

CONSORTIUM MATERIALS TECHNOLOGY for demonstration and development of thermal energy processes

FeCrAl alloys as components in biomass- and waste- fired boilers

Kristina Hellström, Niklas Israelsson, Jan-Erik Svensson, Bo Jönsson, Dilip Chandrasekaran, Johanna Nockert-Olovsjö, Anna Jonasson, Bengt-Åke Andersson, Paul Cho, Per Kallner, Pamela Henderson

KME-507

FeCrAl alloys as components in biomass- and waste- fired boilers

Kristina Hellström, Niklas Israelsson, Jan-Erik Svensson, Bo Jönsson, Dilip Chandrasekaran, Johanna Nockert-Olovsjö, Anna Jonasson, Bengt-Åke Andersson, Paul Cho, Per Kallner, Pamela Henderson

Preface

The project has been performed within the framework the fifth stage of the material technology research programme KME.

KME, Consortium Materials technology for demonstration and development of thermal Energy processes, was established 1997 on the initiative of the Swedish Energy Agency. In the consortium, the Swedish Energy Agency, seven industrial companies and 18 energy companies participate. The programme stage has been financed with 60.2 % by participating industrial companies and with 39.8 % by Swedish Energy Agency. The consortium is managed by Elforsk.

The programme shall contribute to increasing knowledge to forward the development of thermal energy processes for various energy applications through improved expertise, refined methods and new tools. The programme shall through material technology and process technology developments contribute to making electricity production using thermal processes with renewable fuel more effective. This is achieved by

- Forward the industrial developments of thermal processes through strengthen collaboration between industry, academy and institutes.
- Build new knowledge and strengthen existing knowledge base at academy and institutes
- Coordinate ongoing activities within academy, institutes and industry

KME's activities are characterised by long term industry relevant research and constitutes an important part of the effort to promote the development of new energy technology with the aim to create an economic, environmentally friendly and sustainable energy system.

Abstract

The corrosion resistance of certain components in a waste-fired boiler can be improved significantly if the existing material is replaced with FeCrAl material, such as thermo shield tubes and shielding of superheaters. The results also surprisingly show that the pre-oxidation is not favorable when the material is used at lower temperatures, below 700 °C. This means that production of major boiler components in FeCrAl material would be greatly facilitated.

Sammanfattning

Karaktäristiskt för överhettarkorrosion i biomass- och avfallseldade pannor är kombinationen av relativt låga metalltemperaturer och en kemiskt aggressiv miljö. De material som konventionellt används i dessa starkt korrosiva applikationer är främst kromoxidbildande material. Arbetet inom HTC har visat att vissa kemiska reaktioner, speciellt bildningen av alkali kromat (VI), som utarmar den skyddande oxiden på krom tenderar att omvandla oxiden till dåligt skyddande järnoxid vilket kan leda till en plötslig ökning av korrosionshastigheten (breakaway corrosion). En möjlig strategi för att undvika problemet skulle vara att använda en helt annan typ av material som bildar ett skyddande oxidskikt som inte attackeras av alkali i det intressanta temperaturområdet. Ett alternativ skulle vara aluminiumoxidbildande legeringar, t.ex. de välkända FeCrAl stålen, i dessa miljöer. Nyttan med gruppen FeCrAl legeringar bygger på bildandet av ett långsamt växande och mycket skyddande Al₂O₃ skikt på materialytan. Emellertid kan användbarheten av aluminiumoxidbildare ifrågasättas vid temperaturer typiska för överhettare (<600 °C). Detta är främst på grund av den långsamma diffusionen av aluminium i legeringen vid dessa temperaturer. Byte av de högtemperaturlegeringar som används för närvarande i dessa tillämpningar till mer korrosionsbeständiga legeringar kan göra det möjligt att utforma nya anläggningar för högre ångtemperaturer, och därmed få ut mer "grön" el per enhet bränsle.

Detta projekt undersökte FeCrAl-legeringars användbarhet i avfalls- och biomassaeldade pannor. På laboratoriet undersöktes om ett Al_2O_3 ytskikt, etablerat genom föroxidering, kan skydda materialet vid exponering i en pannmiljö. Ett FeCrAl material, Kanthal® APMT, med och utan föroxidering exponerades sedan i fält tillsammans med ett referensmaterial, Sanicro28, på en korrosionsprob vid 600 och 700 °C i 24-1000 timmar. Även okylt icke föroxiderat APMT och Inconell 625 exponerades vid en rad olika temperaturer (350-900°C). Materialen analyserades sedan med avseende på materialförlust samt korrosionsprodukter.

Laboratorieundersökningarna visar att ett tjockare aluminiumoxidytskikt förblir intakt under en längre tid än ett tunnare men flagar så småningom av. Flagningen initieras genom oxidbildning vid defekter. Tillsammans med den medföljande volymexpansionen och klorering av legeringen sprider sig flagningen över ytan. I fältexponeringarna visade legeringen APMT överlägset bäst förmåga att motstå korrosion. Den kromoxidbildande legeringen Sanicro28 visar metallförluster som är mer än dubbelt så stora som för APMT vid 600 och 700 °C. Överraskande nog var metallförlusten högre på de föroxiderade materialen. Dessa resultat är i linje med resultaten från KME 414. Också de okylda materialtesterna (350-700 °C) visar att APMT klarar en avfallseldad miljö bättre än det kromoxidbildande referensmaterialet Inconell 625. Vid de högre temperaturerna behöver uppföljande undersökningar utföras för att kunna dra några slutsatser.

Resultaten visar att korrosionsbeständigheten av vissa komponenter i avfallseldade pannor kan förbättras betydligt om befintligt material ersätts med FeCrAl material, exempelvis termoskyddsrör och överhettare (som skikt p.g.a. tryckbelastningen). Det överraskande resultatet att för-oxidering inte är gynnsam när materialet används vid temperaturer under 700 °C innebär att produktionen av stora pannkomponenter i FeCrAl skulle bli mycket enklare.

Nyckelord: FeCrAl-legring, för-oxidation, ångöverhettare, aluminiumoxid, alkalisalt.

Summary

Characteristic of superheater corrosion in biomass- and waste- fired boilers is the combination of relatively low metal temperatures and chemically aggressive environment. The materials conventionally used in such highly corrosive applications are predominantly chromium oxide forming material. Work in HTC has shown that certain chemical reactions, especially the formation of alkali chromate (VI), which depletes the protective oxide in chromium and tends to transform the oxide into poorly protective iron oxide which can lead to a sudden increase in the corrosion rate (breakaway corrosion). One possible strategy to avoid this problem would be to use a completely different type of material that forms a protective oxide layer that is not attacked by alkali in the interesting temperature range. An alternative would be to use the alumina forming alloys, such as the familiar FeCrAl steels in these environments. The usefulness of the group FeCrAl alloys is based on the formation of a slow growing and highly protective Al₂O₃ layer on the material surface. However, the usefulness of alumina formers is questionable at temperatures typical of the superheaters (< 600 °C). This is mainly due to the slow diffusion of aluminum in the alloy at these temperatures. Replacing the alloys currently used in these applications with more corrosion resistant alloys may make it possible to design new facilities for higher steam temperatures, and thus get more "green" electricity per unit of fuel.

This project investigated the usefulness of iron-chromium-aluminium alloys in waste- and biomass- fired boilers. In the laboratory, it was examined if an Al_2O_3 surface layer, established by pre-oxidation, can protect the material during exposure in a boiler environment. A FeCrAl material, Kanthal® APMT, with and without an Al_2O_3 layer was then exposed in the field together with a reference material, Sanicro 28, on a corrosion probe at 600 and 700 °C for 24-1000 hours. Also, uncooled non pre-oxidized APMT and Inconel 625 were exposed at a range of temperatures (350-900 °C). The materials were then analyzed with respect to loss of material and corrosion products.

The laboratory investigations show that a thicker alumina surface layer stays intact for a longer time than a thinner but eventually spalls off. The spallation is initiated by oxide formation at defects. Together with the accompanying volume expansion and alloy chlorination, the spallation spreads over the surface. In the probe exposure alloy APMT showed by far the best ability to withstand corrosion. The metal loss of the chromia forming Sanicro28 was more than twice that of Kanthal APMT at 600°C and 700°C. Surprisingly, the metal loss was higher on the pre-oxidized material. These results are in line with results from KME 414. Also the uncooled material test (350-700°C) show that Kanthal APMT manages a waste fired environment better than the chromia forming Inconel 625. At the higher temperatures more exposures are needed to draw any conclusions.

The results show that the corrosion resistance of certain components of the waste-fired boilers can be improved significantly if the existing material is replaced with FeCrAl material, such as thermo shield tubes and superheaters (as coatings due to the pressure load). The surprising result that the pre-oxidation is not favorable when the material is used at temperatures below 700°C means that production of major boiler components in FeCrAl material would be greatly facilitated.

Keywords: FeCrAl alloy, pre-oxidation, superheater, alumina, alkali salt.

Table of contents

1	Intr	oductio	n	1
	1.1	Backgr	ound	1
	1.2	Descrip	otion of the research field	1
	1.3	Resear	ch task	2
	1.4			
	1.5	Project	organisation	4
2	Des	cription	of the test materials	6
3	Des		of analytical instruments	8
	3.1		netric analysis	
	3.2		ng Electron microscopy (SEM)	
	3.3		diffraction (XRD)	
	3.4		romatography (IC)	
	3.5		Electron Spectroscopy (AES)	
	3.6	Tome of	of Flight-Secondary Ion Mass Spectrometry (Tof-SIMS)	9
4			exposures	10
	4.1	•	mental set-up	
		4.1.1	Horizontal furnace exposures	
		4.1.2	Thermo gravimetric analysis (TGA)	11
5		d expos	ures	12
	5.1	Plant d	lescription Händelö	
		5.1.1	The boiler	
		5.1.2	The fuel preparation	
		5.1.3		
		5.1.4	·	
	5.2	Plant d	lescription Idbäcken	20
	5.3		otion of the corrosion probe tests and probe	
		5.3.1 5.3.2	The probe test	
	5.4		Operational conditions during probe exposure otion of the un-cooled field tests	
	5.4	5.4.1		
		5.4.2	Description of the un-cooled field tests at Idbäcken	
		3.4.2	Description of the un-cooled held tests at lubacken	20
6	Res		have about a	31
	6.1		tory studies	
		6.1.1 6.1.2	Sample preparation before exposure	
		6.1.3	The influence of KCl	35
		6.1.4	Pre-oxidation	
		6.1.5	The influence of KCl and pre-oxidation	
		6.1.6	Summary of the laboratory results	
	6.2		tudy	
	0.2	6.2.1	The corrosion probe study	
		6.2.2	Thermal shield tubes, Händelö and Idbäcken	
		6.2.3	Shield sheets at the tertiary superheater, Händelö and	
		0.2.0	Idbäcken	101
		6.2.4	Shield sheet at the vortex finder, Händelö	
7	Δna	lysis of	the results	112
•	Alla	, , , , , , ,	tile i esuits	

KME

8	Conclusions	117
9	Goal fulfilment	120
10	Suggestions for future research work	121
11	Literature references	122
12	Publications	124

1 Introduction

1.1 Background

For Sweden to be able to develop a sustainable energy system several high temperature corrosion problems must be solved. Corrosion problems in biomass or waste-fired combustion plants are important issues in this context. New more corrosion-resistant materials could mean less maintenance, less downtime, higher steam data, increased electrical output, etc.

The corrosion problems affecting the components in waste- and biomass-fired boilers can be addressed by changing the environment or by improving the component materials. This project investigates whether components in biomass and waste-fired combustion plants can be replaced with more corrosion-resistant, FeCrAl materials. Exposure of a selected number of components, manufactured in FeCrAl materials, will be performed in an industrial waste fired boiler. The purpose is to examine the corrosion properties of commercial FeCrAl materials in these types of environments and make comparisons with the conventional component materials. This will provide a better understanding of the corrosion process in this type of environment and materials. The results will give guidance about where FeCrAl materials may be used in combustion plants. This could enable new designs of biomass- and waste- fired combustion facilities with higher steam temperatures making this important source of sustainable energy more competitive.

1.2 Description of the research field

Characteristic of corrosion in biomass-and waste-fired boilers is the combination of relatively low metal temperatures and a chemically aggressive environment. The materials conventionally used in these highly corrosive applications are mainly chromium oxide forming material. Recent work within the HTC has shown that certain chemical reactions, especially the formation of alkali chromate (VI), which depletes the protective oxide in chromium oxide tends to transform to poorly protective iron oxide which can lead to a sudden increase in the corrosion rate (break away corrosion). We have primarily worked with two novel reactions that can achieve this effect, evaporation of chromic acid and the formation of alkali chromate ¹⁻⁶.

$$\frac{1}{2} \operatorname{Cr}_2 O_3(s) + \frac{3}{4} O_2(g) + H_2 O(g) \rightarrow \operatorname{Cr} O_2(OH)_2(g)$$
 (1)

$$\frac{1}{2} \operatorname{Cr_2O_3(s)} + \frac{3}{4} \operatorname{O_2(g)} + \operatorname{H_2O(g)} + 2 \operatorname{KCl(s)} \to \operatorname{K_2CrO_4(s)} + 2 \operatorname{HCl(g)}$$
 (2)

Both reactions deplete the protective oxide in chromium, which makes it difficult for the alloy to retain its corrosion resistance. Chlorine is another factor that also tends to accelerate corrosion of these materials, especially in waste-fired plants. Once the protective oxide has been destroyed, for example

by alkali salts forming alkali chromate, the oxide is easily penetrated by chloride ions which lead to more serious corrosion.

A possible strategy to avoid the problem would be to use a completely different type of material that forms a protective oxide layer which is not attacked by alkali. One option would be to use alumina-forming alloys, such as the familiar FeCrAl steels, in these environments. FeCrAl alloys are primarily used at very high temperatures 900 - 1300 °C, for example as heating elements in industrial furnaces. FeCrAl alloys are ferritic iron-based steel with a typical concentration of 18-25 wt. % chromium and ~ 5 wt. % aluminium ⁷. In addition, small amounts of reactive elements are added (yttrium, zirconium and hafnium) to enhance corrosion resistance and to improve the mechanical properties. The benefits of the group FeCrAl alloys are based on the formation of a slow-growing and very protective a-Al₂O₃ layer 8-10. However, the usefulness of aluminum oxide formers can be questioned at low temperatures (<900 °C). This is because the alloy does not form a protective corundum-type oxide at low temperatures. The metastable aluminium oxides formed at lower temperatures have less protective properties. While the protective property of this oxide is not well known, it may provide better protection than chromia. The aluminium diffusion is very slow in the alloy at low temperatures, which means that a protective oxide layer may not form at all. Instead, perhaps a non-protective combination of aluminium, iron and chromium oxide is formed. This could be circumvented by pre-oxidation of the material so that a protective a-Al₂O₃ layer is formed on the surface before exposure.

1.3 Research task

The aim of this project will be to identify and understand the usability and the limitations of alumina forming materials as components in biomass- and waste fired combustion plants. The work will be focused on identifying mechanisms behind the corrosion and to find ways to alleviate the high temperature corrosion problems. The project will include exposures of the material in well-controlled laboratory environments as well as exposures in the complex environment in the field. The project will combine a number of analysis methods which will give us a thorough understanding of the formed oxide and the oxidation process.

1.4 Goal

This project can be seen as a continuation of KME 414 where we investigated the possibility to use FeCrAl materials as layers on superheaters in biomass-and waste- fired boilers at 600 °C. The laboratory studies showed that KCl accelerates the corrosion of the two FeCrAl alloys Kanthal APMT in a similar manner as has been shown earlier in the case of chromium oxide forming high temperature steel. This is because the exposure temperature is too low for the two alloys to form a protective aluminum oxide layer. Instead, a mixed (Fe, Cr, Al) oxide is formed that reacts with KCl, O_2 and H_2O forming potassium chromate during oxidation. The resulting chromium depleted oxide is poorly protective. In the field corrosion exposure, alloy APMT showed by far the best ability to resist corrosion. Both the

"conventional" FeCrAl alloy Kanthal[®] AF and the chromium oxide forming 304L show metal losses of approximately twice that of APMT. Pre-oxidation of the samples had a positive effect on the ability of FeCrAl APMT alloy to resist KCl induced corrosion in relatively mild conditions in the laboratory exposures. In contrast, pre-oxidation had no positive effect on the corrosion behavior in the environment of the fire side in the waste-fired boiler. The difference between the effects of oxidation in the two cases is assigned provisionally to the differences in the corrosive environment.

In the current project, we want to investigate why field and laboratory exposures differed from each other in KME 414 and also if alumina-forming materials can be used in biomass-and waste fired boilers where the material temperature is higher (700 - 900 °C), where the protective aluminum oxide can be more easily formed and maintained. Of interest are also applications at lower temperatures. Components of interest to test are, among others;

- Tube shields in connection to the sand loop seal
- Components in the cyclone outlet (850-900 °C)
- Thermal shielding tubes (Termoskyddsrör) (400-900 °C)
- Tube shields (for superheater tubes) (400-500 °C)
- Layers on superheaters

The work will be focused on identifying mechanisms behind the corrosion and to find ways to alleviate the high temperature corrosion problems.

This project involves two parts; a) an initial study in the laboratory environment and b) field exposures in a waste fired boiler and possibly in a biomass-fired boiler. The materials that will be exposed are FeCrAl alloys and a reference material (used in the application today). The exposure environment in the laboratory mimics the environment in biomass- and waste fired boilers.

The following scientific issues will be highlighted:

- What is the nature of the oxides formed at 600 850 °C in an oxidizing environment?
- How is the oxide formation affected by the presence of water vapor?
- How is the oxide formation affected by the presence of small amounts of alkali compounds (chlorides, carbonates and sulphates)?
- Can the corrosive effect of alkali salts be mitigated by pre-oxidation?
- How does the protective aluminum oxide break down in the presence of alkali salts?

Laboratory study:

The laboratory exposures will be conducted in a synthetic environment that mimics the corrosive environment in real boilers. The exposures will be performed in a thermo balance and in tube furnaces. We will examine:

Influence of O₂ and H₂O

The effect of water vapor on the oxidation of Kanthal[®] APMT will be studied in an oxygen containing environment at 600 – 900 °C.

• Influence of the presence of KCl.

Kanthal APMT will be exposed to KCl in a gas environmnet containing both O_2 and H_2O . The research focus on the initial corrosion attack (<168 hours).

• Influence of pre-oxidation in the presence of KCl

Kanthal[®] APMT is pre-oxidized to form a protective aluminum and is thereafter exposed to KCl in a gas environment containing both O_2 and H_2O .

Field study:

A series of probe-exposures will be conducted in Händelöverket, boiler P14. The material will be Kanthal $^{\circ}$ APMT with and without pre-oxidation and Sanicro 28 as a reference material. The exposure temperature will be 600 and 700 $^{\circ}$ C and the exposure times will be 24, 400 and 1000 hours.

In addition un-cooled exposures will be performed in Händelöverket, boiler P14 and Idbäcken. Selected components manufactured by Sandvik Heating Technology is inserted in and removed from the boiler by E.ON and Vattenfall to be analyzed by Chalmers.

1.5 Project organisation

The personnel at HTC (Chalmers) involved in the project and the following people at the industrial partners has participated in the project:

Bo Jönsson, Sandvik Heating Technology
Dilip Chandrasekaran, Sandvik Heating Technology
Johanna Nockert, Sandvik Heating Technology
Paul Cho, Metso Power
Margareta Lundberg, Metso power
Anna Jonasson, E.ON Värme Sverige
Bengt-Åke Andersson, E.ON Värme Sverige
Per Kallner, Vattenfall
Pamela Hendersen, Vattenfall
Jan-Erik Svensson, HTC
Niklas Israelsson, HTC
Kristina Hellström, HTC

The work within the project was divided between the project participants.

- The laboratory study was conducted on material manufactured by Sandvik Heating Technology, and the exposures and analysis were performed at HTC.
- The cooled probe exposures were conducted on materials manufactured by Sandvik Heating Technology and processed by Metso. The samples were measured at HTC before exposure. The exposures were performed at Händelö by Metso with assistance from E.ON. The analyses of these samples were performed at HTC.
- The test material (Kanthal® APMT) for the un-cooled field exposures at Händelö was supplied by Sandvik and the reference material by E.ON. The material was measured by Sandvik before exposure. The exposures were performed by E.ON and the analyses by HTC.
- The test material (Kanthal® A1) for the un-cooled field exposures at Idbäcken was purchased by Vattenfall. The exposures were performed by Vattenfall and the analyses by HTC.
- HTC has led the project

The budget for the project was: HTC 2600 kkr (financed through KME), Kanthal 3000 kkr (in kind), Metso Power 400 kkr (in kind), E.ON Värme Sverige 300 kkr (in kind), Vattenfall 200 kkr (in kind), in total 6500 kkr for a period of 4 years.

2 Description of the test materials

An overview of the tested materials and their typical chemical composition is given in Table 2 1. Three commercial FeCrAl alloys (Kanthal APMT, Kanthal APM and Kanthal A1) and three FeNiCr alloys (Sanicro 28, Inconel 625 and 253Ma) were investigated. The FeCrAl materials were tested with and without pre-oxidation.

FeCrAl alloys are ferritic iron based steels. Small amounts of reactive elements such as yttrium, zirconium and hafnium are usually added to increase oxidation resistance. The main difference between the FeCrAl alloys is the manufacturing technique. Kanthal® A1 is a cast material manufactured by conventional melting followed by hot rolling, pickling and cold-rolling. Kanthal® APMT is a powder metallurgy manufactured material produced from gas atomized rapidly solified powder particles having the nominal FeCrAl composition. These FeCrAl powders with the addition of small RE-oxide particles are hot isostatically pressed at high temperatures, around 1150°C in vacuum. Both the Kanthal® materials are alumina-formers.

The FeNiCr alloys are chromia-formers and are included in the study to compare alumina- and chromia-forming materials.

Element/ Material	Cr	AI	Ni	С	Si	Mn	Мо	Mg	Ti	RE	Fe
Kanthal [®] APMT	22	5.0		*	≤ 0.7	≤ 0.4	3.0	*	*	Y, Zr, Hf	Bal.
Kanthal [®] A1	21.5	5.8		≤ 0.08	≤ 0.7	≤ 0.4					Bal.
Kanthal [®] APM	22	5.8		≤ 0.08	≤ 0.7	≤ 0.4					Bal.
Sanicro 28	27		31		0.7	2	3.5				35
Inconel 625	21.5		≥ 58				9			Nb, Ta	≤ 5
253MA	21		11	0.08	1.6	≤ 0.8				Се	Bal.

Table 2-1. The chemical composition in mass% of Kanthal® APMT, Kanthal® A1, Kanthal® APM, Sanicro 28, Inconel 625 and 253MA.

3 Description of analytical instruments

3.1 Gravimetric analysis

To get a rough estimation of the corrosion attack the weight of the samples were recorded on a six-decimal Sartorious balance before and after exposure.

3.2 Scanning Electron microscopy (SEM)

The morphology, microstructure and elemental composition of the sample surface was investigated by an FEI Quanta 200 FEG ESEM. The instrument is equipped with a field emission electron gun (FEG) and an Oxford Inca energy dispersive X-ray (EDX) system. The samples were examined with SEM/EDX for elemental mapping and quantification. A Leo ULTRA 55 FEG SEM was also used for imaging at high magnification.

3.3 X-ray diffraction (XRD)

To determine the crystalline corrosion products a Siemens D5000 powder diffractometer was used. The instrument was equipped with a grazing-incidence-beam attachment together with a Göbel mirror. The sample was exposed to a source of CuKa radiation ($\lambda = 1.5418$ Å) with an incident angle of 0.5°. The moving detector collected data in the range of 20° < 20 < 60° with step size of 0.05°. Silicon powder was added to the sample surface for calibration. The background was subtracted from the diffraction measurements.

3.4 Ion chromatography (IC)

To establish the amount of water-soluble anions (CrO_4^{2-} , Cl^-) on the surface after exposure a Dionex ICS-90 system was used. The anions were analysed with an IonPac AS4A-SC analytic column and 1.8 mM Na₂CO₃/1.7 mM NaHCO₃ as elution. To determine the remaining amount of water-soluble cations (K⁺), the samples were analysed with a Dionex ICS-900 system with an IonPac CS12A analytic column. The samples were leached in 5 ml Milli-Q water using ultrasonic agitation for 10 + 10 min. The elution was 20 mM sulfonic acid and the flow rate was 2 ml/min for both anions and cations. The detection limits for the different species are: Cl^- = 0.03 µmol, K⁺=0.03 µmol and CrO_4^{2-} = 0.01 µmol =2.10⁻⁹ mol/cm²

3.5 Auger Electron Spectroscopy (AES)

Auger electron spectroscopy was used to estimate oxide thickness and to determine elemental depth distribution. The AES analyses were performed with a PHI 660 Scanning Auger Microprobe (SAM) using an accelerating voltage of 10 kV and a beam current of 200 nA. AES depth profiling was performed using ion sputtering with 3.5 keV Ar+. Two areas were analysed,

one smaller 10 x 10 μm^2 and one larger 90 x 120 μm^2 . They exhibit almost the same oxide thickness and elemental depth distribution. Only results from the small areas are shown in this study.

Quantitative analyses were performed using the peak-to-peak height of the Auger transitions of a specific element together with sensitivity factors provided by PHI, except for the Al and O, which were calibrated against pure Al_2O_3 . Since the sensitivity factor for oxygen in Cr_2O_3 and Fe_2O_3 are different from that for Al_2O_3 the oxygen signal will be slightly off when mixtures of the oxides are present. The computer software PHI-Matlab and linear least square (LLS) routines were used to separate the oxide and metal components in the depth profiles. This ensures that the detected Fe, Cr and Al in the oxide part of the depth profiles really are in oxidized form and consequently do not originate from the metal substrate.

3.6 Tome of Flight-Secondary Ion Mass Spectrometry (Tof-SIMS)

The Time of Flight-Secondary Ion Mass Spectrometry analyses were performed with a PHI TRIFT II instrument using a pulsed Liquid Metal Ion Gun (LMIG) enriched with 69Ga+ ions. Depth profiles were obtained by sputtering à surface area of 50 \times 50 μm^2 with a continuous non-pulsed beam with primary ion energy of 15 kV and a current of 20 nA. Positive and negative static SIMS mode was used to analyse an area of $25 \times 25 \mu m^2$ in the centre of the sputtered area. All SIMS spectra were calibrated using the exact positions of peaks with a known mass/charge ratio, such as aluminium (26Al+), chromium (52Cr⁺), iron (56Fe⁺) and the Ga primary ion (69Ga⁺). The intensities are expressed as peak areas rather than peak heights, because the energy distribution is not the same for all secondary ions. Before imaging the sample surfaces, an optimum sputtering time to remove surface contamination while at the same time save the remnants of previous surface deposit was 6 minutes using 2 nA, 25 kV 69Ga+ rastered over a 200 x 200 µm² area. The images were acquired during a sampling time of 8 minutes in both positive and negative mode.

4 Laboratory exposures

4.1 Experimental set-up

4.1.1 Horizontal furnace exposures

The exposures were carried out in a horizontal furnace fitted with a 45 mm (inner diameter) SiO_2 -glass tube (*Figure 4-1*). Three sample coupons were placed vertically on an alumina holder. The alumina holder was placed on an alumina boat and inserted in the middle of the furnace. To avoid interaction between the samples, the coupons were placed parallel to the direction of the gas flow. The samples were exposed at 600 °C. The temperature was calibrated to \pm 3 °C and the constant temperature zone was 4 cm. To create a gas-flow containing water vapor, a humidifier was used. The gas was piped trough heated water followed by passage through a cooling system. The cooling system consisted of a heat-exchanger set at the dew point, which gave the desired amount of water vapor. All parts of the gas system carrying humid gas were kept at a temperature above the dew point to prevent condensation.

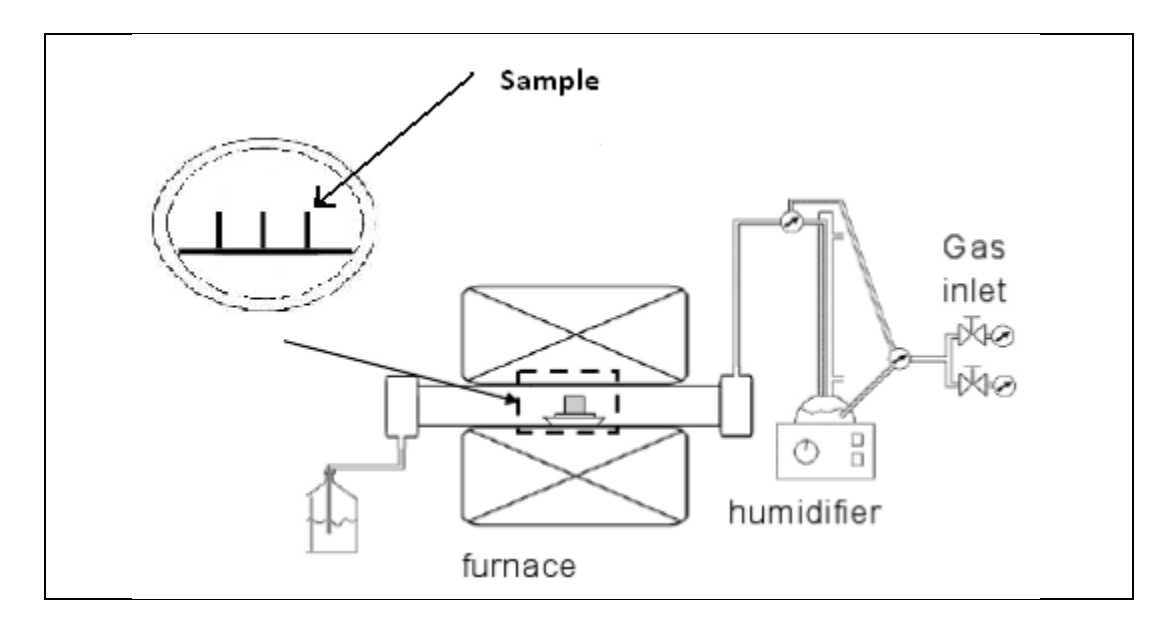


Figure 4-1. Experimental setup of the furnace and surrounding equipment.

Figure 4-1. Experimentell utformning av ugnen och kringutrustning.

4.1.2 Thermo gravimetric analysis (TGA)

By using a thermo balance the mass gain can be measured in situ throughout the experiment. In order to follow the initial oxidation kinetics, exposures were performed in a SETARAM TAG24 thermogravimetric analysis system, which consists of two furnaces and a balance (*Figure 4-2*). The furnaces are fitted with two identically shaped SiO_2 –glass exposure tubes. The reference and sample are positioned in individual exposure tubes and connected to the balance. The mass change between the reference and the sample is recorded. Thus, it is important to ensure that the environments for the reference and sample are as similar as possible. In this case, the reference was the inert material Al_2O_3 , which had the same shape as the sample. A gas stream of the same velocity flowed down the two exposure tubes. The balance was protected from the oxidizing gas by the passage of an inert gas into the balance.

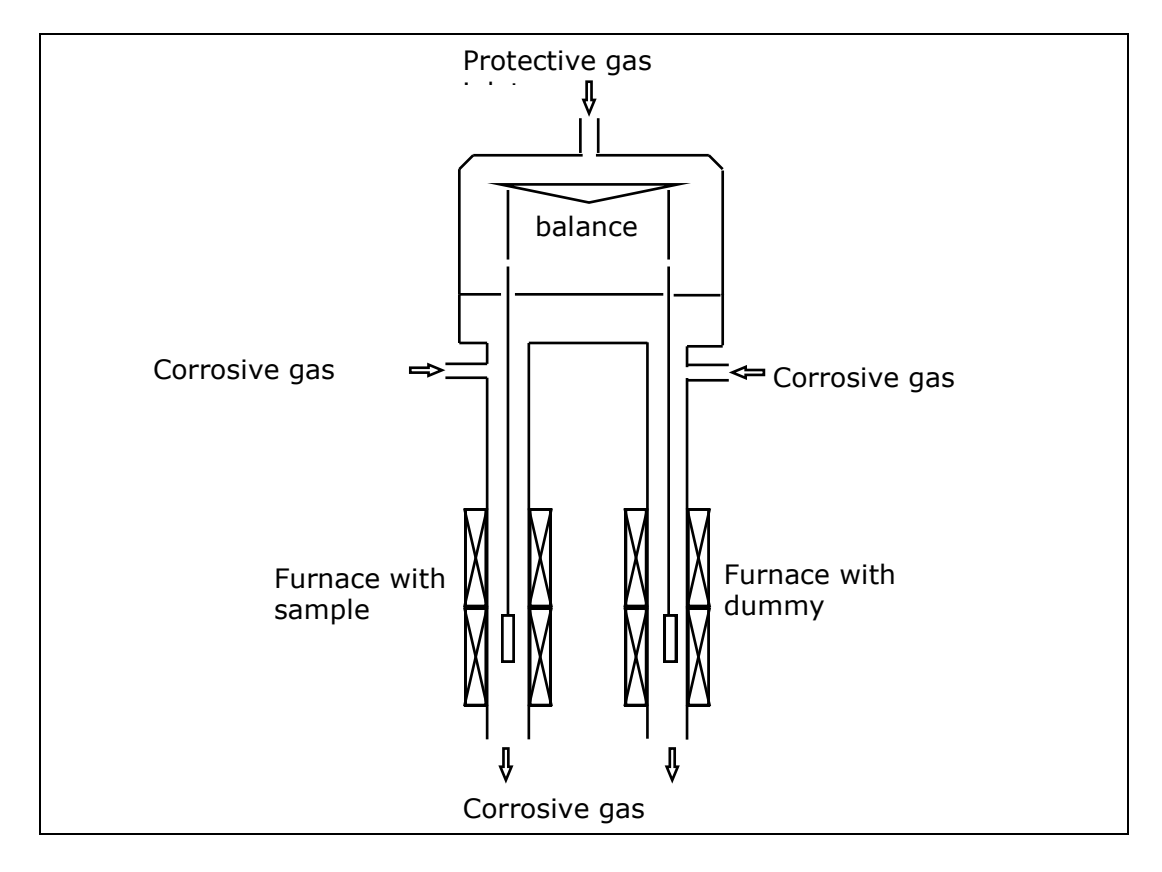


Figure 4-2. Schematic drawing of a SETARAM TGA24.

Figure 4-2. Schematisk bild på SETARAM TGA24.

5 Field exposures

5.1 Plant description Händelö

a) The waste fired plant P14 at Händelö, shown in *Figure 5-1*, has a capacity of 200 000 metric tonnes/year. The plant is a modern Energy-from-Waste plant with great fuel flexibility. The waste burned is household waste and industrial waste. It is also possible to burn 20% sewage sludge from sewage water treatment plants. The plant consists of a boiler, steam turbine, flue gas cleaning and fuel preparation.



Figure 5-1. The waste incinerator plant P14 at Händelöverket.

Figur 5-1. Den avfallseldade förbränningsanläggningen P14 vid Händelöverket.

5.1.1 The boiler

The boiler, Figure 5-2, is a Circulating Fluidised Bed (CFB) boiler with a thermal capacity of 75 MW supplied by Kvaerner Power (today: Metso Power). The boiler produces steam, primarily used for production of electricity, industrial process steam, and district heating. Some boiler data are shown in Table 5-1, Table 5-2 and Table 5-3.

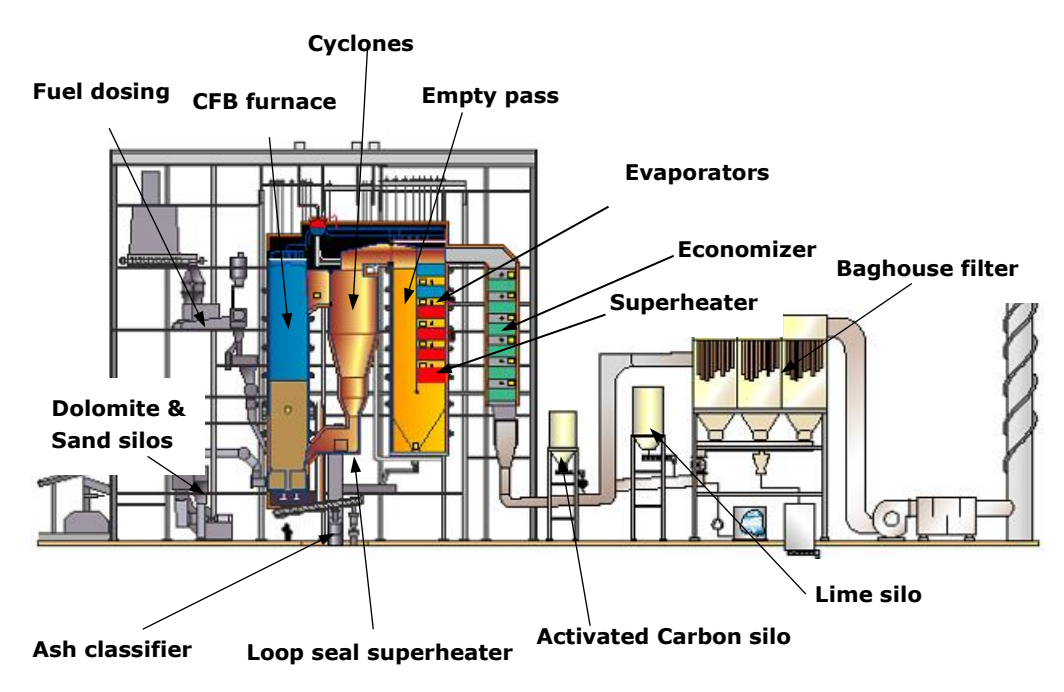


Figure 5-2. Händelö/Norrköping P14 CFB boiler.

Figur 5-2. Händelö/Norrköping P14 CFB panna.

The boiler is designed for fuel flexibility, using a fuel mix of 30-50% combined household waste, 50-70% classified industrial waste and up to 20% sewage sludge.

The design of the Metso CFB boiler used for combustion of MSW/RDF (Municipal Solid Waste, Refused Devised Fuels) fuels comprises some characteristic features to be outlined in the following text. The main parts in the boiler system are a water-cooled furnace with two integrated water cooled cyclones and loop seals, containing the final superheaters, and an external ash-classifier, *Figure 5-2*. The cyclones are followed by a single pass radiation cavity (empty pass) and a convection pass with superheater banks, boiler banks and economizer banks. The boiler is equipped with a conventional steam soot blowing system cleaning the banks in the convection pass. Afterwards the empty pass has been equipped with two water cannons and the economizer with sonic cleaning, which is used together with the original installed steam soot blowers.

The boiler is top supported and designed for natural circulation characterised by the steam separating system including the steam overflow headers, in combination with the downcomers, which run from the top to the bottom of the boiler. Saturated water from the drum is distributed through a number of downcomers to the bottom part of the boiler, the wall tubes in the furnace, the cyclone loop seal and the radiation cavity/back pass enclosure. The water/steam mixture is transferred back to the steam drum by a number of steam separating connecting pipes. The circulating system is integrated between all components.

The furnace front and rear wall are bent into a U-shape to form a water cooled windbox for primary air, below the fluidized bed furnace. The primary windbox also serves as a combustion chamber for the start-up burner, located at the furnace front wall.

All four walls of the furnace are refractory lined, except for a smaller surface area on the upper part of the sides and front wall, for erosion protection and to sustain furnace temperature above 850°C during 2 seconds after the last injection of air. The latter is a European requirement when firing waste. It is also required to install auxiliary burners in the furnace to secure the furnace temperature 850°C before adding the RDF during start up and in case of a sudden drop in the furnace temperature during boiler operation.

Coarse fuel ash entering the furnace is transported through the bottom bed, by means of the directed primary air nozzles, to discharge openings in the bottom plate from where it is fed to the ash classifier. The classifier operates as a high velocity fluidized bed, which elutriates the small bed particles from the coarse particles in the discharged ash and send them back to the furnace. In addition, the coarse ash is cooled by the added air before it leaves the classifier, which minimizes the loss of sensible heat.

The boiler features two hot gas cyclones for separation of the bed material entrained by the flue gas and leaving the furnace at the furnace top. The separated material is returned to the lower part of the furnace via a loop seal. The loop seal contains a bubbling fluidized bed and is equipped with a number of air nozzles to ensure material transport. Moreover, it is designed to prevent flue gas from the furnace entering the cyclones through the bed material return leg.

The loop seal, which is a feature of the CFB process, offers a location of the final superheater (SH) for two reasons; 1. The heat transfer coefficient in the bubbling bed is 5 to 10 times higher than in the back pass. Hence, the SH area required is reduced by 80 to 90%. 2. The gaseous atmosphere in the loop seal contains less of chlorine and water vapor since the chlorine and water released during the combustion of the RDF is in a gaseous form in the cyclone and therefore follows the flue gas to the back pass. Only the particles separated by the cyclone reach the loop seal.

The cyclones are constructed from water-cooled membrane walls, which form part of the water circulation system. The feature of this design is that the cyclones are part of the natural water circulation circuit and therefore expand in the same way as the furnace and back pass enclosure. This feature allows the cyclones to be gas-tight welded to the furnace and the back pass, thus avoiding all expansion bellows of huge dimensions always causing a lot of maintenance problems and costs. The cyclone interior is fully refractory lined with a thin layer for erosion protection, which minimizes the amount/thickness of refractory and further reduces the maintenance costs and shortens the start-up time. An SNCR-system is installed, with ammonia injection in both cyclones.

The cyclones are followed by an empty pass for lowering the flue gas temperature to a temperature, which makes the ash "dry" and non-sticky to the back pass tube banks. This will minimize deposit formation and corrosion attacks. The bottom of the empty pass is equipped with an ash extraction conveyor system.

The risk of combined corrosion and erosion in the back pass calls for low flue gas velocities and low flue gas temperature. This will result in large superheater and evaporator surfaces.

A new evaporator bundle has been installed 2006 before the secondary superheater to reduce the flue gas temperature by 50°C. This bundle and four additional rows of boiler tubes protect the secondary superheater at the gas inlet side.

The secondary superheater in the back pass has compound tubes with Sanicro28/ St45.8/III and three loops of Sanicro63/St45.8, no 1, 14 and 26. The steam temperature increases from approximately 350°C and controlled up to 400°C in parallel flow with the gas.

The primary superheater was replaced in the spring 2007. It now has tube materials 16Mo3 (the cold part) and 13CrMo44 (the warmer part). The steam temperature increases from 290°C up to approximately 370°C in counter flow with the gas. The gas inlet temperature is about 500°C. All superheater tubes in the first and last rows, near the soot blowers, are protected by tube shields.

Water/steam		
Feed water temp	°C	135
Steam flow	kg/s	27.5
Steam pressure	MPa	6.5
Steam temperature	°C	450
Miscellaneous		
Boiler efficiency	%	89.7
Exit flue gas	°C	165-170
temperature		
Unburned in bottom ash	%	<0,1
Unburned in fly ash	%	< 0,5

Table 5-1. Operating data at MCR (Maximum Continues Rate).

Boiler part	Material	Max gas temperature °C	Max steam or water temperature °C	
Furnace	Sanicro 28 / St45.8/III	900	290	
Radiation cavity (empty pass)	St45.8/III	850	290	
Tertiary superheater	TP347H	900	450	
Evaporator bank	St45.8/III	650	290	
Secondary superheater gas inlet	Sanicro 28 / St45.8/III	630	400	
Secondary superheater gas outlet	Sanicro 28 / St45.8/III	500	340	
Primary superheater gas inlet	13CrMo44	500	370	
Primary superheater gas outlet	16Mo3	440	290	
Evaporator bank	St45.8/III	440	290	
Economiser	St 35.8/III	350	240	

Table 5-2. Boiler material and temperatures at MCR.

Boiler part	Tube surface temperature °C	Fin temperature °C	
Furnace	315	340	
Radiation cavity gas inlet	300	310	
Radiation cavity gas outlet	295	300	
Tertiary superheater	500		
Evaporator bank	295		
Secondary heater gas inlet	360		
Secondary superheater gas outlet	415		
Primary superheater gas inlet	380		
Primary superheater gas outlet	300		

Table 5-3. Max tube and fin surface temperature at MCR.

The P14 boiler is integrated with the other boilers at the plant. The water treatment, district heating system, steam turbine and the condenser are commonly used. The plant is supervised from one control room.

5.1.2 The fuel preparation

The fuel preparation plant, Figure 5-3, consists of a receiving bunker (78 m long, 12 m wide and 8 m deep) with a total volume of more than 7000 m^3 . Two overhead travelling cranes with crab buckets feed the two redundant preparation lines. The crushing/grinding is performed in two steps and

magnetic sorting in three steps, before the boiler. M & J delivered the primary shredders and there are also two secondary shredders, which have replaced the hammer mills. The prepared waste is transported to an intermediate storage, an A-barn, before it is transported to the boiler silos. Sydkraft (today E.ON) has designed the waste preparation system, while the parts are delivered from a number of suppliers.

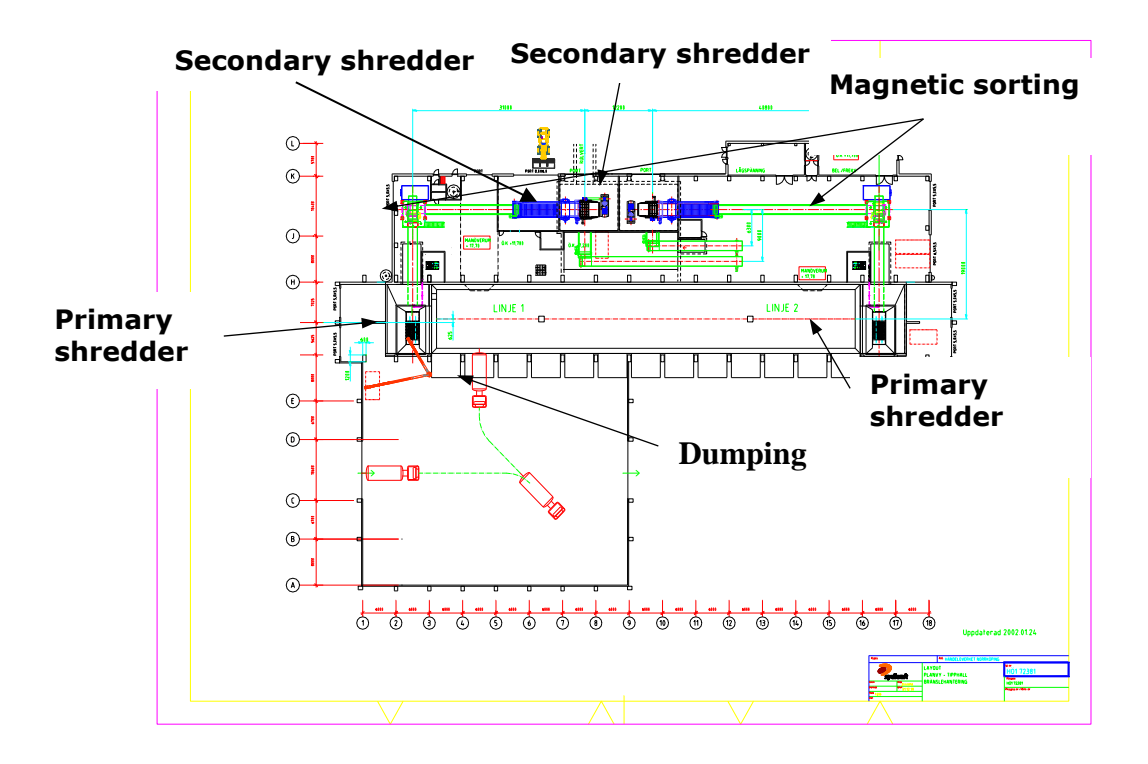
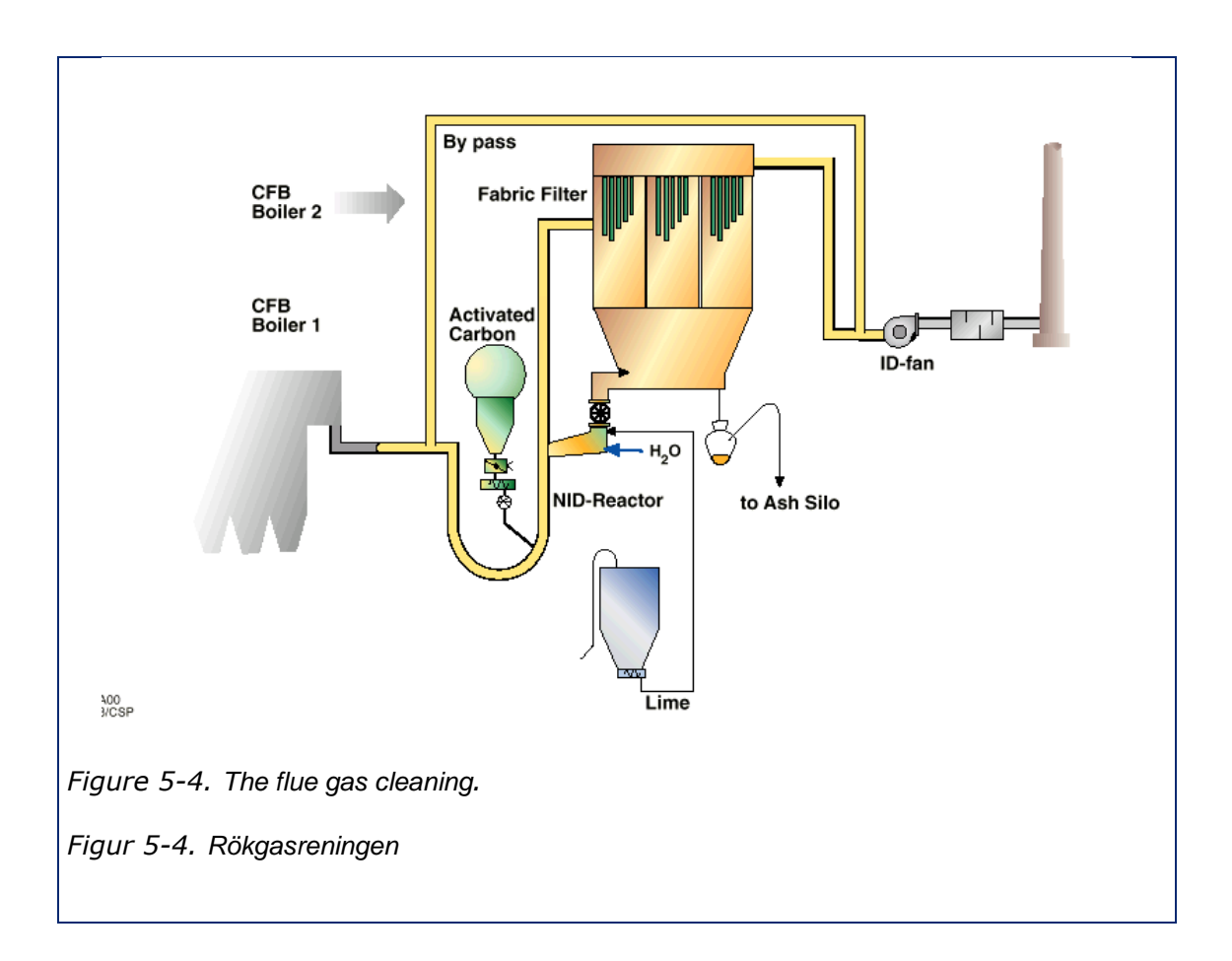


Figure 5-3. The fuel preparation.

Figur 5-3. Bränsleberedningen

5.1.3 The flue gas cleaning

Alstom Power has delivered the flue gas cleaning system, *Figure 5-4*, which is a semidry system without flue gas condensation. The NID-system includes a mixer, a reactor and a fabric filter. Burnt lime is mixed with water in an extinguisher. The hydrated lime is mixed with recirculated filter ash and additional water in a mixer. Next, the moisturized dust is fed into the flue gases in a reactor chamber where activated carbon is added. The particles are removed from the flue gas by a fabric filter. The lime binds to chlorine and sulphur while the activated carbon is used to remove dioxins and heavy metals. The major part of the removed fly ash is recirculated through the mixer and reactor system.



5.1.4 Fuel specification

The fuel consists of a mix of municipal solid waste, industrial waste and some percentage of different types of bio fuels. In *Figure 5-5*, the total distribution of fuels during the period July 2011 - December 2011 is presented. The distribution of fuels reveals that in total, the fuel consists of more than 95% waste fuel. During normal operation, the fraction of waste fuels is 100%. The other types of fuels are related to the startup sequence of the boiler when, according to the incineration directive, no waste fuels are allowed. The bio fuels are also used when the regular fuel feeding system is out of order.

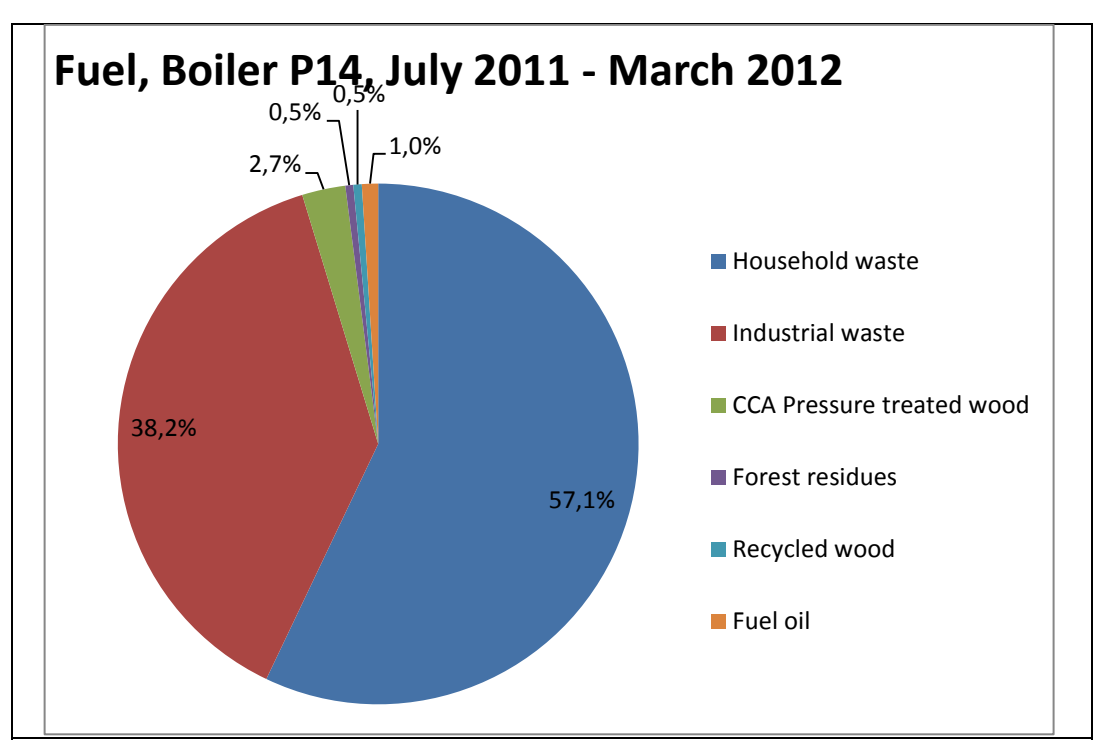


Figure 5-5. Distribution of fuel mix in Boiler P14, July 2011 – March 2012 Figur 5-5. Bränslefördelning i Panna 14, juli 2011 – mars 2012

The different fuels, composing the fuel mix, can be described as:

- <u>Household waste:</u> Solid waste comprising of garbage that originates from private households. Also called domestic waste or residential waste.
- <u>Industrial waste:</u> Solid, semi-solid, liquid, or gaseous fuel that consists of unwanted or residual materials (not including hazardous or biodegradable wastes) from industrial operation.
- <u>CCA Pressure treated wood:</u> Used wood which has been treated with chromated copper arsenate.
- <u>Forest residues:</u> Forest residues are defined as the biomass material remaining in forests that have been harvested for timber, and are almost identical in composition to forest thinnings. Because only timber of a certain quality can be used in lumber mills and other processing facilities, biomass material/forest residue is left in the forests during harvesting operations. Forestry residues include logging residues, excess small pole trees, and rough or rotten dead wood. These residues could be collected after a timber harvest and used for energy purposes.
- Recycled wood; Recycling wood chips are produced from shredded and screened used wood.
- <u>Fuel oil;</u> Fuel oil is a fraction obtained from petroleum distillation, either as a distillate or a residue. Number 1 fuel oil is used in P14. Number 1 fuel oil

is a volatile distillate oil intended for vaporizing pot-type burners. It is the kerosene refinery cut that boils off right after the heavy naphtha cut used for gasoline.

Table 5-4 below shows the average values of several fuel analyses performed 2010-2011. The samples are taken on mixed waste after fuel preparation and storage, on the way into the boiler. The complete fuel analyses are shown in Attachment 1 and were performed by SP.

	H _i MJ/kg	Water content %	Ash %	Carbon %	Oxygen %	Hydrogen %
As delivered	12,3	32,3	11,3	32,9	46,4	8,0
Dry sample			16,7	48,6	26,2	6,4
	Sulphur	Chlorine	Nitrogen			
	%	%	%			
As delivered	0,14	0,7	0,5			
Dry sample	0,21	1,1	0,8			

Table 5-4. Typical fuel data, P14, Händelö

5.2 Plant description Idbäcken

Situated some 120 km south of Stockholm, the Idbäcken CHP plant provides energy to the city of Nyköping. Nyköping has about 30 000 inhabitants and the Idbäcken plant provides half of its electricity requirements, *Figure 5-6*. It also supplies some 14000 households with district heating. The plant is owned and operated by Vattenfall AB and consists of a Bubbling Fluidised Bed (BFB) steam boiler (Boiler 3) for Combined Heat and Power (CHP) operation, two circulating Fluidised Bed (CFB) boilers for hot water production and a hot water accumulator. It has been in operation since the end of 1994.

Boiler 3, the CHP unit, originally operated on a mixture of biomass and coal. Over the years the amount of coal has been reduced and the amount of waste wood increased. Since the summer of 2008, the plant operates on 100% waste demolition wood.

The CHP unit produces 35 MW of electricity and 69 MW of heat. A flue-gas condenser yields 12 MW additional heat at full boiler load. The final steam temperature is 540°C and the pressure 140 bar. A schematic diagram of the boiler is given in *Figure 5-7*.

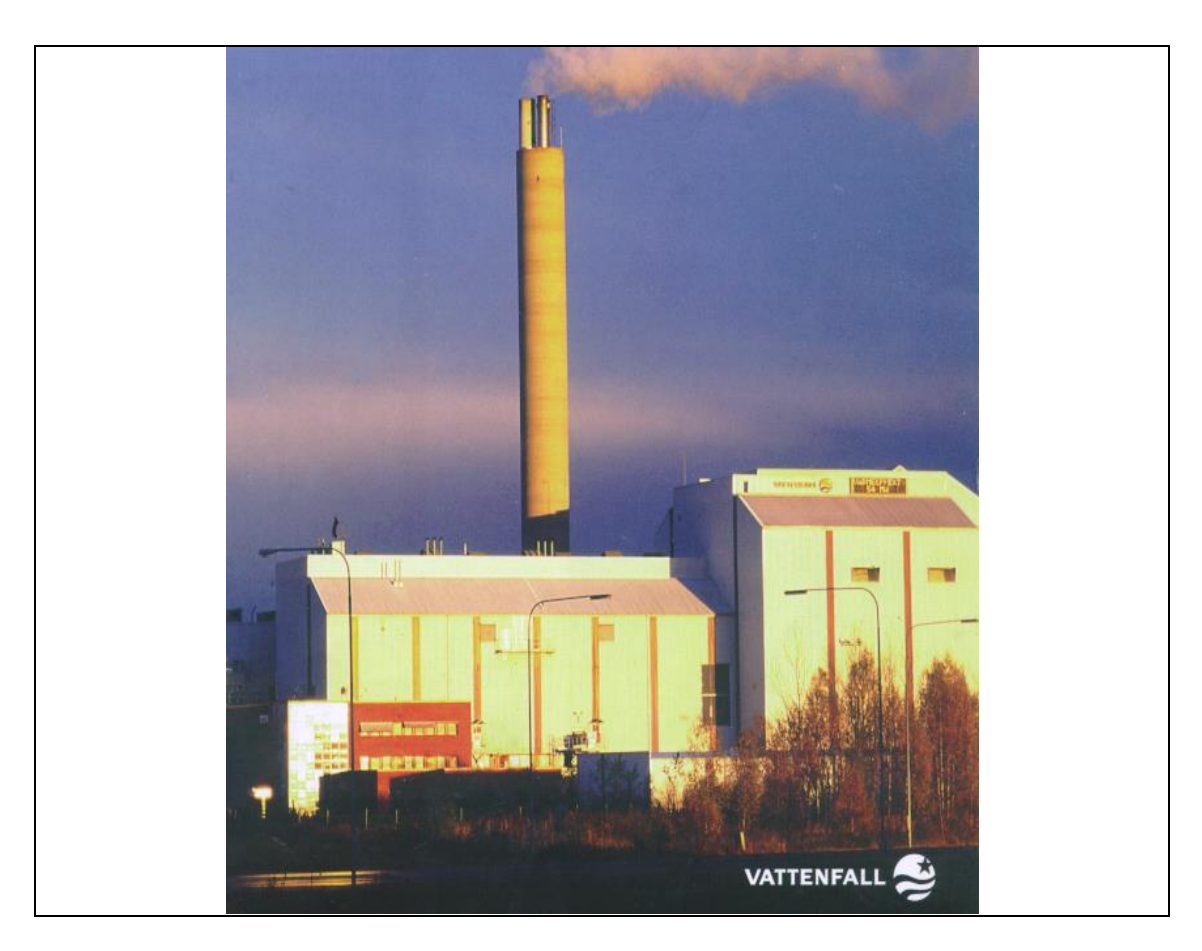


Figure 5-6. View of Vattenfall's plant at Nyköping.

Figur 5-6. Vy av Vattenfalls anläggning I Nyköping.

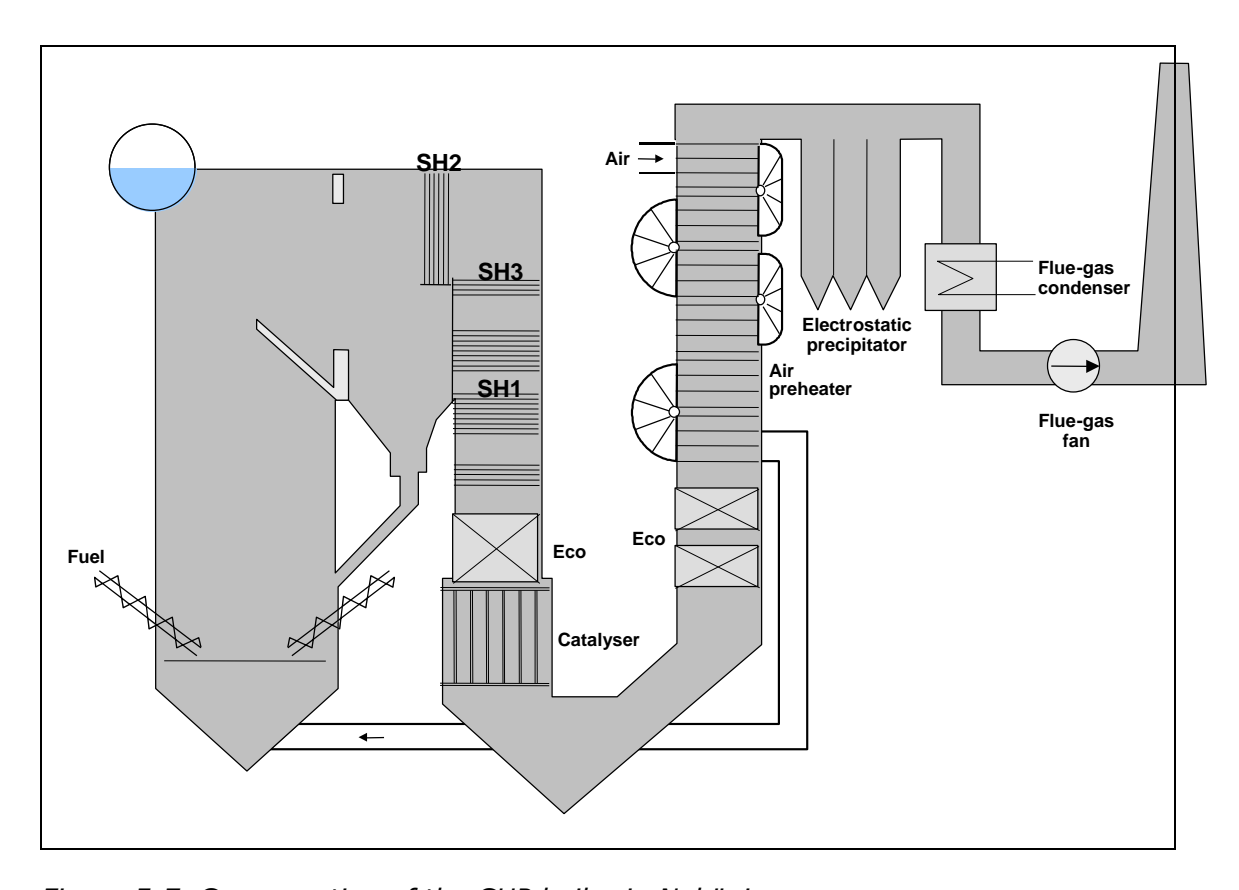


Figure 5-7. Cross-section of the CHP boiler in Nyköping.

Figur 5-7. Tvärsnitts bild på CHP kokaren I Nyköping.

Boiler 3 in Nyköping contains three sets of superheaters as shown in the figure. SH2 is a pendant superheater and the first that the flue gases meet on their way out from the furnace. SH2 is made of X20 and Esshete 1250. The next SH is no. 3, the final superheater, made of TP 347H. SH1 is made of 10CrMo910.

To reduce corrosion, ChlorOut is sprayed into the flue gases upstream of superheater 2.

5.3 Description of the corrosion probe tests and probe

The aim of the probe test is to reveal the corrosion behavior of potential new superheater materials and enable the comparison and ranking of different materials. Corrosion probe test were conducted 3 times. One probe was put into Händelöverken, P14, 5/11-2012 and removed 6/11-2012 making a total of 24 hours exposure. Another probe was put in at the same time, 5/11-2012, and removed 17/12-2012 making the total exposure 1000 hours. A third probe was exposed from 6/11-2012 to 23/11 making the total exposure 400 hours.

5.3.1 The probe test

Description of the probe test arrangement

Figure 5-8 shows a schematic drawing of the probe test arrangement. The probe is installed into the boiler through a hole with a minimum diameter of 50 mm. The probe is cooled with pressurized air. Therefore, a pressurized air (6 Bar) connection is needed for the control unit. One temperature measurement at a specific sample ring in the probe is used to control the amount of cooling air. The control temperature can be adjusted to required level; usually it is the temperature of the studied superheater material. The probe is installed to the boiler, so that the thermocouples are at "wind" side (against the flue gas flow) of the probe. The probe is left in the boiler for needed amount of time.

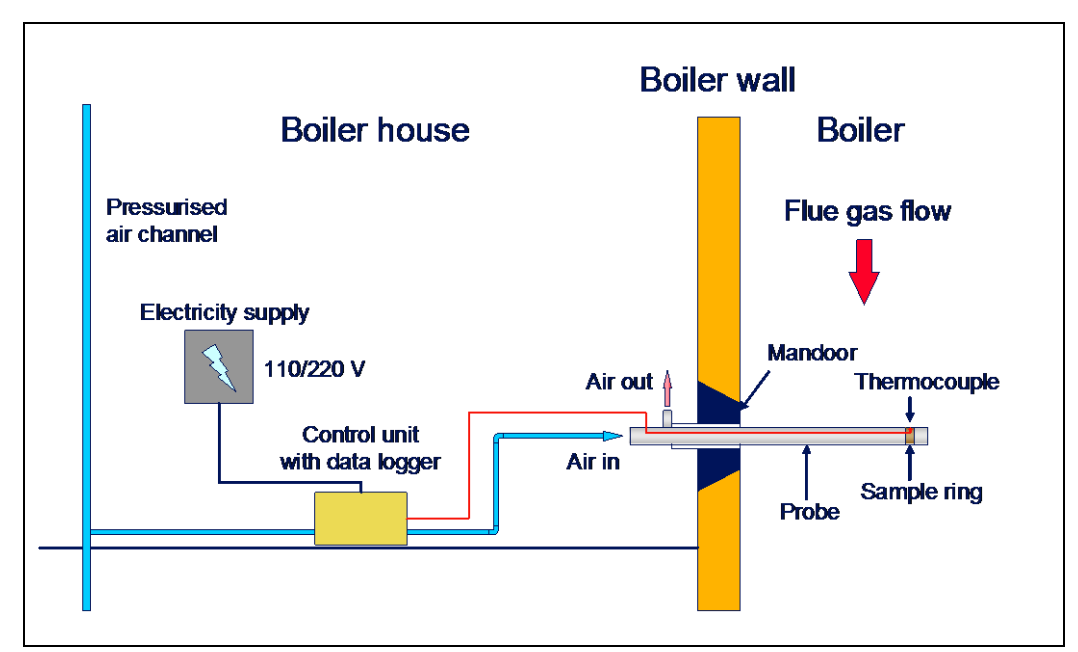


Figure 5-8. A schematic drawing of the probe test arrangement.

Figur 5-8. Schematisk bild på sondprobuppställningen.

Description of the probe

In corrosion probe tests the durability of different materials is studied in the actual atmosphere. The probe is built up as an isothermic probe; it consists of nine material rings and divided to three temperature zones, where the temperatures of the rings in each zone are almost the same. The temperatures of the material rings are measured and saved to data logger. The probe is cooled with pressurized air and the cooling air flow is controlled with a PID controlled pressurized air valves. The amount of lost material can be determined from the rings. The rings can be studied with different analysis techniques to find the corrosion products and determine the corrosion mechanisms. Usually 1000 hours expose time is enough to measure the

corrosion speed and determine the corrosion mechanisms. In *Figure 5-9* a schematic sketch of the probe is presented and *Figure 5-10* shows a photo of a corrosion probes.

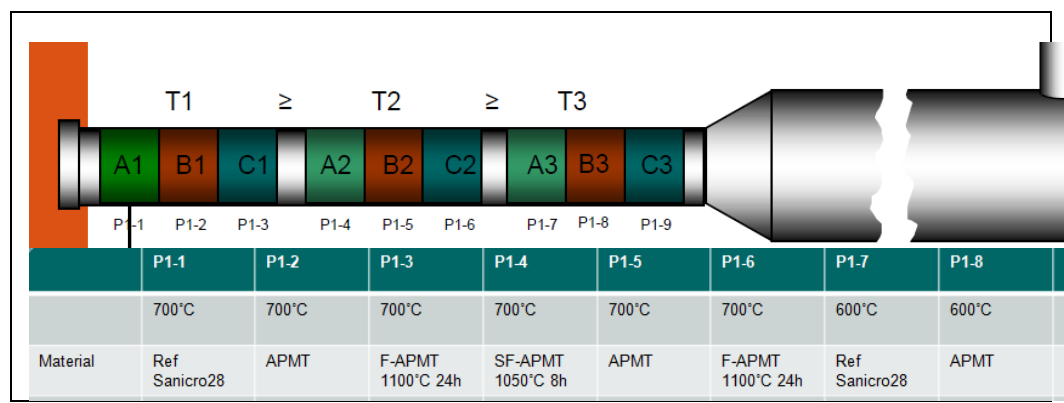


Figure 5-9. A schematic sketch of the corrosion probe.

Figur 5-9. Schematisk bild på korrosionsproben.



Figure 5-10. A photo of the sample rings on the corrosion probe before exposure.

Figur 5-10. Ett foto på provringarna på korrosionsproben innan exponering.

The probe test

The samples were mounted on the probe in the order; Sanicro 28 to the left followed by Kanthal® APMT, pre-oxidised Kanthal® APMT, standard pre-oxidized Kanthal® APMT, Kanthal® APMT, pre-oxidised Kanthal® APMT, Sanicro 28, Kanthal APMT and pre-oxidised Kanthal APMT as shown in *Figure 5-10*. The pre-oxidized Kanthal® APMT was oxidized at 1100 °C for 24 hours and the standard pre-oxidized Kanthal® APMT was oxidized at 1050 °C for 8 hours to establish a protective Al_2O_3 scale on the surface prior to exposure. During exposure, the control temperature was set to 700 °C for the first 6 samples and 600 °C for the additional three samples. The control temperature was

measured from the middle sample in each test groups. The placement of the probe in the boiler was after the cyclone and before empty shaft as shown in Figure 5-11 with a blue star. This place was chosen because of the gas temperature (above $800~^{\circ}$ C). Three probes were left in the boiler for 24, 400, and 1000~ hours. After probe exposure, the test rings were transported together with moisture absorbing medium to HTC, Chalmers for analyses.

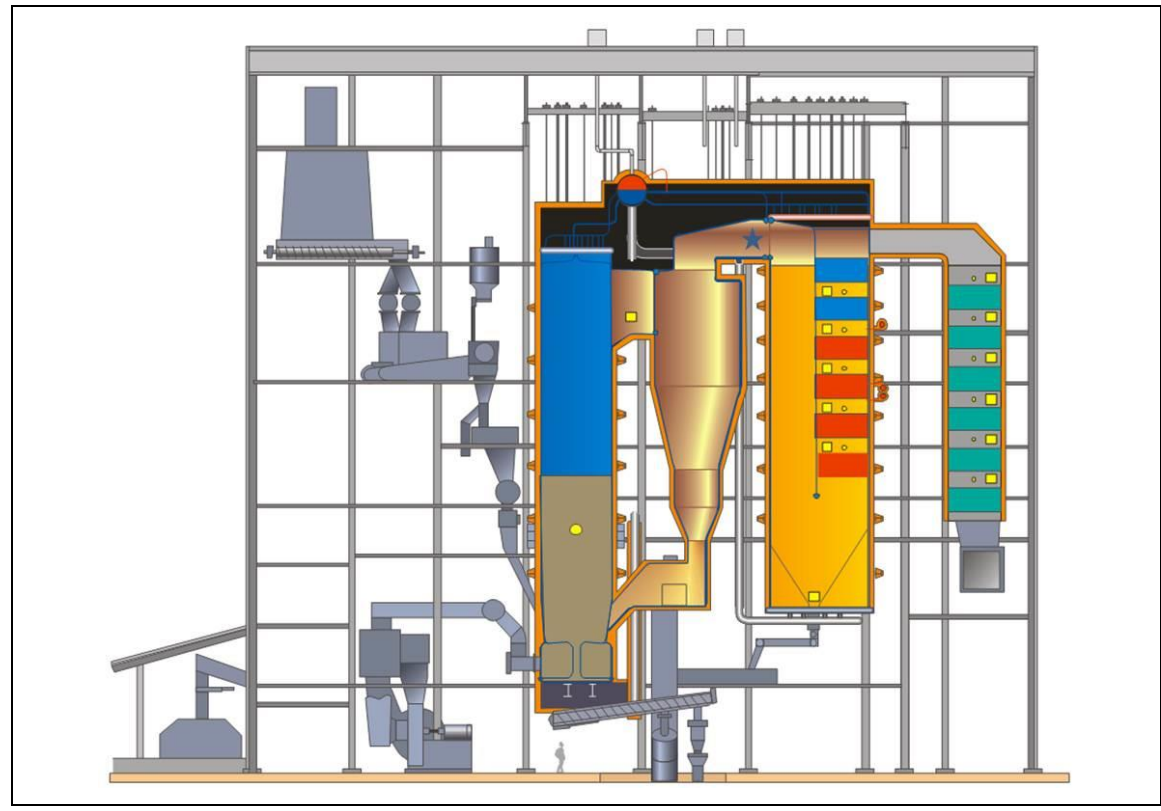


Figure 5-11. Side view of the Händelö/Norrköping P14 CFB boiler showing the placement of the probe with a blue star.

Figur 5-11. Sid-vy av Händelö/Norrköping P14 CFB pannan med markering för probplaceringen med en blå stjärna.

5.3.2 Operational conditions during probe exposure

The operational conditions for P14 during the test period ($5/11\ 2012\ -\ 17/12\ 2012$) have been relatively stable, see *Figure 5-13*.

5.4 Description of the un-cooled field tests

Un-cooled field tests have been performed in two different boilers; the waste fired boiler at Händelöverken (P14) and the biomass fired boiler at Idbäcken. In Händelö, standard pre-oxidized FeCrAl material, Kanthal® APMT, and a reference material, IN 625, has been tested as thermal tube shields. In

addition, standard pre-oxidized Kanthal $^{\circledR}$ APMT has been tested as tube shield for the tertiary superheaters located at the sand loop seal, the reference material was then 253Ma. The test tube shield was placed on top of the original tube shields. Standard pre-oxidized APMT was also tested as shield sheet at the vortex finder. The standard pre-oxidation was performed at 1050 $^{\circ}$ C for 8 hours to establish a protective Al_2O_3 scale on the surface prior to exposure.

Pre-oxidized Kanthal[®] APMT was also tested as tube shields for the tertiary superheaters in Idbäcken. It was not possible to get thermal tube shields of the material Kanthal[®] APMT that fitted in Idbäcken within the time frame of this project. In Idbäcken the FeCrAl material Kanthal[®] A1 is already used as thermal tube shields in the boiler. Therefore, we choose to include some thermal tube shields of Kanthal[®] A1 in Idbäcken located at different positions and temperatures. The aim of the un-cooled field tests is to reveal the corrosion behavior of FeCrAl materials at different locations and temperatures in boilers.

5.4.1 Description of the un-cooled field tests at Händelöverken

The locations of the thermal shield tubes exposed at Händelöverken in P14 is shown in *Figure 5-12*. The blue boxes mark the location where the thermal shield tubes made of the test material Kanthal APMT were exposed. Thus, the test material was exposed at a range of different temperatures (~ 380 – 840 °C) in the environment of a waste-fired boiler. The red boxes mark the location where the reference thermal shield tubes were exposed. The blue circle marks the position of the vortex finder on which a shielding sheet of the material Kanthal APMT is placed. The temperature in this region is usually around 850 °C. The green circle marks the position of the tertiary superheater tube on which a shielding tube of the material Kanthal APMT is placed on top of the original tube shield. The temperature in this region is usually around 870°C.

The thermal shield tubes were inserted into the boiler 2011-07-25. 2011-11-11 the thermal shield tube KT039 broke down. The thermal shield tube made of the test material that was closest in temperature was also taken out for comparison, namely KT041. Two references were inserted instead. 2012-03-13 the thermal shield tube at position KT039 were broken again. The rest of the thermal tube shields were taken out 2012-04-15. The position KT041 was then broken. Since the reference material does not seem to be a sustainable alternative at positions KT039 and KT041, thermal tube shields of the test material Kanthal[®] APMT were inserted at these positions 2012-04-29. The life length of this material was to be investigated at these positions and compared to the reference material.

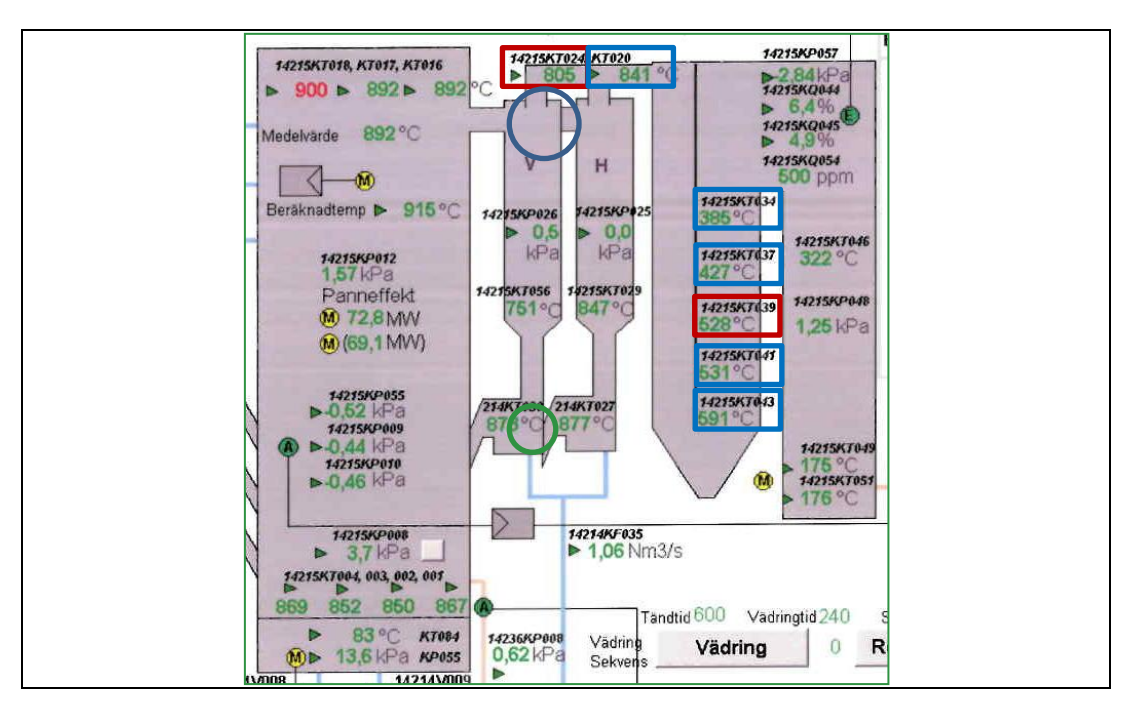


Figure 5-12. An illustration of the boiler P14 in Händelöverket with the positions of the thermal tube shields made of the test material marked with blue boxes and red boxes for the reference material.

Figur 5-12. En illustration av Händelöverket, P14, med positionerna av termoskyddsrören gjorda av testmaterialet markerade med blå rektanglar och referensmaterialet med röda rektanglar.

Operational conditions during the un-cooled field test exposures at Händelö.

The un-cooled material (thermal tube shields, shielding sheet at the vortex finder and tube shields at the tertiär superheaters) were exposed at Händelöverken, P14, from 2011-07-25 to 2012-04-15. The operational condition for P14 during the test period is illustrated in *Figure 5-13* showing the temperature given by the thermo couples. The initially low values given by the thermo couples at the positions KT020 and KT034 is due to a technical fault. Hence the initially values does not correspond to the heat in the boiler at these positions.

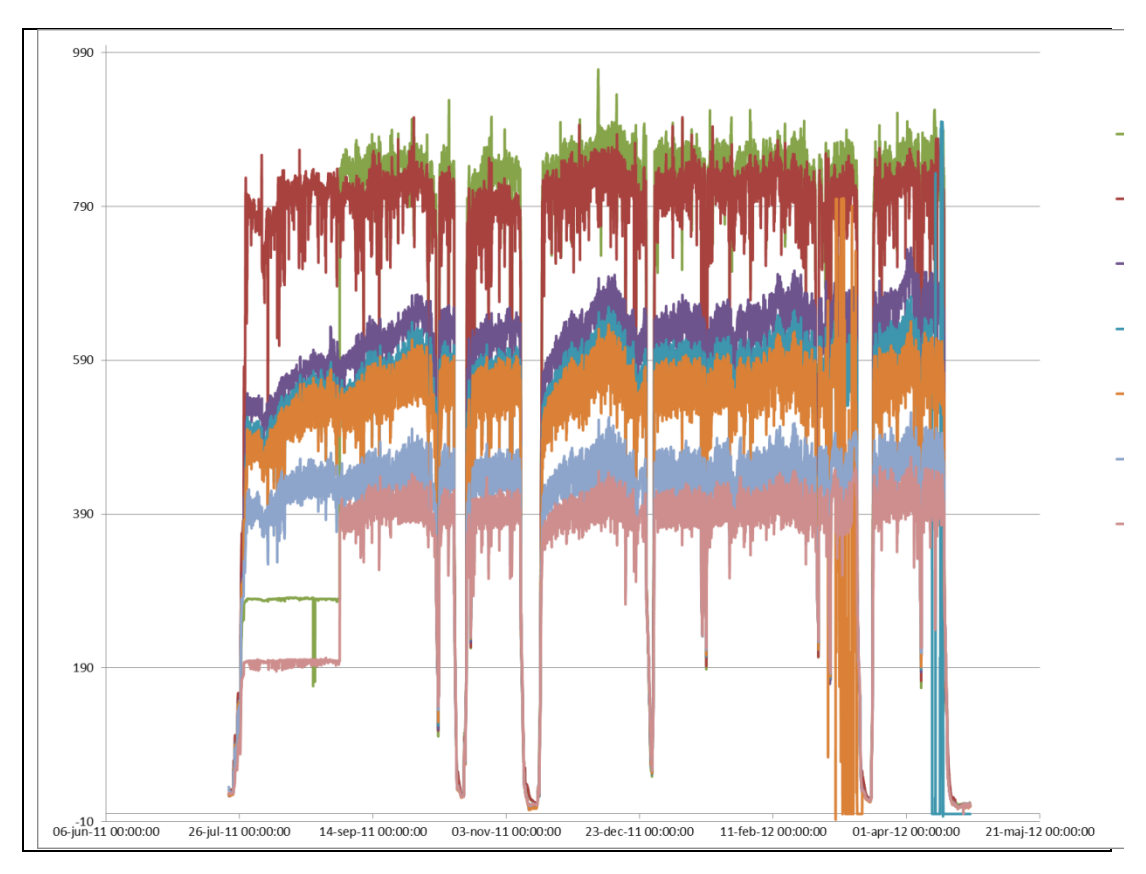


Figure 5-13. Temperatures given by the thermo couples in Händelöverken, P14, from 2011-07-25 to 2012-04-15.

Figur 5-13. Temperaturer från termogivarna i Händelöverken, P14, från 2011-07-25 till 2012-04-15.

5.4.2 Description of the un-cooled field tests at Idbäcken

The thermal shield tubes placed at Idbäcken that were followed by the project were made of the FeCrAl material Kanthal $^{\$}$ A1. The thermal shield tubes followed were placed at level 6 at the fireside, marked A, where the temperature is around 800 °C, underneath level 6 before the superheaters, marked B, where the temperature is around 650 °C and at level 3 by the hopper of the blow soothing where the temperature is around 380 °C (*Figure 5-14*).

A shielding tube of the material Kanthal[®] APMT was placed at the tertiary superheater tubes, marked sh 3 in *Figure 5-14*.

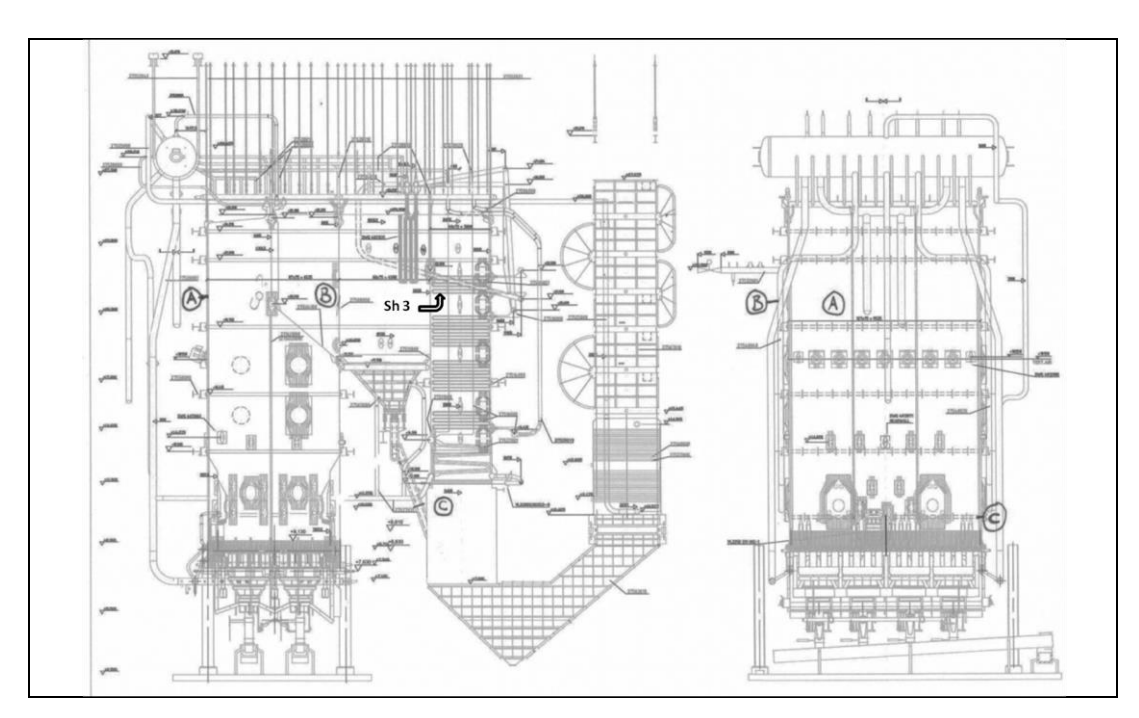


Figure 5-14. An illustration of the boiler at Idbäcken with the positions of the thermal tube shields (marked A, B and C) and the tertiary tube shield (marked sh 3).

Figur 5-14. En illustration av pannan i Idbäcken med positionerna av termoskyddsrören (markerade med A, B och C) och tubskyddet vid tertiäröverhettaren (markerad med sh 3).

Operational conditions during the un-cooled field test exposures at Idbäcken

The un-cooled material exposed at Idbäcken were thermal tube shields and tube shields at the tertiary superheaters. The thermal shield tube (A) was exposed from 2011-10-24 to 2012-03-08, (B) from 2011-12-12 to 2012-06-28 and (C) from 2011-12-12 to 2012-15. The tube shield at the tertiary superheaters was exposed from 2011-08-01 to 2012-06-28. The operational condition during the test period is illustrated in Figure 5-15 showing the temperature given by the thermo couples. There have been several short failures, two longer ones and a stop for summer revision. All the thermocouples (A, B and C) were taken out before the summer stop. Thermocouple C was put in again after the revision.

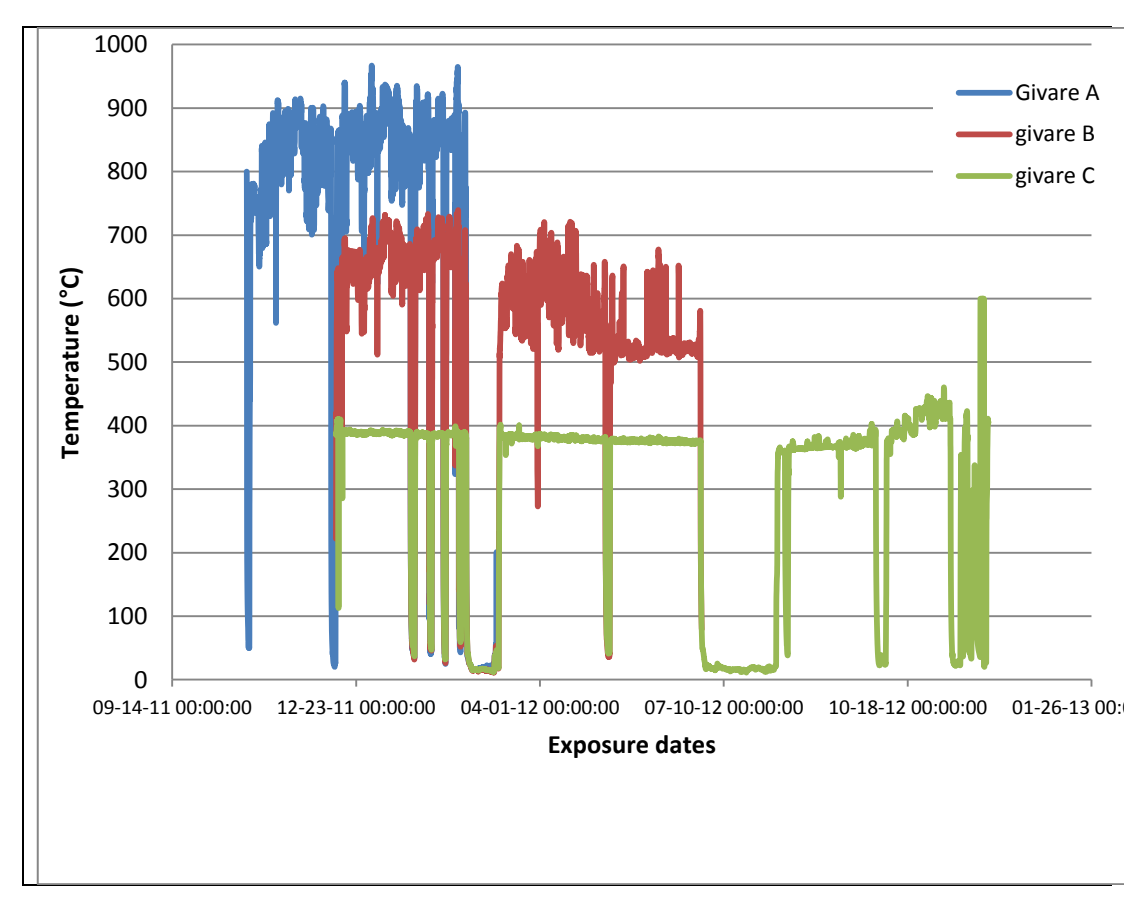


Figure 5-15. Temperatures given by the thermo couples in Idbäcken.

Figur 5-15. Temperaturer från termogivarna i Idbäcken.

6 Results

6.1 Laboratory studies

6.1.1 Sample preparation before exposure

Sample preparation is very important in order to obtain reproducible oxidation results. The growth kinetics and morphology are affected by e.g., contaminants and variations in surface roughness.

The material was cut into 15*15*2 mm and 10*8*2 mm coupons. The larger coupons were used in the furnace exposures and the smaller coupons for the TGA runs. The samples were first ground with silicon carbide paper and then polished down to 1 μ m with diamond suspension and ethanol based lubricant. The samples were then cleaned with detergent and water followed by three steps using ultrasonic agitation. All steps lasted for 10 minutes and were in the following order: water, acetone, and ethanol. Finally the coupons were dried in a cold air flow to avoid getting rests of solvent on the surface. After the grinding and polishing process the samples have a mirror like appearance shown in.

To investigate the effects of KCl(s) on the corrosion behavior, a saturated KCl solution was applied on the surface. The solution was sprayed on the sample surface and dried with a warm (\sim 35 °C) air flow. To avoid formation of large droplets during the process, alternating spraying and drying was performed to get an even distribution of the crystals. The samples were then allowed to stabilize in a desiccator for one hour before measuring the weight on a microbalance. The amount of approximately 0.1-0.2 mg/cm² KCl was applied and the salt crystals were in the order of 10-100 μ m.

6.1.2 The influence of O₂ and H₂O

Oxidation of Kanthal® APMT at 600 °C in the absence of KCl resulted in very low mass gains in both O_2 and O_2 + H_2O as shown by the *in-situ* TG measurements (*Figure 4-1*). The results indicate that mass gain is somewhat greater in the presence of water vapour. The relatively high noise in the TG measurement in O_2 + H_2O is due to the presence of the humidifier. After completion of the TG exposures (168 hours) the mass gains were 3.4 μ g/cm² in O_2 and 6.1 μ g/cm² in O_2 + O_2 as determined ex-situ.

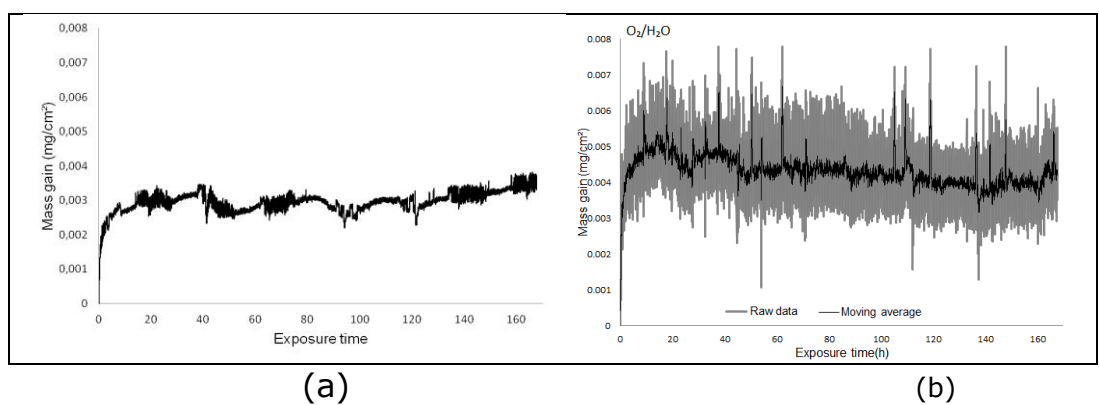


Figure 6-1. TGA curve (In-situ mass gain versus exposure time) for Kanthal® APMT exposed at 600 °C in (a) 5% O_2 or (b) 5% O_2 + 40% H_2O .

Figur 6-1. TGA kurva (in-situ massökning mot exponeringstiden) för Kanthal® APMT exponerad i 600 °C i (a) 5% O_2 eller (b) 5% O_2 + 40% H_2O .

After 24 hours exposure in dry O_2 and in $O_2 + H_2O$, rhombohedral M_2O_3 was identified, corresponding to Cr_2O_3 , $a\text{-}Fe_2O_3$ or a solid solution of the two (*Figure 6-2*). The analysis showed that the peak positions correspond to Cr_2O_3 and not $a\text{-}Fe_2O_3$. However, the peak positions are also compatible with Cr-rich (FeCr) $_2O_3$, especially in dry O_2 . There is no indication of aluminum oxides and little evidence for spinel oxides. After 168 hours, the rhombohedral M_2O_3 peaks have become more pronounced, the peak positions now corresponding to pure Cr_2O_3 (*Figure 6-3*). In addition, a weak peak appears corresponding to spinel oxide (M_3O_4) with a unit cell slightly smaller than that of magnetite. It is suggested that this phase corresponds to FeCr- or FeCrAl-spinel oxide. Similar to the 24hours exposure there is no indication of crystalline aluminas. In general the XRD intensities are higher in O_2 than in $O_2 + H_2O$ environment while the mass gains are consistently lower. This suggests that the oxide film formed in dry O_2 is more crystalline.

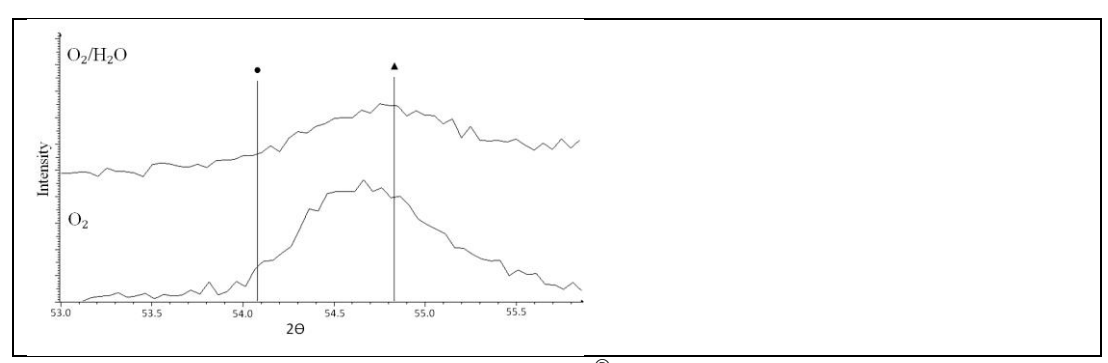


Figure 6-2. XRD diffractograms of Kanthal[®] APMT exposed at 600 °C in 5% O_2 and 5% O_2 + 40% H_2O for 24 hours. The symbols indicate the peak positions of Cr_2O_3 (\blacktriangle) and $Fe_2O_3(\bullet)$ (h,k,l).

Figur 6-2. Röntgen diffraktogram av Kanthal[®] APMT exponerad vid 600°C i 5% O_2 och 5% O_2 + 40% H_2O under 24 timmar. Symbolerna indikerar topp positionerna för Cr_2O_3 (\blacktriangle) and $Fe_2O_3(\bullet)$ (h,k,l).

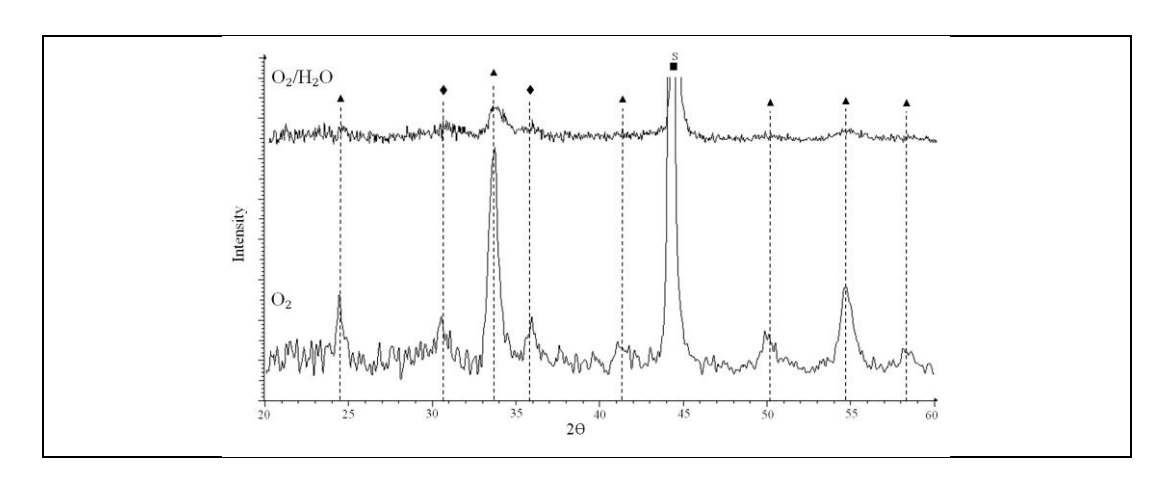


Figure 6-3. XRD diffractograms of Kanthal[®] APMT exposed at 600 °C in 5% O_2 and 5% O_2 + 40% H_2O for 168 hours. The symbols indicate: Cr_2O_3 (\blacktriangle), M_3O_4 (\blacklozenge) and substrate (\blacksquare).

Figur 6-3. Röntgen diffraktogram av Kanthal[®] APMT exponerad vid 600 °C i 5% O_2 och 5% O_2 + 40% H_2O under 168 timmar. Symbolerna indikerar: Cr_2O_3 (\blacktriangle), M_3O_4 (\blacklozenge) och substrat (\blacksquare).

Figure 6-4 shows depth profiles acquired by Auger electron spectroscopy after exposure to O_2 and $O_2 + H_2O$ at 600 °C for 24 and 168 hours. In all cases, the oxide film is dominated by alumina with significant amounts of iron and chromium also present. Chromia is enriched in a band in the middle of the oxide film and iron oxide is consistently found outside the chromia band. The AES profiling shows that the oxide formed in dry O_2 is somewhat thinner than in O₂ + H₂O. Thus the oxide is 19 and 24 nm in dry and wet environment, respectively, after 24 hours. After 168 hours the film thickness has grown to 29 and 36 nm, respectively. This is in agreement with the mass gains recorded (ex-situ) in the TG exposures, corresponding to an average thickness of the external oxide of 20 and 36 nm, respectively, after 168hours. The chromia band forms early during exposure and appears not to change with time. If the chromia band is considered to be a marker for the original sample surface, the additional oxide formed between 24 and 168 hours is mainly due to inward growth. The alumina content in the outer part of the scale increases with exposure time.

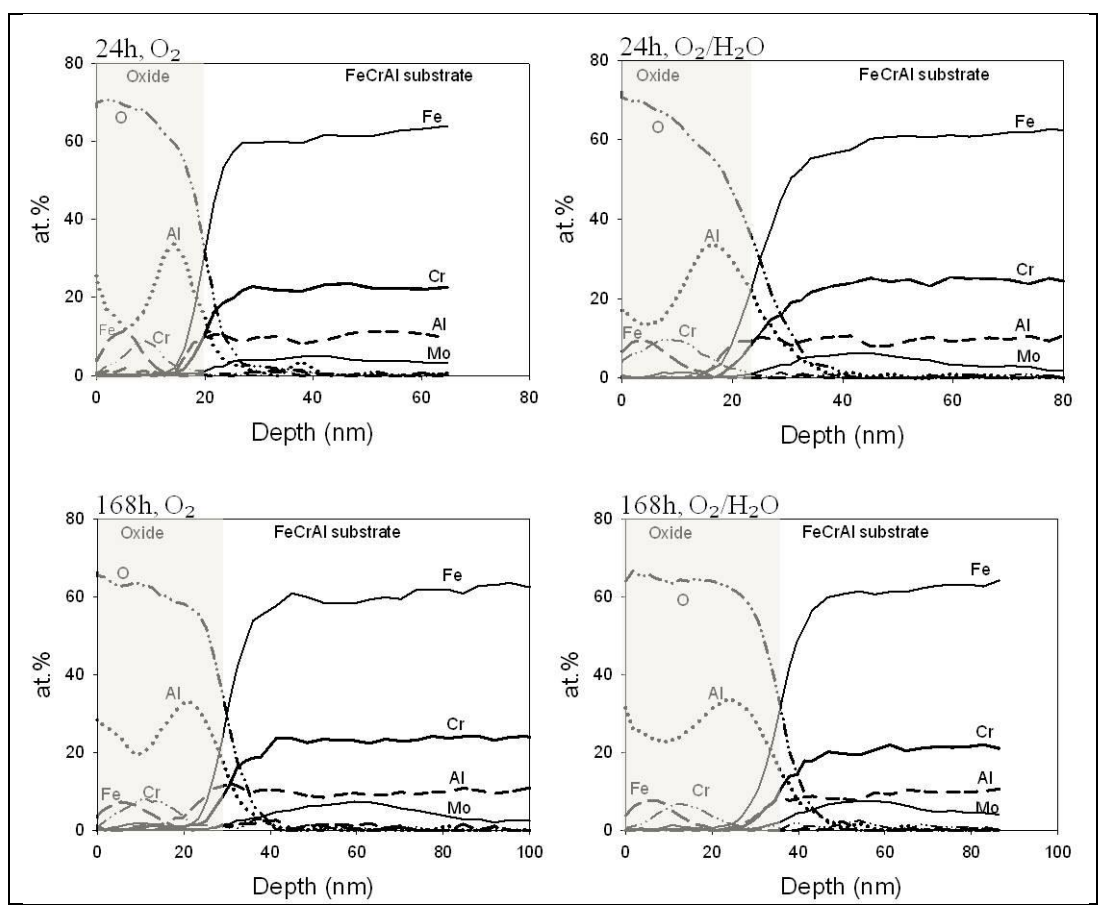


Figure 6-4. AES depth profiles of APMT samples exposed to dry and humid O_2 at 600 °C for 24h and 168h.

Figur 6-4. AES djup profiler från APMT prover exponerade i torr och fuktig O_2 vid 600 °C under 24 och 168 timmar.

The sample surface is smooth and rather featureless after 168 hours oxidation in both environments. High magnification imaging shows 100 nm size plate-like crystallites with sharp edges ($Figure\ 6-5$ A) in the dry case, while in the presence of water vapour the oxide surface is dominated by < 50 nm equiaxed grains ($Figure\ 6-5$ B). In the latter case the surface is corrugated.

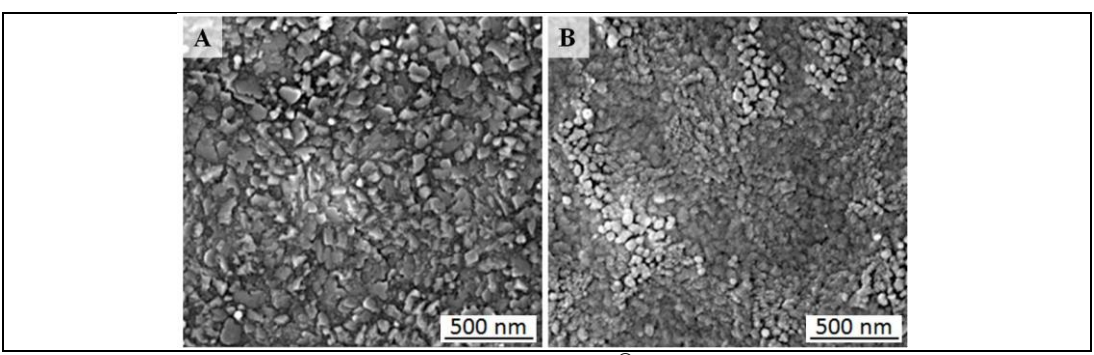


Figure 6-5. In-lens SE image of Kanthal[®] APMT exposed at 600 °C for 168 hours in 5% O_2 (A) and 5% O_2 + 40% H_2O (B).

Figur 6-5. In-lens SE bild av Kanthal[®] APMT exponerad vid 600 °C under 168 timmar i 5% O_2 (A) och 5% O_2 + 40% H_2O (B).

6.1.3 The influence of KCl

Adding KCl to the polished samples before exposing to $O_2 + 40 \% H_2O$ at 600 °C results in much larger mass gains. Sample mass increases rapidly up to 9 hours and then decreases with exposure time. As no spallation was observed, the mass loss implies volatilization from the samples.

Figure 6-6 shows XRD patterns acquired after 24 and 168 hours exposure. KCl is only detected after 1 hour (not shown). Potassium chromate (K_2CrO_4) is detected in all cases except after 168 hours. A rhombohedral corundum-type solid solution (FeCr)₂O₃ forms initially on the surface. The corresponding peak positions shift slightly toward lower angle with exposure time, indicating an increase of cell volume which is attributed to increasing iron content. After 168 hours the positions of the main peaks correspond to hematite (α -Fe₂O₃), representing the iron-rich end point of the solid solution (FeCr)₂O₃. In addition, weak peaks are detected after 24 and 168 hours indicating the presence of Cr_2O_3 .

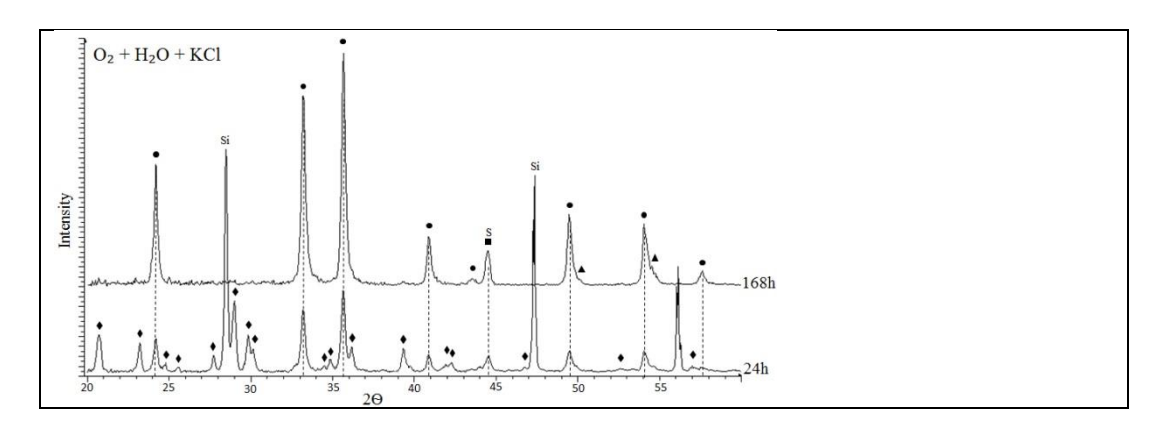


Figure 6-6. X-ray diffractograms of Kanthal[®] APMT exposed at 600 °C in 5% $O_2 + 40\%$ H_2O in the presence of KCl for 24 and 168h. The symbols indicate: K_2CrO_4 (\blacklozenge), $(Fe_2O_3$ (\blacklozenge), Cr_2O_3 (\blacktriangle), and substrate (\blacksquare).

Figur 6-6. Röntgen diffraktogram av Kanthal® APMT exponerad vid 600 °C i 5% O_2 och 5% $O_2 + 40\%$ H_2O i närvaro av KCl under 24 och 168 timmar. Symbolerna indikerar: K_2CrO_4 (\blacklozenge), $(Fe_2O_3$ (\blacklozenge), Cr_2O_3 (\blacktriangle), och substrat (\blacksquare).

Figure 6-7 shows the amount of water-soluble anions and cations extracted from the samples after exposure in the presence of KCl. While the amounts of K^+ and Cl^- both decrease with exposure time, chloride is lost more rapidly. Thus, after one hour, only 57 % of the added chloride was retrieved from the samples, while almost all of the potassium (96 %) was detected. After 9 hours only a small fraction of the added chloride remains on the surface. The analysis shows that substantial amounts of chromate $(CrO_4^{2^-})$ form on the steel surface. The stoichiometric relationship between K^+ , Cl^- and $CrO4^{2^-}$ on the sample surface after 1, 9 and 24 hours indicates that KCl reacts with chromia in the oxide scale according to:

$$1/2Cr_2O_3(s) + 2KCl(s) + 3/4O_2(g) + H_2O(g) \rightarrow K_2CrO_4(s) + 2HCl(g)$$
 (2)

The amount of $CrO4^{2^-}$ peaks at 9 hours. Since scale spallation was not observed, the decrease in $CrO4^{2^-}$ after > 9 hours implies that chromate has decomposed. The decomposition of K_2CrO_4 is attributed to the reduction of chromate by electrons originating from the oxidation of the alloy substrate in an electrochemical process:

$$K_2CrO_4(s) + H_2O(g) + 3e^- \rightarrow \frac{1}{2}Cr_2O_3(s) + 2KOH(I) + \frac{3}{2}O^{2^-}$$

$$Cr(alloy) \rightarrow Cr^{3+} + 3e^-$$

$$\Sigma K_2CrO_4(s) + H_2O(g) + Cr(alloy) \rightarrow Cr_2O_3(s) + 2KOH(I)$$
(3)

In accordance with this hypothesis, large amounts of potassium but very little chromate are present on the surface after long exposure times. The deviations from the stoichiometry of Reaction (2) found after 72 and 168

hours are attributed to the small amounts of K^+ , Cl^- and $CrO4^{2^-}$ that are left, resulting in relatively large measurement errors.

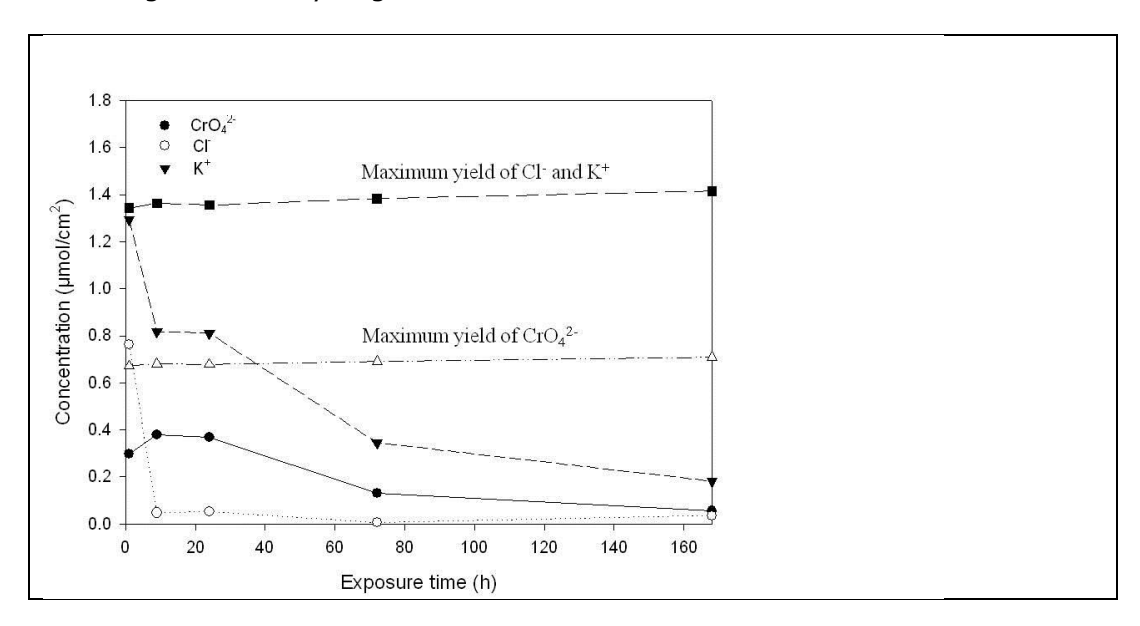


Figure 6-7. Amount of water soluble ionic substances on the sample surface versus exposure time for Kanthal[®] APMT exposed at 600 °C in 5% O_2 + 40% H_2O in the presence of KCl.

Figur 6-7. Mängden vattenlösliga joner på provytan versus exponeringstid för Kanthal[®] APMT exponerad vid 600°C i 5% O_2 och 5% O_2 + 40% H_2O i närvaro av KCl.

The SEM images of an unexposed sample in *Figure 6-8* show 10-100 μ m KCl crystallites on the surface (*Figure 6-8* A). In the backscattered image (*Figure 6-8* A) there are no signs of KCl between the salt particles. However, *Figure 6-8* B, which was acquired with an in-lens SE detector, clearly shows small bright KCl particles between the large crystals. The presence of small amounts of KCl between the large crystals was verified by EDX.

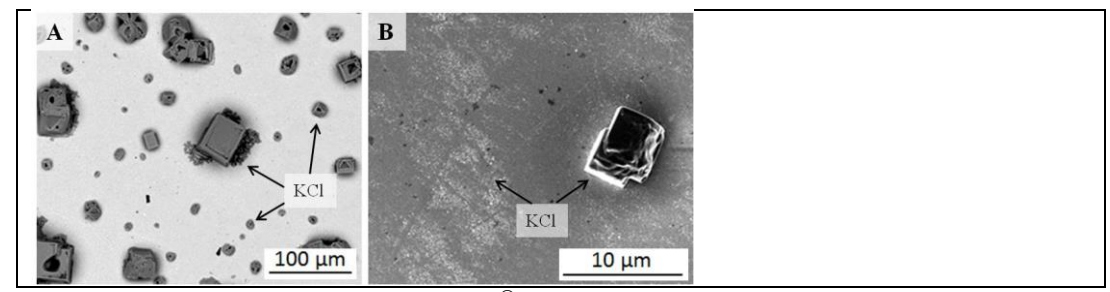


Figure 6-8. SEM images of Kanthal[®] APMT with added KCl before exposure, (A) is a BSE and (B) an SE image taken with an in-lens detector.

Figur 6-8. SEM bilder på Kanthal[®] APMT med pålagd KCl innan exponering, (A) är en BSE och (B) en SE bild tagen med en in-lens detektor.

The presence of KCl on the surface causes rapid corrosion and a surface morphology that change with exposure time. The morphology can be described in terms of a few features; i) partly reacted salt crystals with corrosion products, ii) corrosion product agglomerations formed at completely reacted salt crystals, iii) the oxide between i) and ii), and iii) chromate particles on top of the oxide and on the former salt crystals. These morphological features will be described more in detail below.

SEM analysis after one hour in 5 % O_2 + 40 % H_2O in the presence of KCl shows numerous small particles (1-3 µm) on the alloy surface (Figure 6-9 A and B). Figure 6-10 shows EDX maps of a partly reacted/evaporated KCl crystal surrounded by small particles that sit upon a relatively smooth oxide. The EDX maps show that the small particles mainly contain K, Cr and O, allowing us to conclude that they consist of K₂CrO₄ which was identified by XRD (compare Figure 6-6). The presence of CrO4²⁻ is also verified by the IC analysis (Figure 6-7). As expected, some areas contain large amounts of Cl and K, corresponding to KCl which was identified by XRD. The presence of substantial amounts of unreacted KCl at this stage is also in line with the IC analysis. In addition to the large, partly reacted KCl crystals, small amounts of CI and K are also present in the smooth oxide between the K₂CrO₄ particles, the EDX analysis indicating about 1-2 at % K and Cl. The surface coverage of K₂CrO₄ varies, the chromate particles sometimes forming a circle around the partly reacted KCl crystals (Figure 6-9 B). In some areas the K₂CrO₄ particles agglomerate to form a layer which tends to be cracked (Figure 6-9 A). The cracks are suggested to be due to the relatively large thermal expansion coefficient of K_2CrO_4 , causing tensile stresses during cooling. At this stage, some of the KCl crystals have become more or less overgrown by iron-rich oxide that forms shell-like aggregates, roughly replicating the shape of the original salt particles (Figure 6-9 B).

With time, the scale surface becomes increasingly iron-rich and after 24 hours of exposure most of it consists of iron oxide. The iron oxide appears bright in Figure 6-9 C and D and is considered to correspond to hematite which was identified by XRD (Figure 6-6). At this stage, KCl is absent from the surface, the former salt crystals being replaced by oxide accumulations that often form shell-like structures. Compared to 1 hour, the K2CrO4 particles (dark grey in Figure 6-9 C and D) have grown in size and tend to agglomerate in certain areas after 24 hours of exposure. K₂CrO₄ particles are found on top of some oxide agglomerations (former KCl crystals), in some cases covering them entirely (Figure 6-9 D). Some of the reacted salt crystals are surrounded by a circular halo of thin oxide. On top of the thin oxide there are morphological features with a distribution and shape similar to that of the K2CrO4 particles seen after 1hour (Figure 6-11 A, B). SEM/EDX showed traces of chromate in these features and they are considered to correspond to partly decomposed K₂CrO₄. EDX point analyses show no indication of Cl in the former salt particles and overgrown areas. Small amounts of chlorine (1-2 %) and slightly higher amounts of potassium were detected in areas not yet overgrown by iron oxide. In accordance with the EDX analysis, the IC results show that only 4 % of the added chloride remains on the surface after 24 hours of exposure. After 168 hours the entire surface is overgrown by iron-rich oxide, ridges of iron-rich oxide surrounding the former salt crystals (Figure 6-9 E). EDX point analyses show that the ridges contain slightly more potassium (~2 %) and chromium (~4 %) compared to the base oxide. The surface of the oxide

ridges contains small rounded "pockmark" features, (Figure 6-12) which correspond to the partly decomposed K_2CrO_4 particles observed after 24hours (compare Figure 6-11 B). The oxide formed after 72 hours (not shown) is similar to that observed after 168 hours except that the amount of K_2CrO_4 is greater after 72 hours.

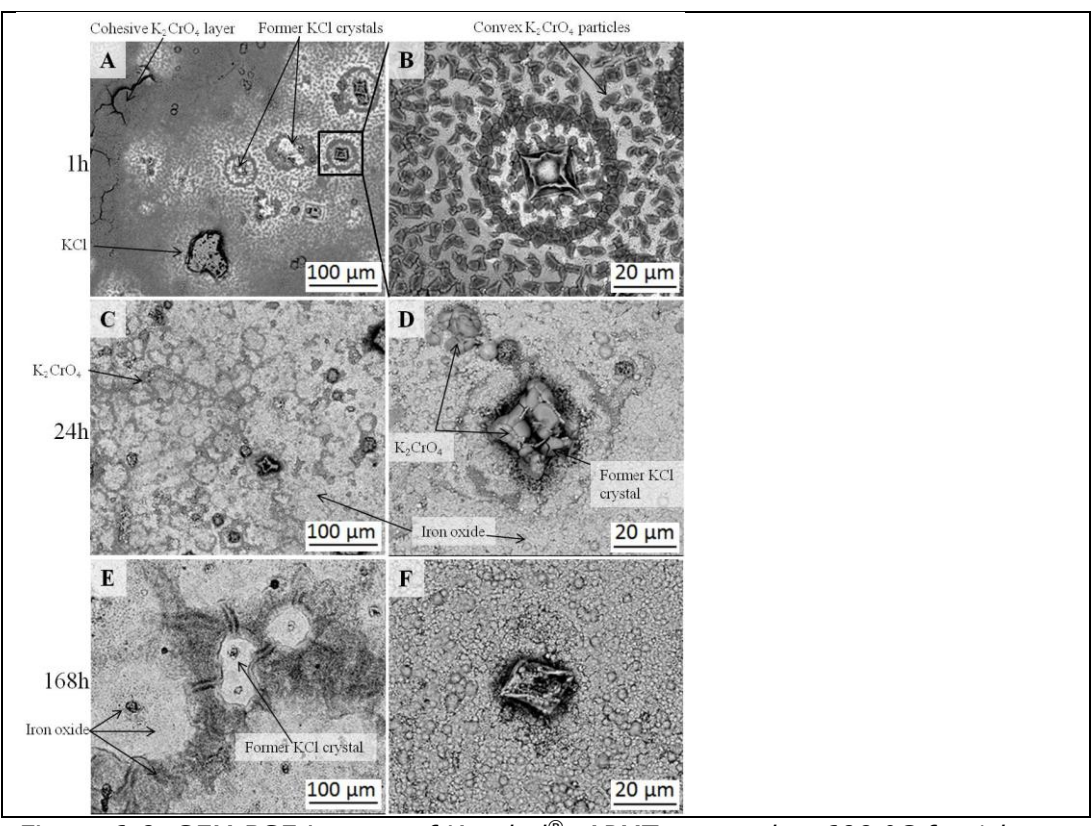


Figure 6-9. SEM BSE images of Kanthal® APMT exposed at 600 °C for 1 hour (A, B), 24 hours (C, D) and 168 hours (E, F) in 5% O_2 + 40% H_2O with KCl.

Figur 6-9. SEM BSE bilder på Kanthal[®] APMT exponerad vid 600 °C under 1 timma (A, B), 24 timmar (C, D) och 168 timmar (E, F) i 5% O_2 + 40% H_2O med KCl.

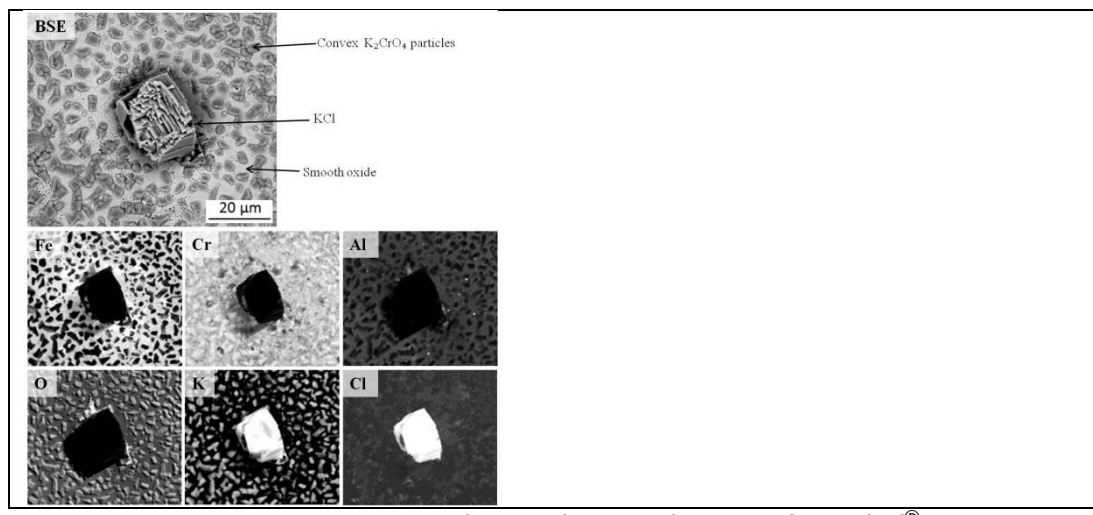


Figure 6-10. SEM BSE image and EDX elemental maps of Kanthal[®] APMT exposed at 600 °C for 1 hour in 5% O_2 + 40% H_2O with KCl.

Figur 6-10. SEM BSE bild med EDX element kartor på Kanthal[®] APMT exponerad vid 600 °C under 1 timma i 5% O_2 + 40% H_2O med KCl.

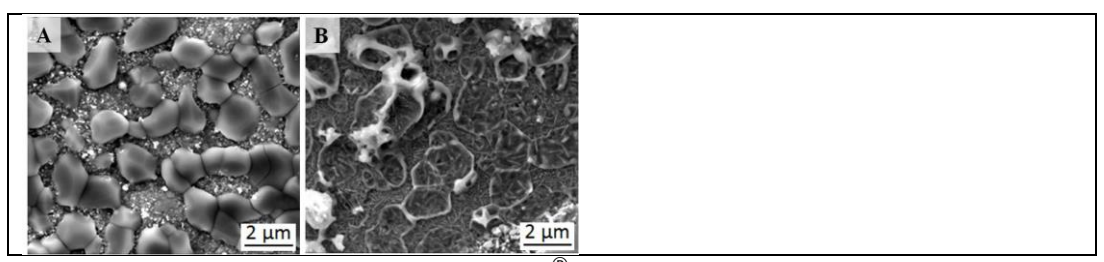


Figure 6-11. SEM SE images of Kanthal[®] APMT exposed at 600 °C for 1 hour (A) and 24 hours (B) in 5% O_2 + 40% H_2O with KCl. Image (A) shows K_2CrO_4 particles on the surface, and image (B) shows the remains of the K_2CrO_4 particles after 24 hours of exposure.

Figur 6-11. SEM SE bilder på Kanthal® APMT exponerad vid 600 °C under 1 timma (A) och 24 timmar (B) i 5% O_2 + 40% H_2O med KCl.

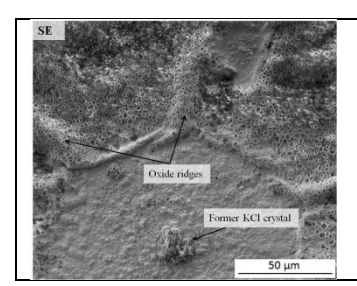


Figure 6-12. SEM SE image of Kanthal® APMT exposed at 600 °C for 168 hours in 5% O_2 + 40% H_2O with KCl.

Figur 6-12. SEM SE bild på Kanthal® APMT exponerad vid 600 °C under 168 timmar i 5% O_2 + 40% H_2O med KCl.

6.1.4 Pre-oxidation

The sample pre-oxidized at 700 °C in 20% O_2 + 80% N_2 for 24 hours in KME 414 has been investigated further in this project. Pre-oxidation in the tube furnace for 24 hours resulted in an average mass gain of 12 μ g/cm². The mass gain is in accordance with the Auger analysis, showing that the oxide film is about 70 nm thick, alumina-rich and contains traces of chromium and iron, as shown in *Figure 6-18* A. The oxide is similar to that formed in the exposures at 600 °C except that it is thicker and more alumina rich. The oxide morphology is smooth with grain size \sim 100 nm and similar to that formed after 168 hours at 600 °C in dry O_2 , see above. Similar to the 168 hours exposure at 600 °C, XRD gave evidence for Cr_2O_3 while no crystalline alumina phases could be positively identified (see *Figure 6-14*).

Additional pre-oxidations were conducted within this project. These preoxidations were performed in 5% O_2 + 95% N_2 for 1 and 24 hours at 900 and 1100 °C, respectively. All pre-oxidations resulted in an α-Al₂O₃ scale according to XRD. Cross sectioned samples revealed the oxide thicknesses (Figure 6-13); about 0.1 and 0.3 µm on the material exposed at 900 °C for 1 and 24 hours and 0.4 and 1.5 μm on the material exposed at 1100 °C for 1 and 24 hours, respectively. The images also reveal a two layered oxide with a darker outer layer and a brighter inner layer. The thickness of the layers differs depending on the pre-oxidation conditions. After 1 hour exposure at 900 °C the inner layer does not seem to be fully continuous and the thickness appears to be about 1/8 of the outer layer. After 24 hours pre-oxidation at 900 °C the outer and inner layer has about the same thickness. The same is valid after 1 hour pre oxidation at 1100 °C. After 24 hours pre-oxidation at 1100 °C the thickness of the inner layer is more than 10 times that of the outer layer. The following exposures with applied KCl on the material surface will reveal which oxide withstands the corrosion attack the best.

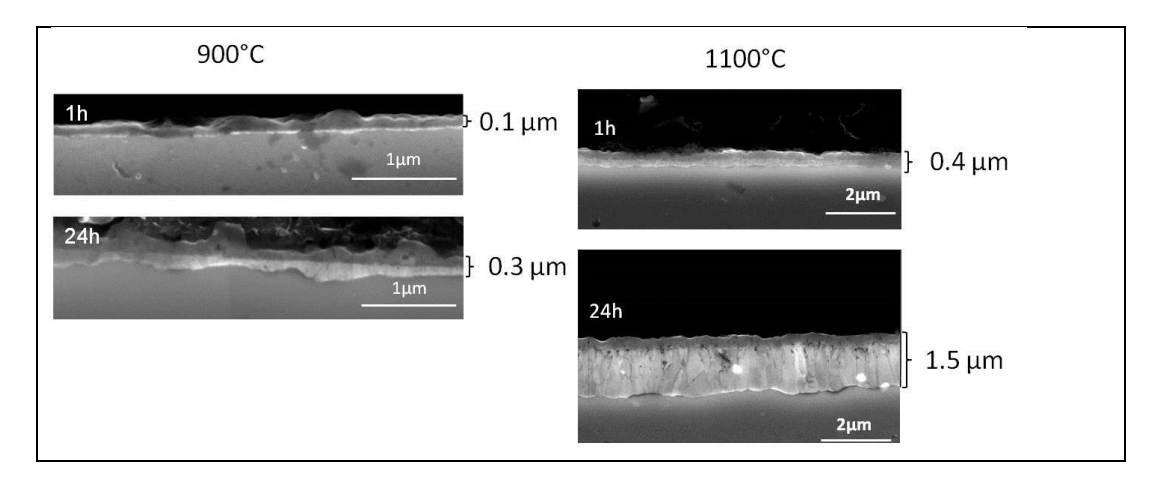


Figure 6-13. Cross-sectioned SEM images of the pre-oxidized APMT samples.

Figur 6-13. SEM bilder av tvärsnittet på föroxiderade APMT prover.

6.1.5 The influence of KCl and pre-oxidation

In KME 414 a sample were pre-oxidized at 700 °C for 24 hours and thereafter oxidized at 600 °C with 0.1 mg/cm 2 KCl in the presence of H $_2$ O. Further examination of that sample has been conducted in this project and the results are presented below.

Exposing the pre-oxidized samples at 600 °C in the presence of KCl initially resulted in a mass loss. After 24hours no further change in mass was registered. The measured mass loss closely corresponds to the amount of salt added before exposure (0.10 mg/cm^2) and is attributed to the volatilization of KCl.

X-ray Diffraction of the sample exposed for one hour, show no additional diffraction peaks except for KCl (not shown). KCl was not detected after longer exposure times. The XRD analysis performed after 24 hours shows diffraction lines that are tentatively attributed to α -alumina (*Figure 6-14*). After 24 hours and especially after 168 hours, a new set of diffraction lines appears that is tentatively attributed to KAlSiO₄ (Kaliophilite). The Cr₂O₃ observed directly after pre-oxidation and after 1h exposure with KCl, is absent after 24 and 168 hours.

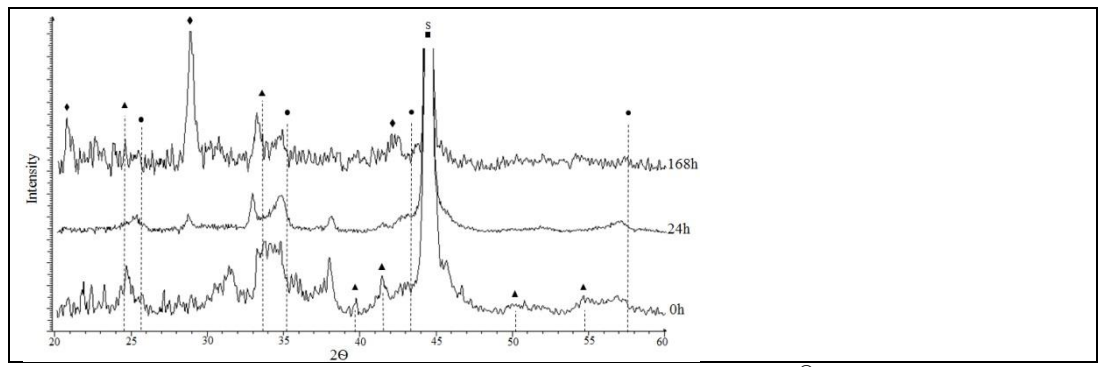


Figure 6-14. X-ray diffractograms of pre-oxidised Kanthal® APMT at 700 °C for 24h and subsequently exposed at 600 °C in 5% O_2 + 40% H_2O in the presence of KCl for 24 and 168h. The symbols indicate: $Cr_2O_3(\blacktriangle)$, α -Al $_2O_3(\bullet)$, KAlSiO $_4(\bullet)$ and substrate(\blacksquare).

Figur 6-14. Röntgen diffraktogram av föroxiderad Kanthal® APMT vid 700 °C i 24 timmar och därefter exponerad vid 600 °C i 5% O_2 + 40% H_2O i närvaro av KCl i 24 och 168 timmar. Symbolerna indikerar: $Cr_2O_3(\blacktriangle)$, α -Al $_2O_3(\bullet)$, KAlSiO $_4(\blacklozenge)$ och substrat(\blacksquare).

Figure 6-15 show the amount of water-soluble anions and cations found on the pre-oxidized samples after exposure with KCl. After one hour 78 % of the added Cl was found and 89 % of K, while no CrO4^{2^-} was detected. The mismatch between the Cl⁻ and K⁺ concentrations and the absence of CrO4^{2^-} implies that K must be present in another form than KCl or K_2CrO_4 . The potassium and chloride concentrations decrease with time in a similar manner and the concentrations are constant after 24 hours. Only traces of chromate $(\text{CrO}_4^{2^-})$ were recorded (corresponding to < 0.5 % of the added K).

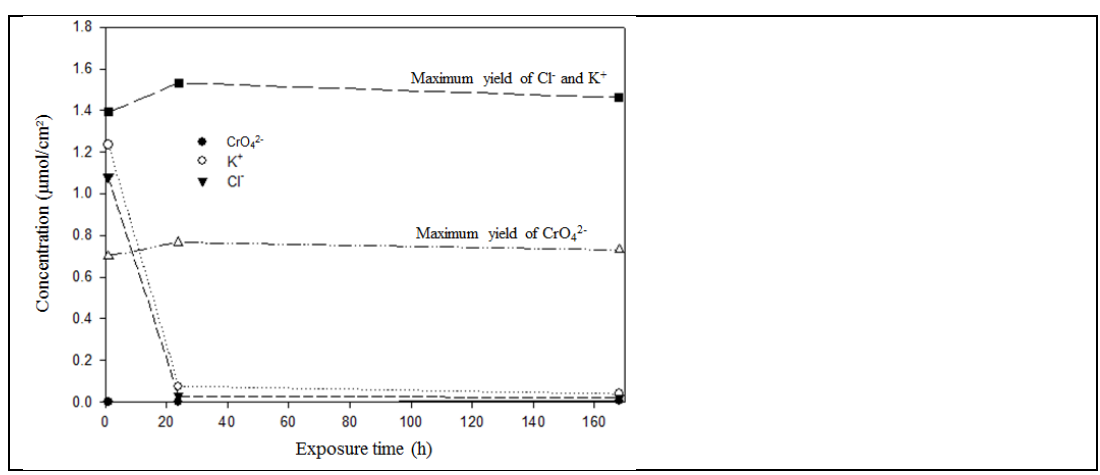


Figure 6-15. Amount of water soluble ionic substances on the sample surface versus exposure time for pre-oxidized Kanthal[®] APMT with added KCl exposed at 600 °C in 5% O_2 + 40% H_2O for 1, 24 and 168 hours.

Figur 6-15. Mängd vattenlösliga joner på provytan mot exponeringstid för föroxiderad Kanthal[®] APMT med pålagd KCl exponerad vid 600°C i 5% O_2 + 40% H_2O under 1, 24 och 168 timmar.

1 hour of exposure in the presence of KCl produced little change in surface morphology (compare Figs. Figure 6-8 A and Figure 6-16 A). This is in marked contrast to the material not subjected to pre-oxidation (compare Figure 6-9 A) However, a few K_2CrO_4 particles are detected on the surface by EDX (Figure 6-16 B). In line with the slow corrosion attack, the KCl crystals are less reacted compared to the exposure without pre-oxidation (see Figure 6-9 and Figure 6-10).

There is no indication of KCl on the surface after 24 hours (Figure 6-16 C and D). Also, the KCl crystals have left no morphological traces on the surface. Compared to the situation after 1hour, the number of K2CrO4 particles has increased, appearing as dark spots in Figure 6-16 c. In comparison to the corresponding exposure without pre-oxidation, the amount of K₂CrO₄ is much smaller, in accordance with the IC analysis. Based on the number density and size of the K₂CrO₄ particles, the amount of chromate on the surface was estimated to be about 10*10⁻⁹molescm⁻². As noted above, the oxide scale formed during pre-oxidation contains a chromium-rich band. Integrating the Cr signal in the Auger profile in Figure 6-18 A indicates that the amount of Cr in the scale corresponds to a 1-1.5 nm layer of pure Cr₂O₃, corresponding to 8-12*10⁻⁹ mol/cm² of Cr. The agreement regarding the amount of Cr implies that the chromium in the pre-oxidation scale is the only source of chromate on the surface. This conclusion is supported by the AES profiling (see below). Typically, the K₂CrO₄ particles are considerably larger than without preoxidation. However, small K₂CrO₄ particles are also observed. At this stage porous oxide agglomerates of different size appear on the surface that are enriched in K and Si and also contain Al, together with some Cr and Fe (see Figure 6-16 D). In addition to the larger porous agglomerates seen in Figure 6-16 D smaller ones (0.5-1 µm) are scattered over the surface (not shown). Iron-rich oxide has started to grow in the vicinity of some of the K2CrO4 particles (Figure 6-17). Otherwise there are no signs of corrosion.

The surface morphology after 168 hours is similar to that described after 24hours, showing little evidence for corrosion attack. At this stage the K_2CrO_4 particles are replaced by porous agglomerates with similar size and distribution. It is proposed that these agglomerates are the remnants of decomposed K_2CrO_4 particles. According to EDX point analyses, the porous agglomerates (see *Figure 6-16* F) are enriched in Si, K and O and also contain considerable amounts of Al. It is proposed that the porous agglomerates correspond to KAlSiO₄ detected by XRD. This suggests that KCl has reacted with alumina and with the silica which was detected at the scale/gas interface after pre-oxidation, according to Reaction (4):

$$H_2O(g) + 2SiO_2(s) + 2KCl(s) + Al_2O_3(s) \rightarrow 2HCl(g) + 2KAlSiO_4(s)$$
 (4)

 Δ Go (873K) = 53.756 kJ/mol which corresponds to Peq HCl(g) = 0.015atm (in 40% H₂O)¹¹.

Because the oxide formed in the pre-oxidation is relatively inert and slow-growing it is not considered likely that the decomposition of K_2CrO_4 on the pre-oxidised samples is mainly due to Reaction (3). Instead the following reaction is considered:

$$2SiO_2(s) + K_2CrO_4(s) + Al_2O_3(s) \rightarrow 1/2Cr_2O_3(s) + 2KAlSiO_4(s) + 3/4O_2(g)$$
 (5)

 Δ Go (873K) = -36.719 kJ/mol ¹¹.

According to Reaction (5), the large porous agglomerates are expected to contain chromia. It was not possible to decide whether this is the case by SEM/EDX because of the chromium signal from the underlying oxide and from the substrate. Alternatively, the following reaction would leave no chromia in the product:

$$2H_2O(g) + 2K_2CrO_4(s) + 2Al_2O_3(s) + 4SiO_2(s) \rightarrow 2H_2CrO_4(g) + 4KAlSiO_4(s)$$
 (6)

 Δ Go (873K) = 88.760 kJ/mol which corresponds to Peq H₂CrO₄ (g) = 884.10-6atm (in 40% H₂O)¹¹.

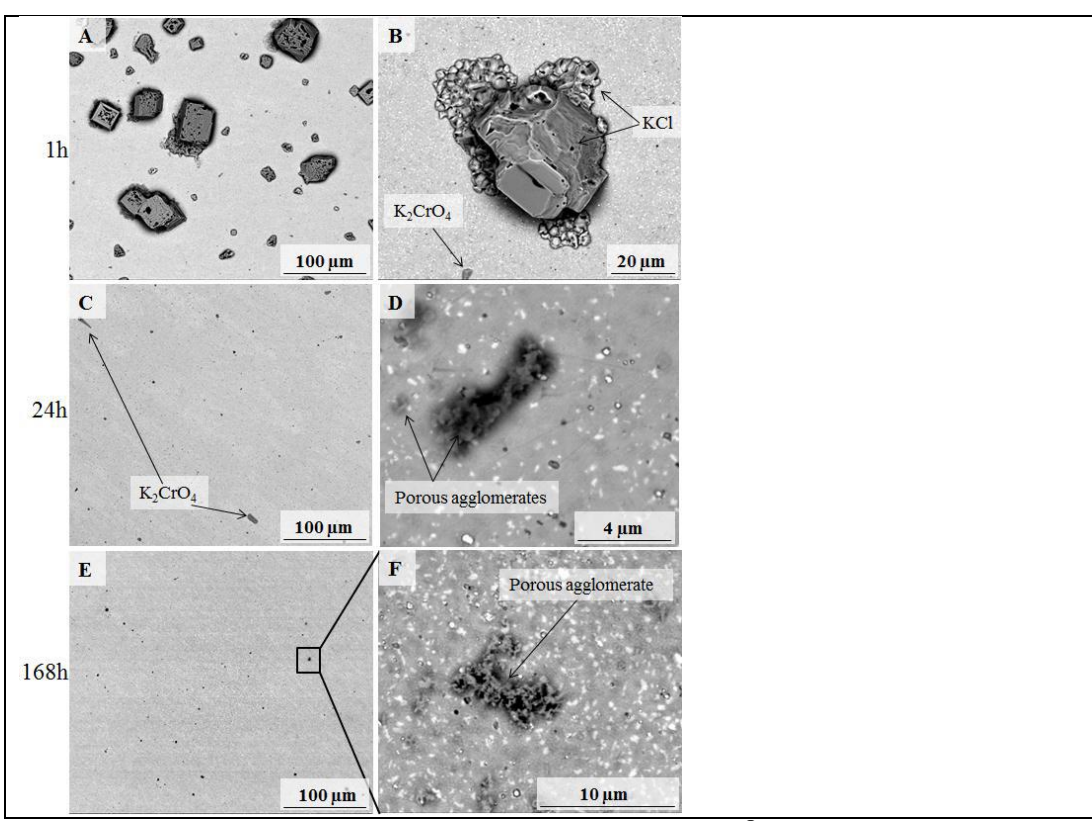


Figure 6-16. SEM BSE images of pre-oxidized Kanthal® APMT exposed at 600 °C with KCl for 1 hour (a, b), 24 hours (c, d) and 168 hours (e, f) in 5% O_2 + 40% H_2O .

Figur 6-16. SEM BSE bilder på föroxiderad Kanthal® APMT exponerad vid 600 °C med KCl under 1 timma (a, b), 24 timmar (c, d) och 168 timmar (e, f) i 5% $O_2 + 40\% H_2O$.

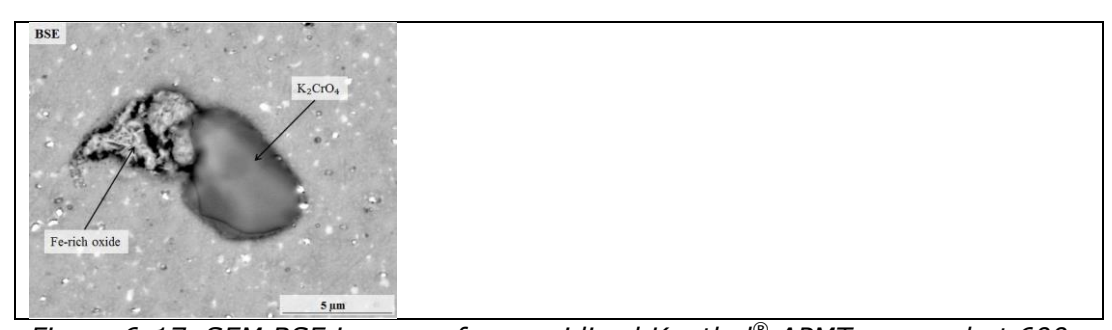


Figure 6-17. SEM BSE images of pre-oxidized Kanthal $^{\rm @}$ APMT exposed at 600 $^{\rm o}$ C with KCl for 24 h.

Figur 6-17. SEM BSE bilder på föroxiderad Kanthal® APMT exponerad vid 600 °C med KCl under 24 timmar.

After 1hour exposure at 600° C in the presence of KCl, AES depth profiling shows little change compared to the pre-oxidized sample, except that K is present at the surface (*Figure 6-18* B). The alumina scale grows somewhat

thicker up to 24 hours (to about 80 nm), no further thickness increase being detected after 168 hours. The depth profiles acquired after 24 and 168 hours of exposure with KCl (*Figure 6-18* C and D) indicate that potassium is mainly situated in the outer 20 nm of the oxide. However, there are also traces of potassium deeper into the scale. It may be noted that the chromia-enriched band observed in *Figure 6-18* A and B has disappeared after 24 and 168 hours. Considering the simultaneous occurrence of K_2CrO_4 on the scale surface (see *Figure 6-16* B and C) it is proposed that most of the chromia in the scale has reacted with KCl according to reaction (2). Iron in the scale behaves similar to chromium and tends to disappear with time. However, we do not observe iron-containing corrosion products on the surface in sufficient quantity to account for the missing iron oxide within the scale. Mo is present in the alloy substrate and its distribution does not change upon exposure. Chlorine is not shown in the depth profiles because of the overlap of Auger electron energies with Mo in the alloy.

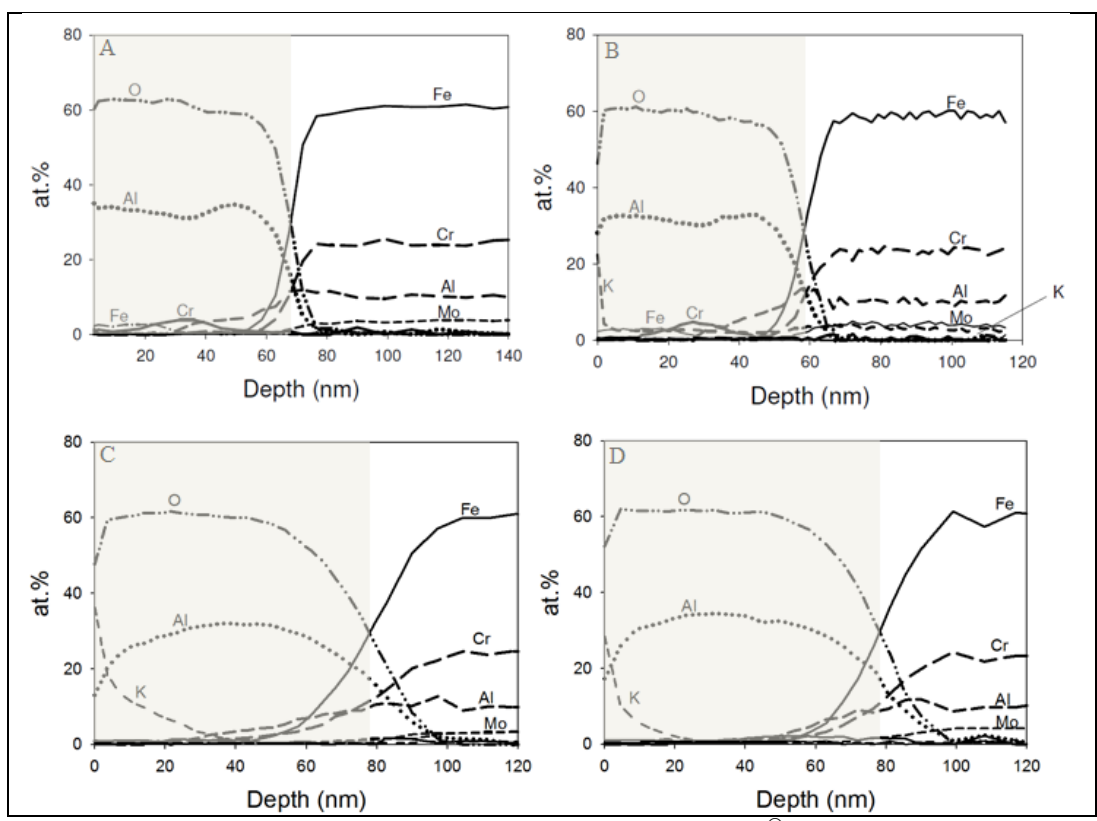


Figure 6-18. AES depth profiles of pre-oxidized Kanthal® APMT at 700 °C for 24 hours (A), pre-oxidized Kanthal® APMT with added KCl and exposed additionally (B) 1, (C) 24 and (D) 168 hours at 600 °C.

Figur 6-18. AES djup profiler av föroxiderad Kanthal[®] APMT i 700 °C under 24 hours (A), föroxiderad Kanthal[®] APMT med pålagd KCl och exponerad ytterligare (B) 1, (C) 24 och (D) 168 timmar i 600 °C.

Because of the difficulty of analyzing Cl in the presence of Mo, a complementary analysis by SIMS was carried out. It may be noted that while

the SIMS analysis has very high sensitivity (better than Auger) it is not quantitative. However, SIMS is still useful for comparing the concentration and distribution of a certain element in the scale, depending on *e.g.*, as a function of exposure time.

Figure 6-19 shows depth profiles for positive and negative ions from a preoxidized sample and from samples oxidized 24 and 168 hours in the presence of KCl. The AlO²⁻ ion signal in Figure 6-19 is used to indicate the interface between aluminium oxide and the metal substrate. The SIMS depth profiles for pre-oxidised Kanthal[®] APMT (Figure 6-19a) is in general agreement with the AES depth profile of the same material (Figure 6-18A), showing an Al-rich oxide containing both chromium and iron. The analysis further indicates that silicon is enriched at the scale surface. The traces of K and Cl found at the surface after pre-oxidation are due to contamination. After 24 and 168 hours oxidation of the pre-oxidized material in the presence of KCl, the main change indicated by SIMS is an enrichment of K in the outer part of the oxide, in agreement with the AES results. There is a decrease in the chromium and iron SIMS signals which is also in agreement with the AES analysis. Importantly, there is no indication that the chlorine penetrates the oxide and accumulates at the oxide/metal interface.

SIMS depth profiling was not performed on the sample oxidized with KCl for 1 hour. However, imaging with SIMS 12 showed a dendritic network of potassium and chlorine which corresponds to the distribution of the added salt, being similar to that observed by SEM on the unexposed material with added KCl (*Figure 6-8* B).

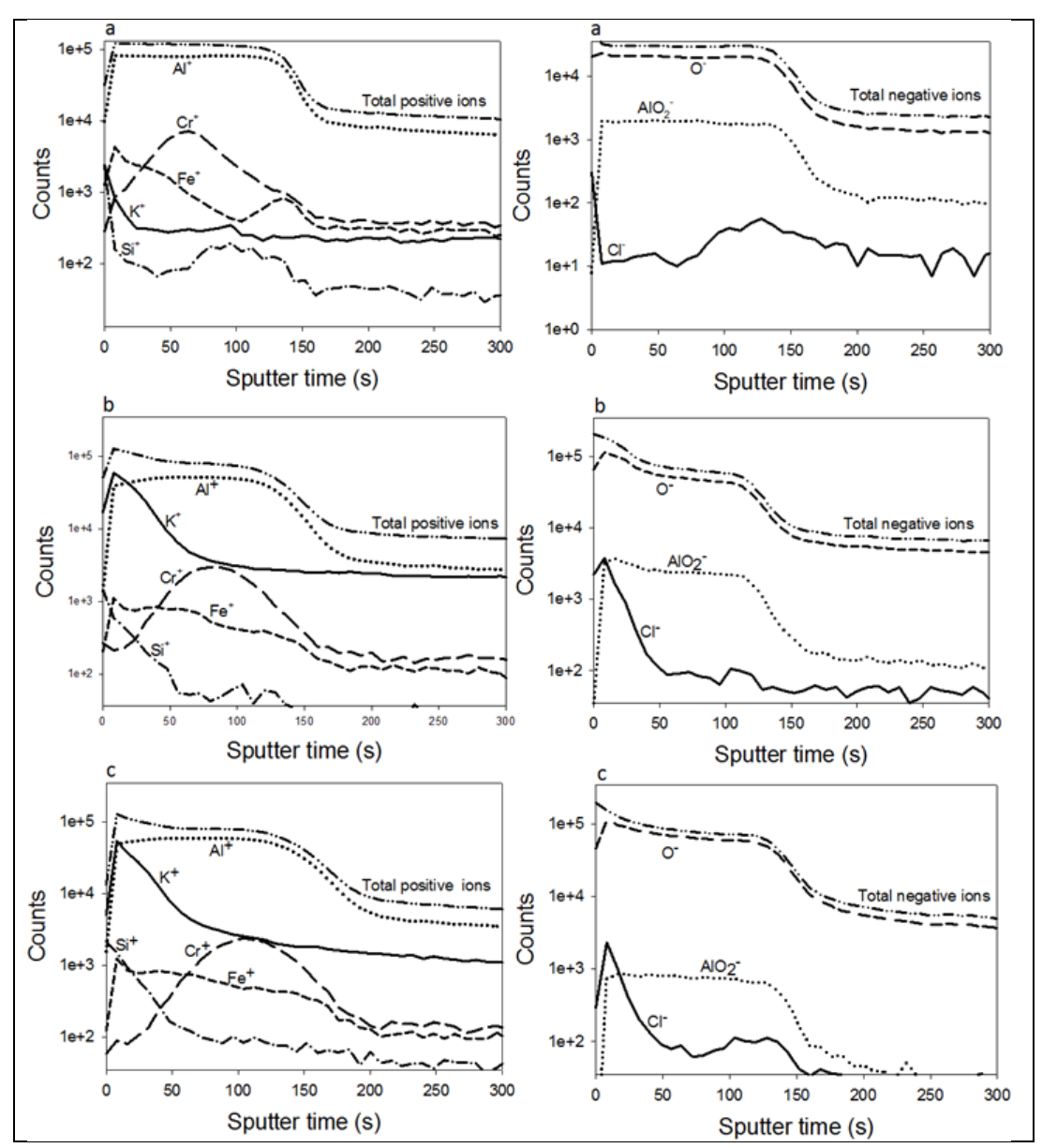


Figure 6-19. ToF-SIMS depth profiles in the oxide scales formed on Kanthal® APMT samples after pre-oxidation for 24 h at 700 °C in 20% O_2 (a), pre-oxidized Kanthal® APMT with added KCl and exposed additionally 24 and 168 hours at 600 °C in 5% O_2 + 40% H_2O (b) and (c).

Figur 6-19. ToF-SIMS djup profiler av oxidskiktet bildad på Kanthal[®] APMT prover efter för-oxidering i 24 tim i 700°C i 20% O_2 (a), föroxiderad Kanthal[®] APMT med pålagd KCl och exponerad i ytterligare 24 och 168 timmar vid 600°C i 5% O_2 + 40% H_2O (b) och (c).

After the pre-oxidations conducted in this project 0.2 mg/cm 2 KCl (compared to 0.1 mg/cm 2 KCl in KME 414) was applied on the material surface and then exposed at 600 °C for 24 hours in 5% O $_2$ + 40% H $_2$ O + 55% N $_2$. The procedure was repeated until corrosion of the surface was visible. After the

first exposure with KCl the material pre-oxidized for 1 hour at 900 °C were corroded all over the surface, the material pre-oxidized for 1 hour at 1100 °C where corroded on about $\frac{3}{4}$ parts of the surface leaving about $\frac{1}{4}$ of the surface with an intact alumina scale (*Figure 6-20*). The other pre-treated FeCrAl samples protected the material resulting in no visible corrosion with the exception close to the drilled hole.

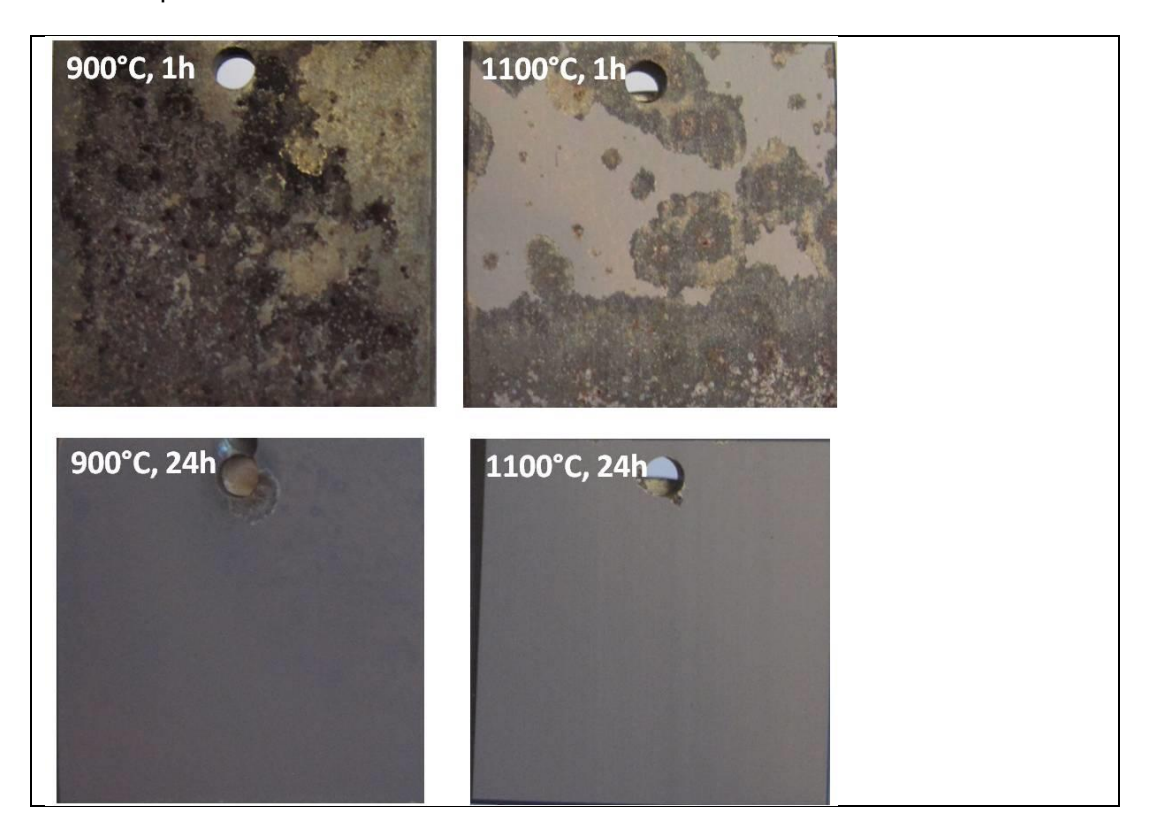


Figure 6-20. SEM images of the surface of APMT pre-oxidized at different times and temperatures and thereafter oxidized in the presence of H_2O and KCl for 24 hours at 600 °C.

Figur 6-20. SEM bilder på ytan av APMT prover föroxiderade vid olika temperaturer och tider och därefter oxiderade I närvaro av H_2O och KCl under 24 timmar i 600 °C.

After a second exposure with KCl, a few percent of the surface was corroded on the material pre-oxidized for 24 hours at 900 °C (*Figure 6-21*). The corrosion started on the surface far from an edge. The material pre-oxidized for 24 hours at 1100 °C showed the same appearance as after the first cycle. However, after a third exposure with KCl also this surface showed signs of corrosion, but only on a minor part of the surface. The corrosion had started at the edges of a drilled hole and at a small area on the polished surface.

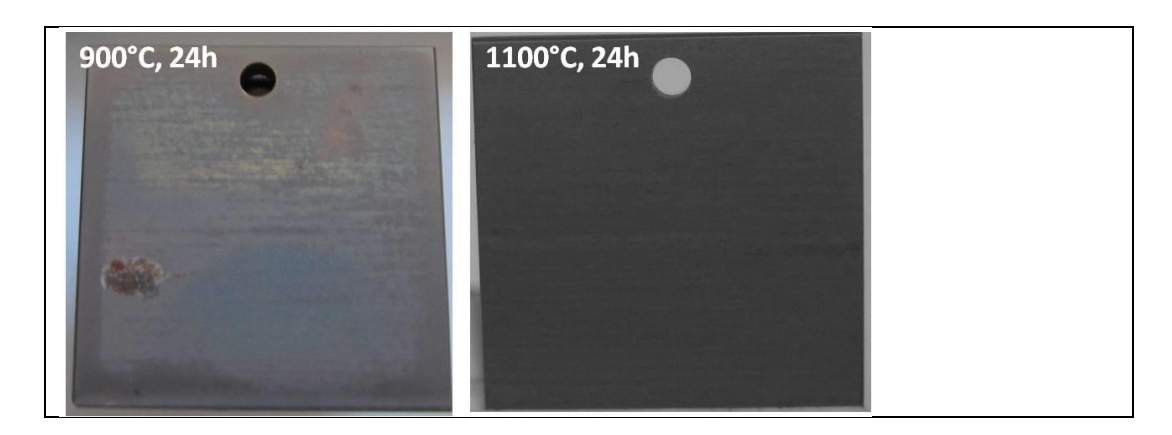


Figure 6-21. SEM images of the surface of APMT pre-oxidized at different times and temperatures and thereafter oxidized two times in the presence of H_2O and KCl for 24 hours at 600 °C.

Figur 6-21. SEM bilder på ytan av APMT prover föroxiderade vid olika temperaturer och tider och därefter oxiderade två gånger I närvaro av H_2O och KCl under 24 timmar i 600 °C.

After an additional exposure with KCl the already corroded areas had become larger, now covering about 5% of the surface (*Figure 6-22*). However, there were no new spots where the corrosion had started, indicating that the corrosion starts at defects in the protective scale.

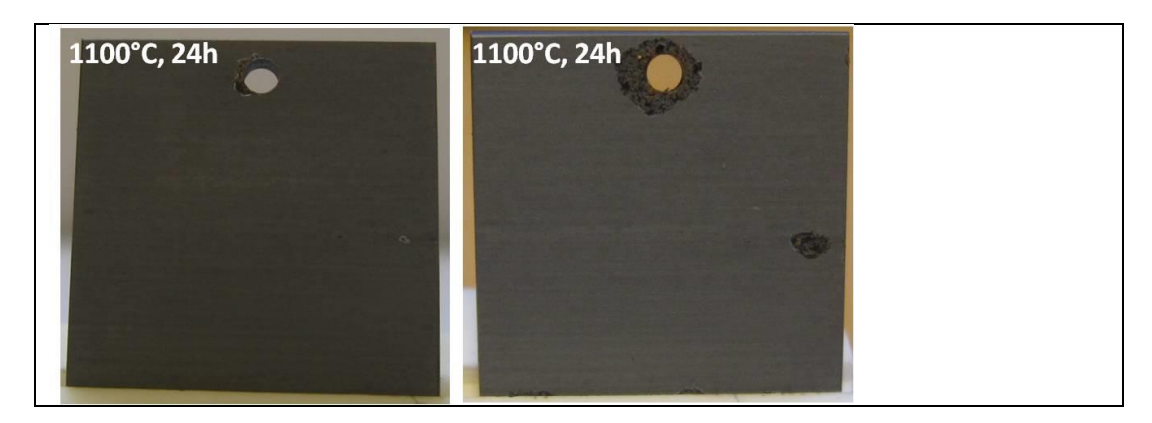


Figure 6-22. SEM images of the surface of APMT pre-oxidized at different times and temperatures and thereafter oxidized 3 (to the left) and 4 (to the right) times in the presence of H_2O and KCl for 24 hours at 600 °C.

Figur 6-22. SEM bilder på ytan av APMT prover för-oxiderade vid olika temperaturer och tider och därefter oxiderade 3 (till vänster) och 4 (till höger) gånger I närvaro av H_2O och KCl under 24 timmar i 600 °C.

SEM investigation of the surface of the material pre-oxidized for 1hour at 900 $^{\circ}$ C and thereafter cycled once in the presence of O_2 , H_2O and KCl reveals an uneven surface with iron-rich oxide protrusions (*Figure 6-23*). The same kind of areas can be seen on the material pre-oxidized for 1 hour at 1100 $^{\circ}$ C and

cycled 1 time. In addition the Al_2O_3 scale from the pre-oxidation is cracked, with iron-rich oxide growing in the cracks as can be seen (*Figure 6-23*).

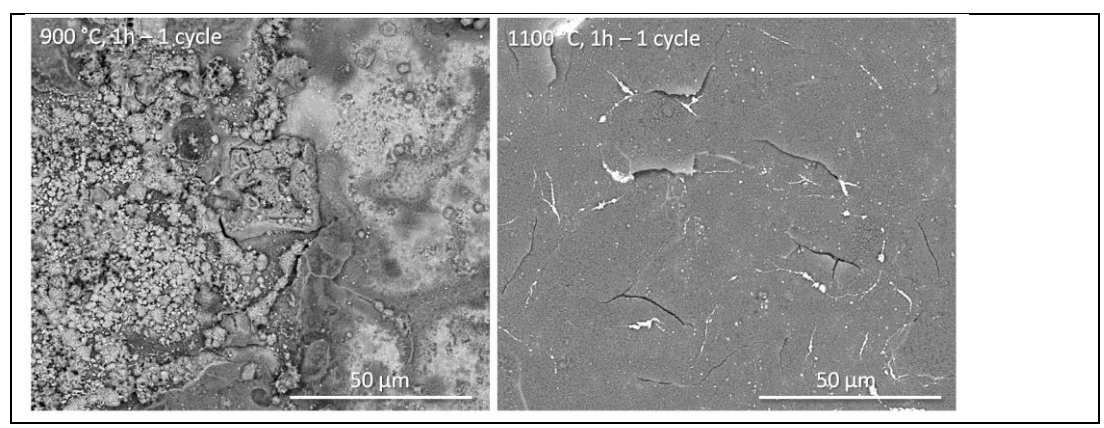


Figure 6-23. SEM image of the surface of APMT pre-oxidized at 900 or 1100 °C for 1 hour and thereafter oxidized in the presence of H_2O and KCl for 24 hours at 600°C.

Figur 6-23. SEM bild på ytan av APMT för-oxiderat vid 900 eller 1100 °C i 1 timma och därefter oxiderat i närvaro av H_2O och KCl under 24 timmar i 600 °C.

Analyses of the surface corrosion product show the formation of K_2CrO_4 and Fe-rich oxide (*Figure 6-24*) comparable with the exposures of non-pre-oxidised FeCrAl samples.

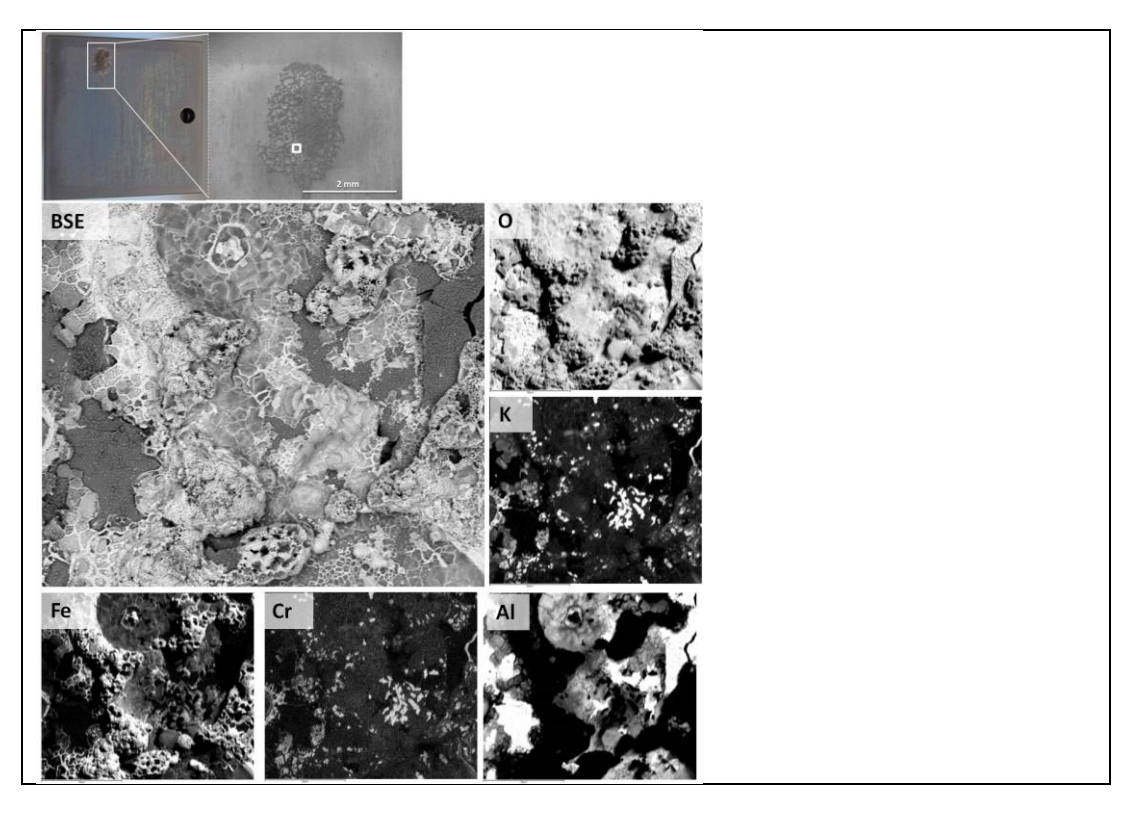


Figure 6-24. SEM image of the surface of APMT pre-oxidized at 900 °C for 24 hour and thereafter oxidized for 2 cycles in the presence of O_2 , H_2O and KCl for 24 hours at 600 °C.

Figur 6-24. SEM bild på ytan av APMT föroxiderat vid 900 °C i 24 timmar och därefter oxiderat i två cykler i närvaro av O_2 , H_2O och KCl under 24 timmar i 600 °C.

Cross sections of these oxides are shown in figure Figure 6-25 and Figure 6-26. The cross section of the material pre-oxidized for 1 hour at 900 °C (Figure 6-25) reveals different stages of the oxidation. Iron-rich oxide forms inward and outward to the alumina scale. The oxide formation mainly seems to start inward and with time also starts to form at the gas/scale interface. A Cr-rich oxide that also contains substantial amounts of iron and aluminum is present closest to the alloy surface. It seems likely that the oxidation starts at defects and spreads below the alumina scale. The volume increase during oxidation then causes tensions in the Al_2O_3 scale that eventually cracks resulting in the formation of oxide protrusions above the scale. Needle-like AIN particles forms in the alloy substrate just beneath the oxide scale. The formation of AIN likely inhibits the healing process of the formed cracks in the alumina scale due to the decreased AI activity in the substrate.

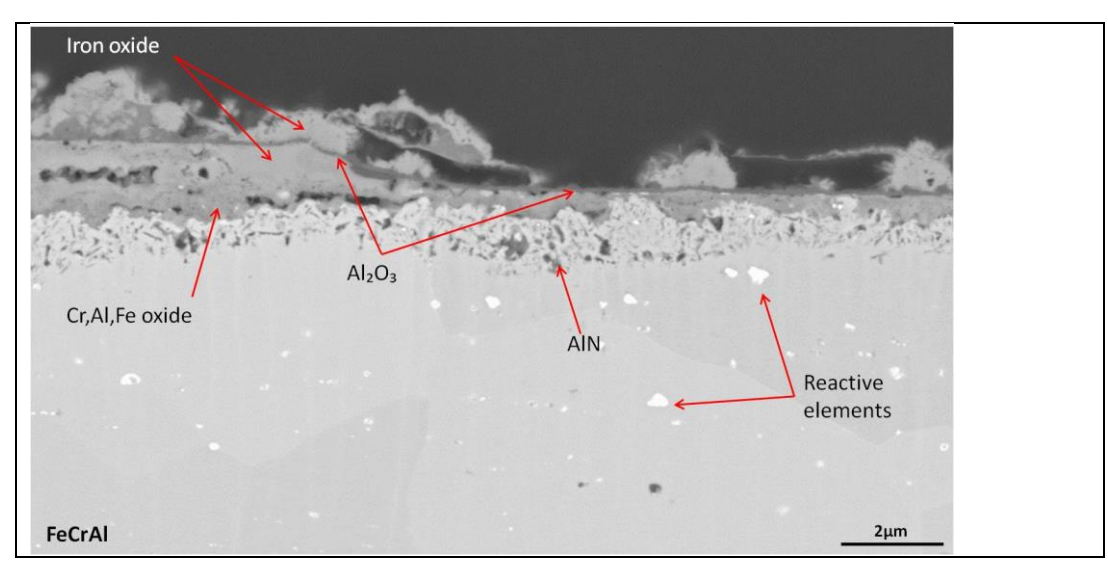


Figure 6-25. SEM image of the cross scetion of APMT pre-oxidized at 900°C for 1 hour and thereafter oxidized in the presence of O_2 , H_2O and KCl for 24 hours at 600°C.

Figur 6-25. SEM bild på tvärsnittet av APMT föroxiderat vid 900°C i 1 timma och därefter oxiderat I närvaro av O_2 , H_2O och KCl under 24 timmar i 600°C.

The cross section of the sample pre-oxidized for 1 hour at 1100 °C and cycled 1 time shows a similar oxide structure as the cross section in *Figure 6-25*. One difference is that the oxide formed in *Figure 6-26* grows mainly inward compared to the alumina scale. An iron-rich oxide protrusion can be seen above the present cracks in the Al_2O_3 scale.

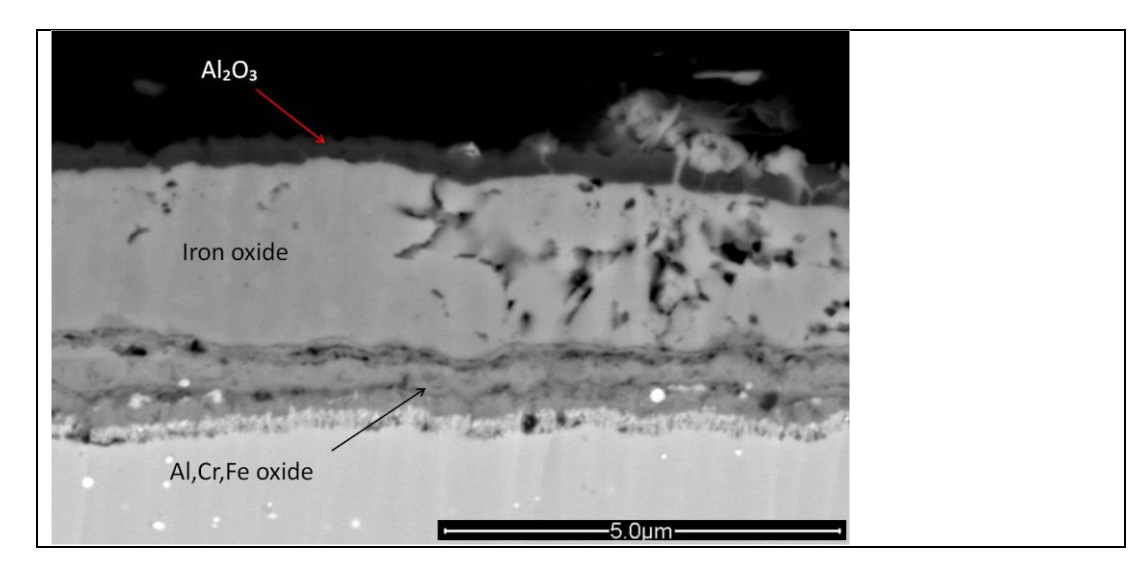


Figure 6-26. SEM image of the cross section of APMT pre-oxidized at 1100 °C for 1 hour and thereafter oxidized in the presence of O_2 , H_2O and KCl for 24 hours at 600 °C.

Figur 6-26. SEM bild på tvärsnittet av APMT föroxiderat vid 1100 °C i 1 timma och därefter oxiderat i närvaro av O_2 , H_2O och KCl under 24 timmar i 600 °C.

6.1.6 Summary of the laboratory results

- Oxidation of the powder-metallurgical FeCrAl alloy Kanthal[®] APMT at 600 and 700 °C in the absence of KCl, results in the formation of a thin oxide layer which is dominated by alumina and contains significant amounts of iron and chromium.
- Oxidation at 900 and 1100 °C results in a duplex continuous a-Al₂O₃ scale.
- \triangleright At 600 °C the oxidation is somewhat faster in O₂ + H₂O environment compared to dry O₂.
- \blacktriangleright KCl strongly accelerates the corrosion of Kanthal® APMT in $O_2 + H_2O$ at 600 °C. Chromia in the scale reacts rapidly with $O_2 + H_2O$ forming K_2CrO_4 and gaseous HCl. Chromate formation depletes the protective scale in Cr, triggering the formation of a fast-growing iron-rich scale.
- ➤ K₂CrO₄ is reduced on the scale surface according to an electrochemical process where the electrons are supplied by means of alloy oxidation.
- There was little evidence for alloy chlorination and it is believed to be of secondary importance in the present case.
- ightharpoonup Pre-oxidation has a beneficial effect on the corrosion behavior on Kanthal® APMT in the presence of KCl at 600 °C.
- ➤ The oxide from the pre-oxidation at 700°C is not completely inert to KCl since K₂CrO₄ forms on the surface.
- \triangleright KAlSiO₄ forms on the pre-oxidized samples exposed to O₂ + H₂O + KCl.
- ➤ KAlSiO₄ are believed to form either by a reaction between KCl, H₂O and the oxide scale or by a reaction between K₂CrO₄, H₂O and the oxide scale.
- > The FeCrAl samples pre-oxidized for 900 and 1100 °C showed protective behavior against KCl-induced corrosion at 600 °C. The formed alumina scale is however broken down with time. The corrosion appears to start at defects in the protective scale resulting in the growth of a Fe-rich oxide underneath the scale, leading to cracks in the alumina scale where oxidation may continue.

6.2 Field study

6.2.1 The corrosion probe study

Treatment of test samples before exposure

Before corrosion probe exposure, the test samples were cleaned ultrasonically first in acetone and then in ethanol. The samples were then dried in flowing air and the weight of the samples was recorded. Two different pre-oxidations were performed of the FeCrAl alloy, Kanthal® APMT, to establish a protective scale before the probe exposure. The pre-oxidation was conducted in a muffle furnace in laboratory air. The material was pre-oxidized at 1050°C for 8 hours or at 1100°C for 24 hours.

To be able to determine material loss of the samples after exposure the wall thickness was measured in a transversal section using a micrometer. The anvil was rounded on the inside and flat on the outside (diameter 6,3mm). The measurements were performed at eight equally spaced positions around the tube formed sample marked 2 to 9 in *Figure 6-27*. The samples were mounted with number 1 facing the windward direction.

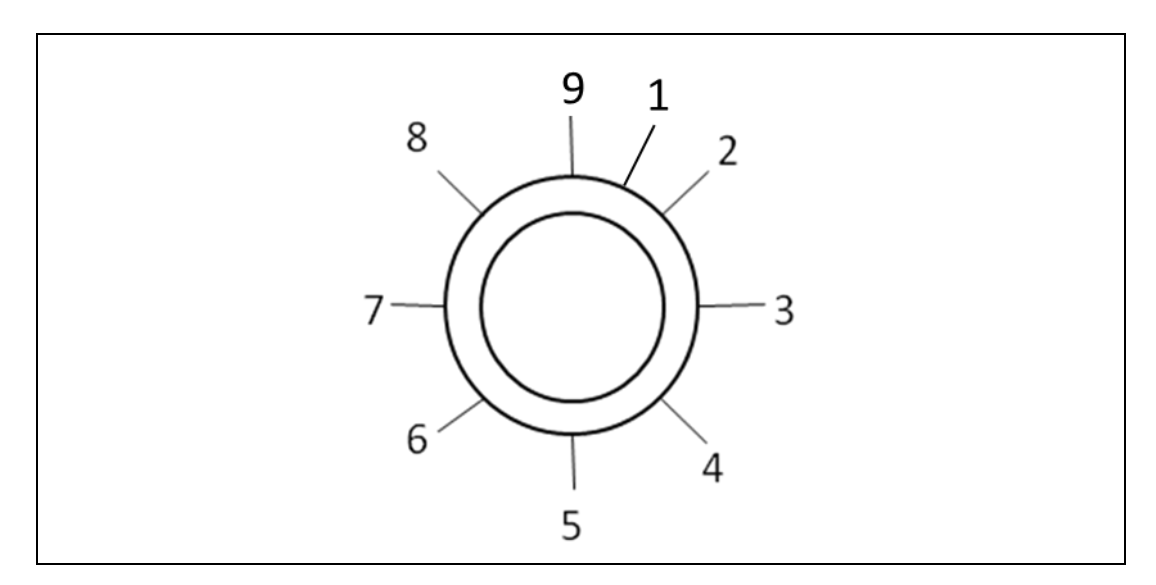


Figure 6-27. Measuring positions on tube samples.

Figur 6-27. Mätpositioner på sondproverna.

Optical inspection of the surface

After 24 hours exposure at 600 °C or 700 °C all the samples were covered by a deposit. However during the demounting of the samples from the probe most of the deposits fell off. *Figure 6-28* shows two optical images of the samples. The upper image is facing the camera with the windward side and the lower one is turned 180°. Some of the deposit fell off during handling and had sample material attached to the inside. The deposits were about one mm thick and were beige-gray in color. The deposit attached to the samples

exposed at 600 °C appeared somewhat thicker than on the samples exposed at 700 °C. The surfaces which had lost their deposits ranged from black to reddish. The rough morphology and the colors observed indicate that the rings were severely corroded. With respect to corrosion resistance no major distinction between the alloys could be made by visual inspection.

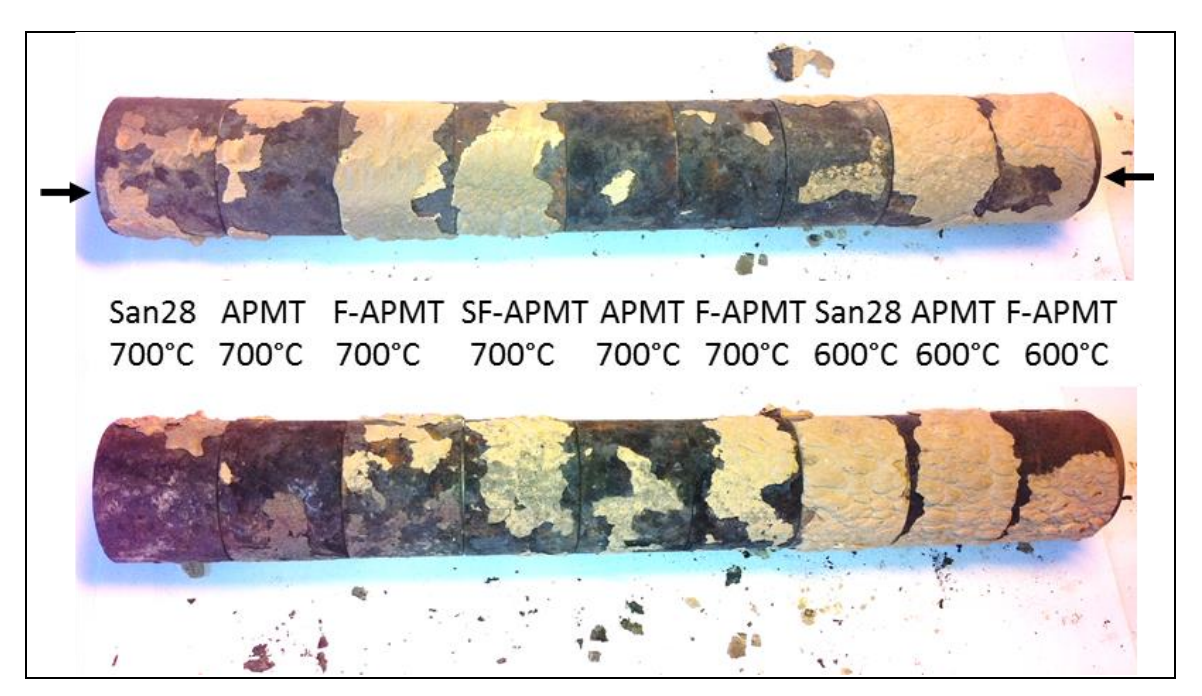


Figure 6-28. Photo showing the samples after probe exposure for 24 h. Sanicro 28 to the left followed by Kanthal® APMT, pre-oxidised Kanthal® APMT, standard pre-oxidized Kanthal® APMT, Kanthal® APMT, pre-oxidised Kanthal® APMT, Sanicro 28, Kanthal® APMT and pre-oxidised Kanthal® APMT to the right. The arrows on the topmost image mark the position of the thermal element (facing the winward side). The samples below have been turned 180°

Figur 6-28. Foto på proverna efter 24 timmars fältexponering. Sanicro 28 till vänster följd av Kanthal® APMT, föroxiderad Kanthal® APMT, standard föroxiderad Kanthal® APMT, Kanthal® APMT, föroxiderad Kanthal® APMT, Sanicro 28, Kanthal® APMT och föroxiderad Kanthal® APMT till höger. Pilarna på översta bilden visar positionen på termoelementen (vänd mot vindsidan). Proverna under har vänts 180°.

Figure 6-29 shows two optical images of the samples exposed for 400 hours. The upper image is facing the camera with the windward side and the lower one is turned 180°. The deposits were about one mm thick and were beigegray in color. The deposit attached to the samples exposed at 600 °C appeared thicker and more adherent than on the samples exposed at 700 °C. The surfaces which had lost their deposits ranged from gray to black. The rough morphology and the colors observed indicate that the rings were severely corroded. With respect to corrosion resistance no major distinction

between the alloys could be made by visual inspection. During separation of the samples from each other all the deposit fell off.



Figure 6-29. Photo showing the samples after probe exposure for 400 h. Sanicro 28 to the left followed by Kanthal® APMT, pre-oxidised Kanthal® APMT, standard pre-oxidized Kanthal® APMT, Kanthal® APMT, pre-oxidised Kanthal® APMT, Sanicro 28, Kanthal® APMT and pre-oxidised Kanthal® APMT to the right. The arrows on the topmost image mark the position of the thermal element (facing the winward side). The samples below have been turned 180°.

Figur 6-29. Foto på proverna efter 400 timmars fältexponering. Sanicro 28 till vänster följd av Kanthal® APMT, föroxiderad Kanthal® APMT, standard föroxiderad Kanthal® APMT, Kanthal® APMT, föroxiderad Kanthal® APMT, Sanicro 28, Kanthal® APMT och föroxiderad Kanthal® APMT till höger. Pilarna på översta bilden visar positionen på termoelementen (vänd mot vindsidan). Proverna under har vänts 180°.

Figure 6-30 shows two optical images of the samples exposed for 1000 hours. The upper image is facing the camera with the windward side and the lower one is turned 180°. Between the sample F-APMT 700°C and San28 600°C there is a ceramic bright colored piece separating the samples. No deposit remained on the samples exposed at 700 °C after demounting. However, again there was a substantial amount of beige-gray, yellow and white colored deposit attached to the samples exposed at 600 °C. The surfaces which had lost their deposits ranged from gray to black. The rough morphology and the colors observed indicate that the rings were severely corroded. With respect to corrosion resistance no major distinction between the alloys could be made by visual inspection. During separation of the samples from each other all the deposit fell off.

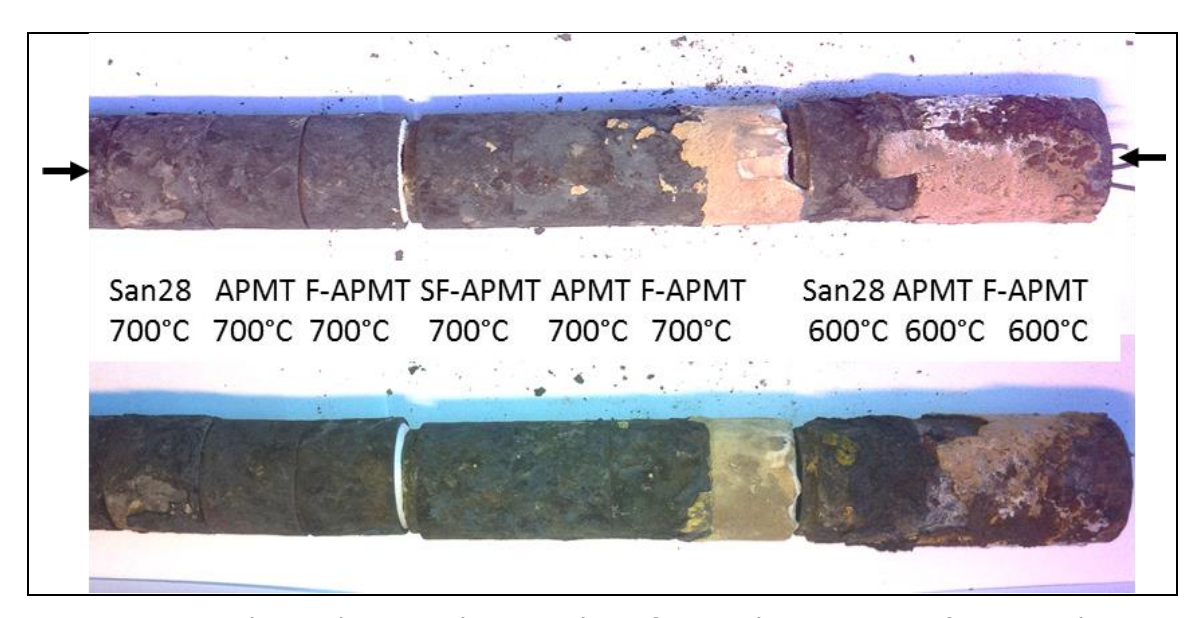


Figure 6-30. Photo showing the samples after probe exposure for 1000 h. Sanicro 28 to the left followed by Kanthal® APMT, pre-oxidised Kanthal® APMT, standard pre-oxidized Kanthal® APMT, Kanthal® APMT, pre-oxidised Kanthal® APMT, Sanicro 28, Kanthal® APMT and pre-oxidised Kanthal® APMT to the right. The arrows on the topmost image mark the position of the thermal element (facing the winward side). The samples on the image below have been turned 180°.

Figur 6-30. Foto på proverna efter 1000 timmars fältexponering. Sanicro 28 till vänster följd av Kanthal[®] APMT, föroxiderad Kanthal[®] APMT, standard föroxiderad Kanthal[®] APMT, Kanthal[®] APMT, föroxiderad Kanthal[®] APMT, Sanicro 28, Kanthal[®] APMT och föroxiderad Kanthal[®] APMT till höger. Pilarna på översta bilden visar positionen på termoelementen (vänd mot vindsidan). Proverna på bilden under har vänts 180°.

Optical inspection of the cross-sections

Figure 6-31 show camera images of polished cross-sections of the samples exposed for 24 – 1000 h at 600 °C. The surface of the samples exposed for 24 h appears smooth, without any visible material loss. After 400 h, the surface of Sanicro 28 is very rugged all around the circumference, indicating substantial material loss. The surfaces of the APMT and pre-oxidized APMT samples also have some rugged areas but to a much lesser extent than Sanicro 28. The uneven surface of pre-oxidized APMT and APMT appears mostly on the half circumference towards the wind side and are also pronounced on top of the rings (from the image view). After 1000 h exposures, Sanicro 28 are rugged all around the circumference again, but surprisingly, to a lesser extent than after 400 h. The pre-oxidized APMT also appears very rugged all around the circumference whereas APMT appears to have the smoothest surface, although less smooth than after 400 h exposure.

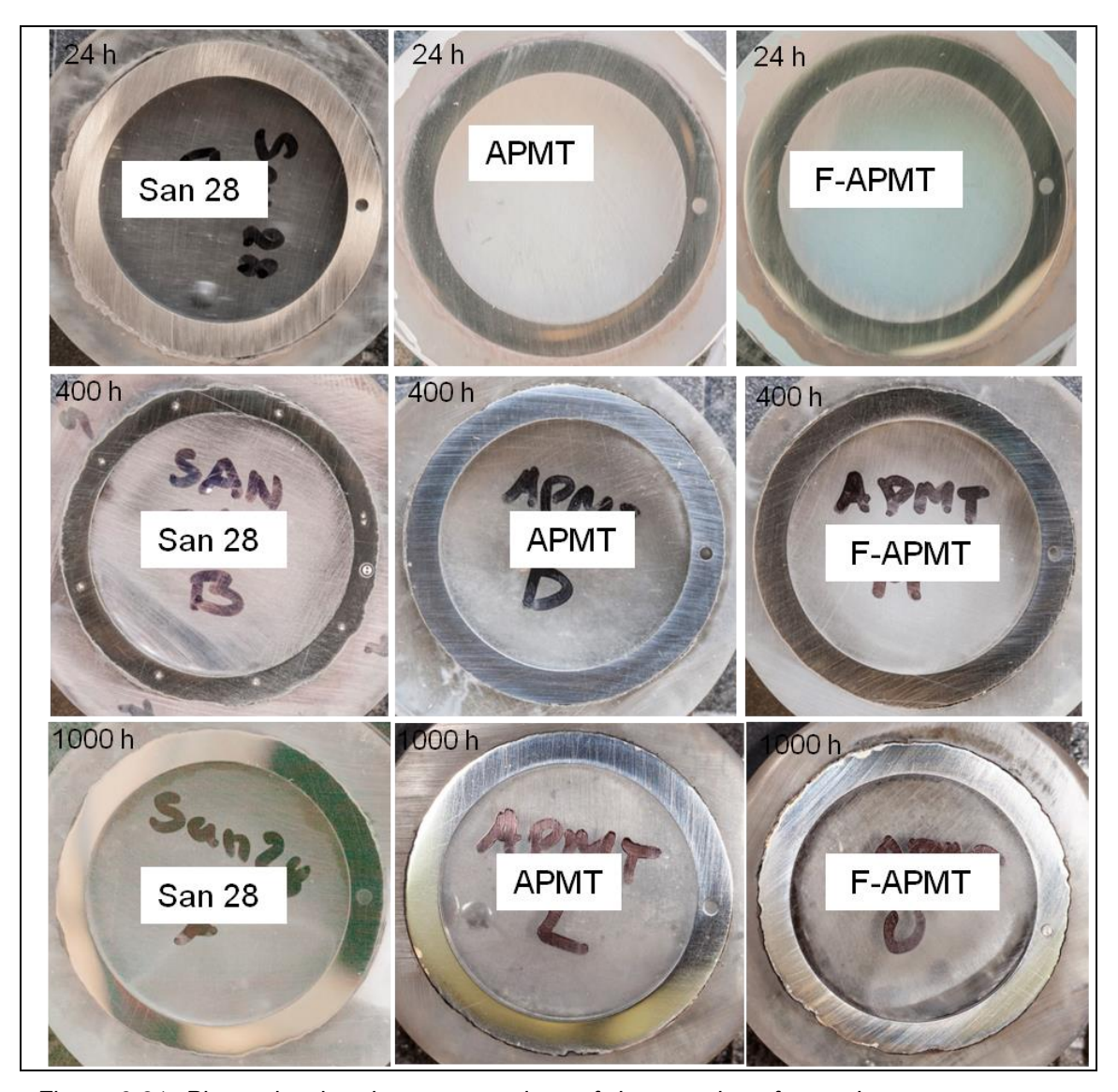


Figure 6-31. Photo showing the cross-sections of the samples after probe exposure at 600°C for 24-1000 h. The pre-oxidized APMT is marked "F-APMT" and Sanicro 28 "San 28".

Figur 6-31. Foto som visar tvärsnittet av proverna som exponerats i fält vid 600°C under 24-1000 timmar. För-oxiderad Kanthal APMT är markerad med "F-APMT" och Sanicro 28 med "San 28".

Figure 6-32 show camera images of polished cross-sections of the samples exposed for 24 h at 700 °C. The surface of the samples exposed appears smooth, without any visible material loss. After 400 h, the surface of Sanicro 28 is very rugged all around the circumference, indicating substantial material loss. The surfaces of the APMT and pre-oxidized APMT samples also have some rugged areas but to a much lesser extent than Sanicro 28. The uneven surface of pre-oxidized APMT and APMT appears mostly on the half

circumference towards the wind side and are also pronounced on top of the as was the case after exposure at 600 °C for 24 h.

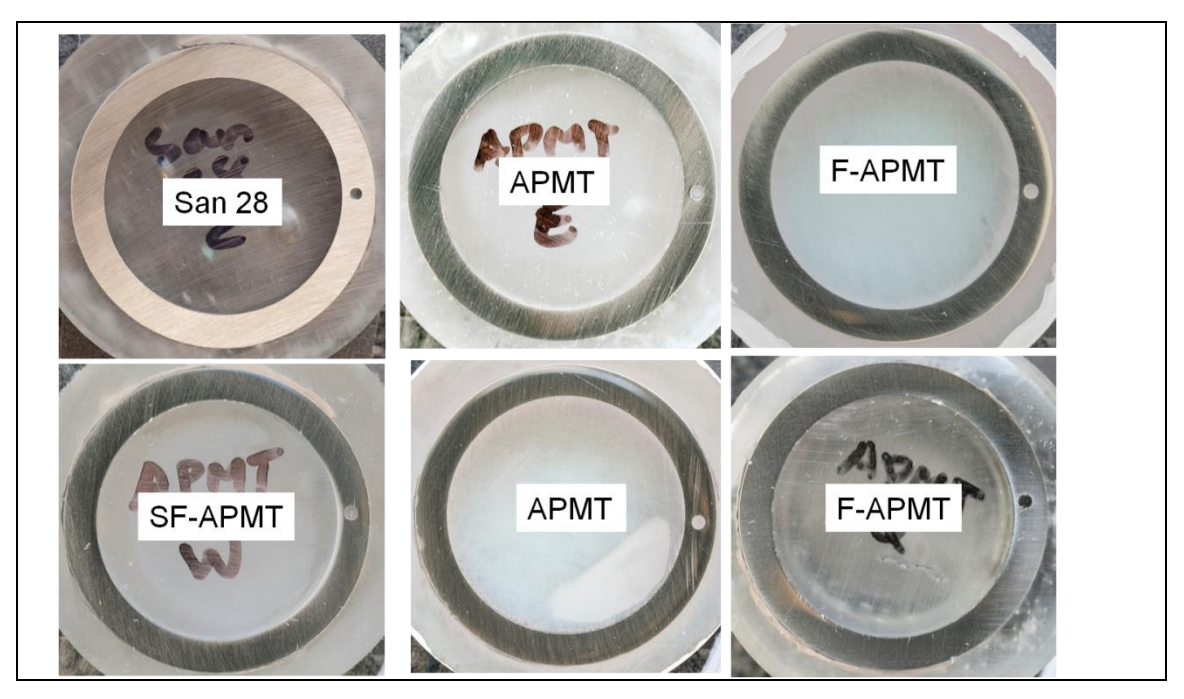


Figure 6-32. Photos showing the cross-sections of the samples after probe exposure at 700°C for 24 h. The pre-oxidized APMT is marked "F-APMT" and Sanicro 28 "San 28".

Figur 6-32. Foto som visar tvärsnittet av proverna som exponerats i fält vid 700°C under 24 timmar. För-oxiderad Kanthal APMT är markerad med "F-APMT" och Sanicro 28 med "San 28".

Figure 6-33 show camera images of polished cross-sections of the samples exposed for 400 h at 700°C. The surface of Sanicro 28 appears very rugged all around the circumference. The APMT samples with and without preoxidation appears rather similar. They are a little bit rugged on the surface but much less than Sanicro 28.

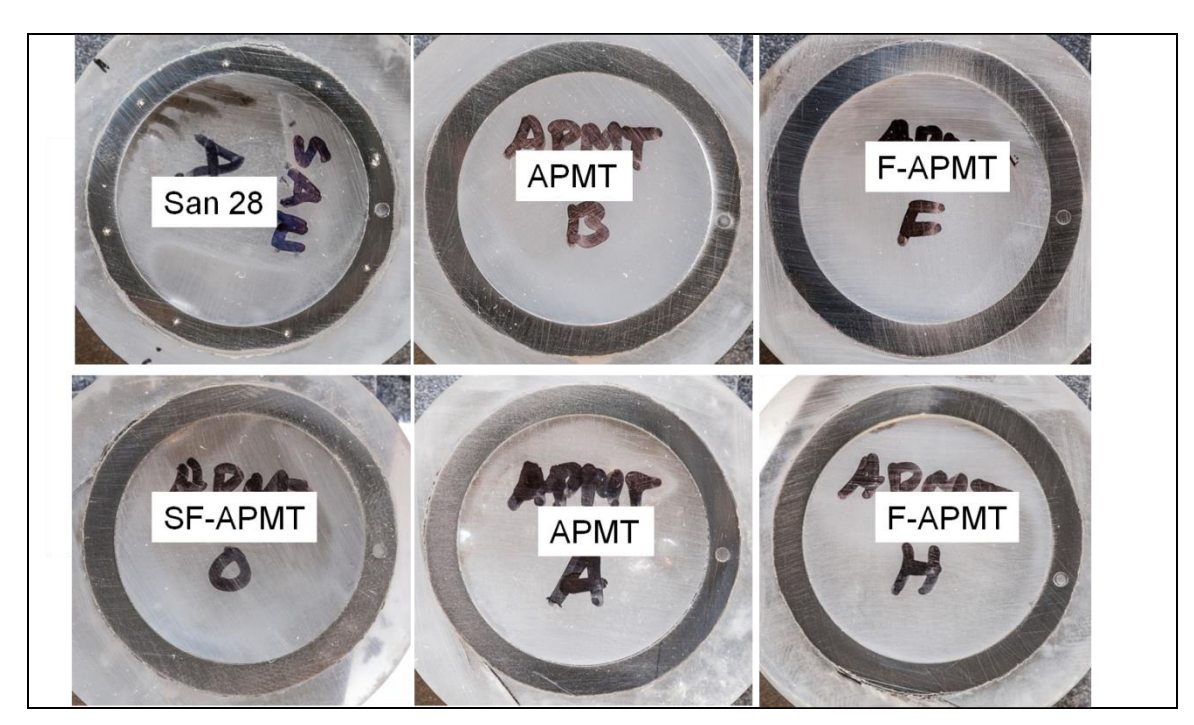


Figure 6-33. Photos showing the cross-sections of the samples after probe exposure at 700°C for 400 h. The pre-oxidized APMT is marked "F-APMT" and Sanicro 28 "San 28".

Figur 6-33. Foto som visar tvärsnittet av proverna som exponerats i fält vid 700°C under 24 timmar. För-oxiderad Kanthal® APMT är markerad med "F-APMT" och Sanicro 28 med "San 28".

Figure 6-34 show camera images of polished cross-sections of the samples exposed for 1000 h at 700°C. The surfaces of the samples appear similar to that obtained after 400h exposure. Thus, Sanicro 28 appears very rugged all around the circumference. The APMT samples with and without pre-oxidation appears rather similar. They are a little bit rugged on the surface but much less than Sanicro 28.

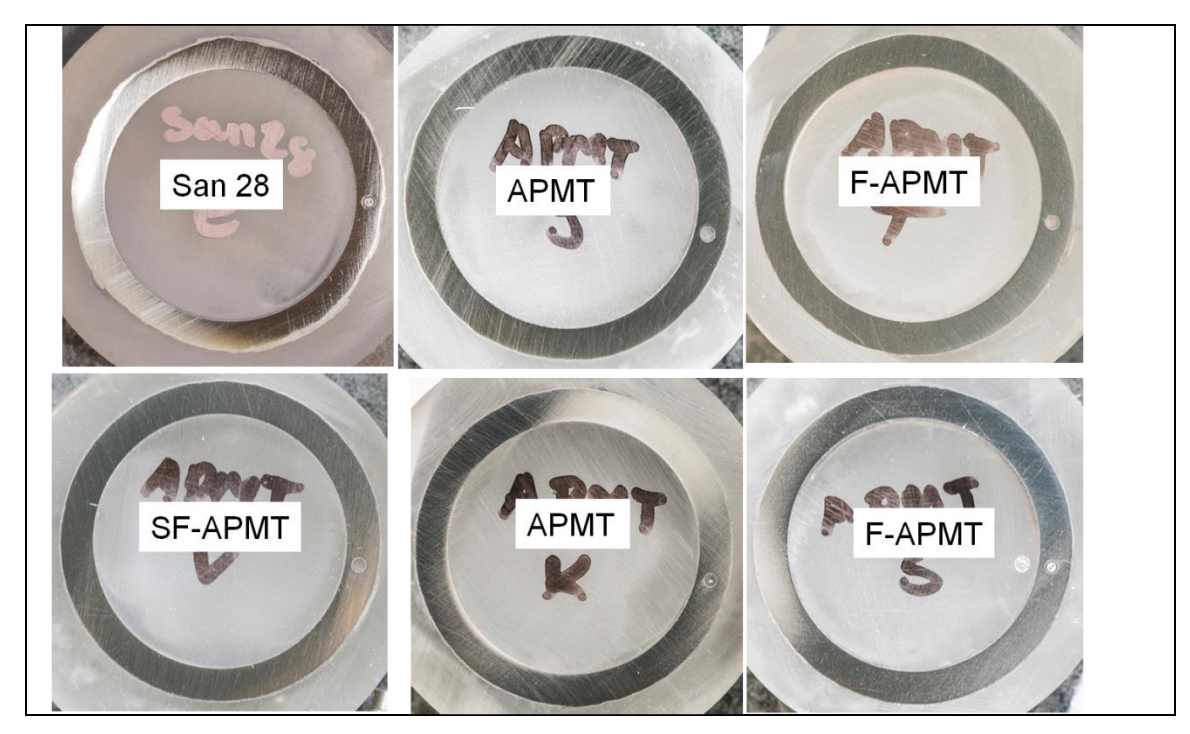


Figure 6-34. Photos showing the cross-sections of the samples after probe exposure at 700°C for 1000 h. The pre-oxidized APMT is marked "F-APMT" and Sanicro 28 "San 28".

Figur 6-34. Foto som visar tvärsnittet av proverna som exponerats i fält vid 1000°C under 24 timmar. För-oxiderad Kanthal[®] APMT är markerad med "F-APMT" och Sanicro 28 med "San 28".

Material loss

The material loss was determined using an image processing program coupled to an excel file. To verify the results of the material loss process, the material loss at the location where maximum material loss had taken place was determined using SEM on one sample. This value was then compared to the value obtained from the excel file and the difference was less than 9%.

Figure 6-35 show the material loss around the circumference of Sanicro 28, APMT, and APMT pre-oxidized at 1100°C for 24 h, after field exposure at 600°C for 400 h and 1000 h. 0° at the x-axes is the position of the thermo couple. The mean, max and min values obtained for the material loss are shown in Table 6-1. The obtained values are in accordance with the cross-sectioned images, the most rugged surface shows the highest material loss values. Thus, after 400 and 1000 h of exposure the material loss of Sanicro 28 is substantially higher than that of the APMT alloy with or without pre-oxidation, In addition, the material loss values are higher for APMT with pre-oxidation compared with that of APMT without pre-oxidation, the average values for 1000 h exposure being 0.75, 0.18 and 0.26 mm respectively. Comparing the material loss of all the samples exposed at 600°C, the material loss appears to be random around the circumference, there is no preferred orientation with higher material loss.

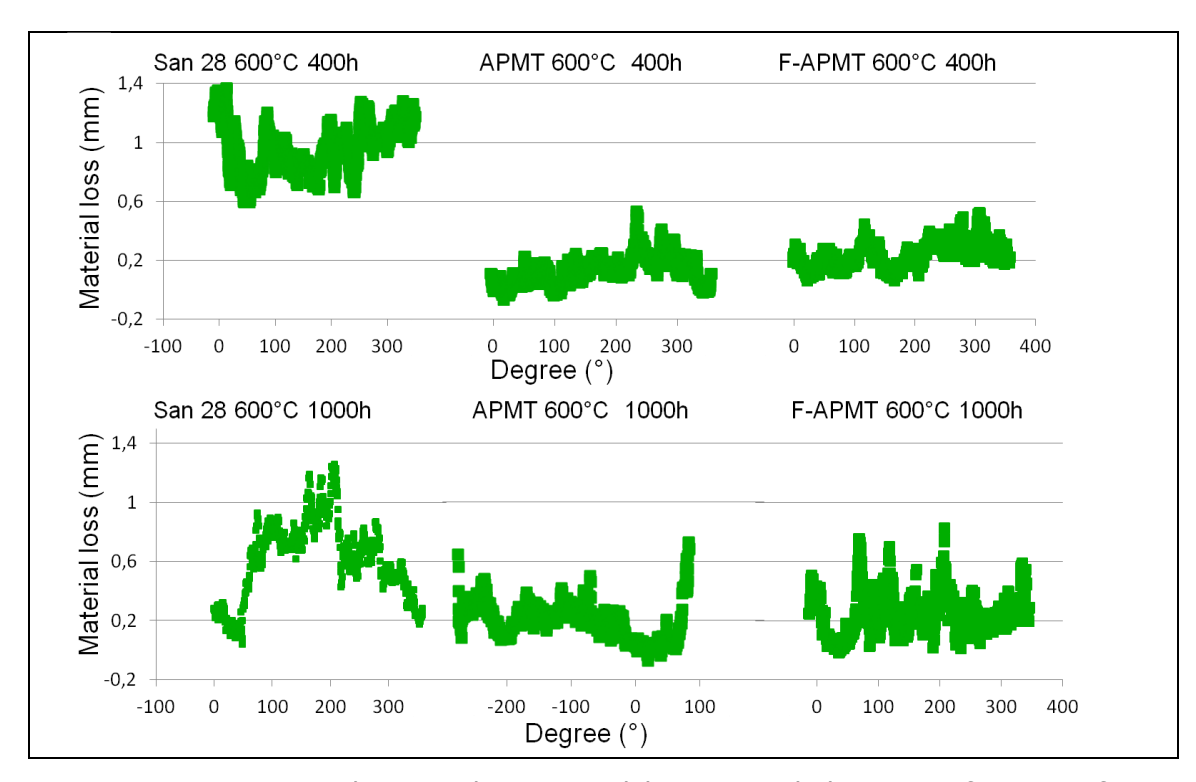


Figure 6-35. Curves showing the material loss around the circumference of Sanicro 28, APMT and pre-oxidized (1100°C, 24 h) APMT after probe exposure at 600°C for 400 h and 1000 h. 0° at the x-axes is the position of the thermo couple.

Figur 6-35. Kurvor som visar materialförlusten runt omkretsen på Sanicro 28, APMT och för-oxiderad (1100°C, 24 tim) APMT efter sond exponering vid 600°C under 400 tim och 1000 tim. 0° vid x-axeln är termoelementets position.

400 h	Min (mm)	Max (mm)	Average (mm)
San 28	0.68	1.15	0.91
APMT	0	0.53	0.15
F-APMT	0.06	0.45	0.25
1000 h	Min (mm)	Max (mm)	Average (mm)
1000 h San 28	Min (mm) 0.43	Max (mm) 1.26	Average (mm) 0.75

Table 6-1. Max, min and average values of the material loss measurements of Sanicro 28, APMT and pre-oxidized (1100°C, 24 h) APMT after probeexposure at 600°C for 400 h and 1000 h.

The material loss values obtained in this project is compared with those obtained in KME 414 during similar exposure conditions (600°C, 1000 h, Händelöverken), see *Table 6-2*. The material loss values coincide very well, the average material loss for APMT in KME 507 being 0.18 mm as compared to 0.16 mm (APMT in KME 414). Furthermore, the values for pre-oxidized APMT were 0.26 mm (KME 507) and 0.42 mm (KME414). However, the pre-oxidations were not performed in the same manner. The pre-oxidation in KME 414 were conducted at 1050°C for 8 h, whereas in KME 507 the pre-oxidation was conducted at 1100°C for 24 h. However, these results re-enforces the conclusion that Kanthal[®] APMT without pre-oxidation withstands the environment better than pre-oxidized APMT and that FeCr-steels at 600°C in a waste-fired boiler.

material	Max (mm)	Average (mm)
APMT (KME 507)	0.50	0.18
APMT (KME 414)	0.42	0.16
F-APMT (KME 507)	0.83	0.26
SF-APMT (KME 414)	0.77	0.42

Table 6-2. Max, min and average values of the material loss of Sanicro 28, APMT and pre-oxidized APMT obtained during field-exposures at 600°C for 1000 h, in this project and in KME 414. The material marked SF-APMT was pre-oxidized at 1050°C for 8 h and F-APMT at 1100°C for 24 h.

Figure 6-36 show the material loss around the circumference of Sanicro 28, APMT and pre-oxidized APMT (SF-APMT and F-APMT) after probe exposure at 700°C for 400 h and 1000 h. The material marked SF-APMT was pre-oxidized at 1050°C for 8 h and F-APMT at 1100°C for 24 h. 0° at the x-axes is the position of the thermo couple. The mean, max and min values obtained for the material loss of these materials is shown in Table 6-3. The obtained material loss values are in accordance with the cross-sectioned images, the most rugged surface shows the highest material loss values. Similar to the values obtained after exposures at 600°C, Sanicro28 had lost substantially more material than the APMT materials with and without pre-oxidation after exposure at 700°C for 400 h and 1000 h, the average value for Sanicro28 being around 0.9 mm as compared to around 0.3 for the APMT materials. Here the similarities with the 600°C exposure stop. After exposure at 700°C and 400 h the APMT materials with and without pre-oxidation show similar material loss values, and after 1000 h the pre-oxidized APMT showed somewhat lower values than APMT without pre-oxidation, the average values being similar (0.3 mm) but the max value being ~0.4 and 0.5 mm respectively. Comparing the material loss of all the samples exposed at 700°C, the material loss appears to be random around the circumference, there is no preferred orientation with higher material loss.

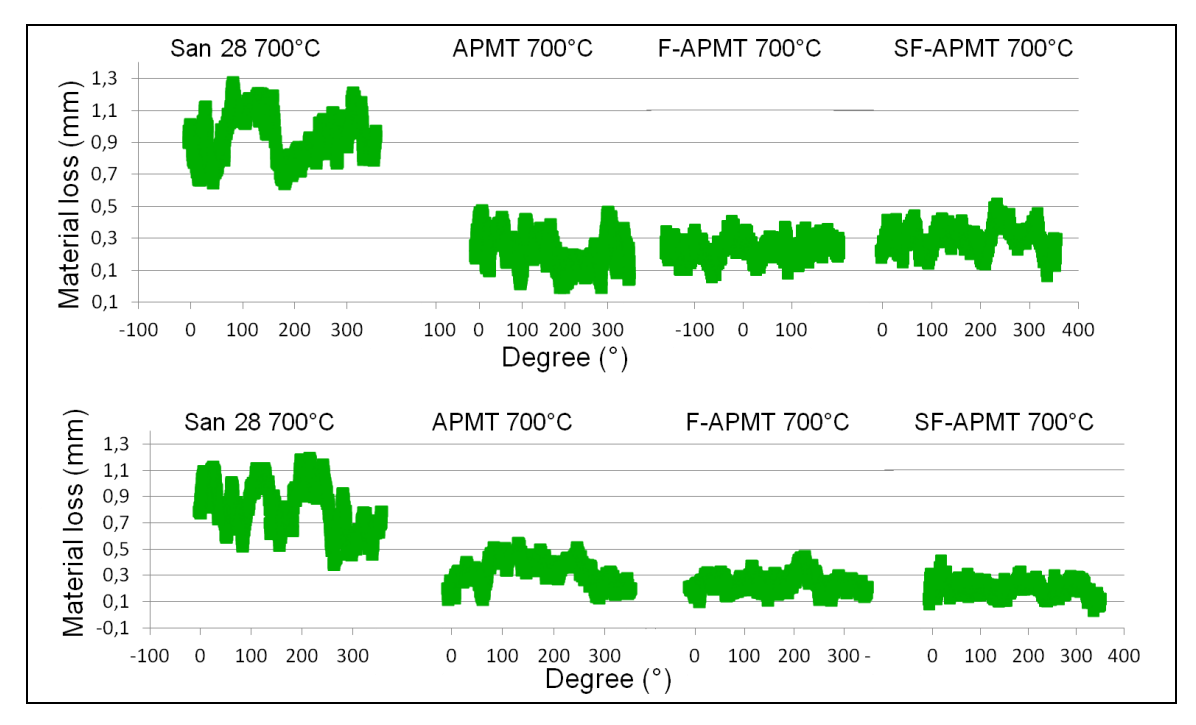


Figure 6-36. Curves showing the material loss around the circumference of Sanicro 28, APMT and pre-oxidized APMT after probe exposure at 700°C for 400 h and 1000 h. 0° at the x-axes is the position of the thermo couple. The material marked SF-APMT was pre-oxidized at 1050°C for 8 h and F-APMT at 1100°C for 24 h.

Figur 6-36. Kurvor som visar materialförlusten runt omkretsen på Sanicro 28, APMT och för-oxiderad APMT efter fält exponering vid 700°C under 400 h and 1000 h. 0° vid x-axeln är termoelementets position. Materialet som märkts SF-APMT för-oxiderades i 1050°C under 8 timmar och F-APMT i 1100°C under 24 timmar.

400 h	Min (mm)	Max (mm)	Average (mm)
San 28	0.64	1.21	0.96
APMT	0 / 0.30	0.39 / 0.84	0.21 / 0.55
F-APMT	0.10 / 0.32	0.41 / 0.67	0.25 / 0.48
SF-APMT	0.13	0.51	0.31
1000 h	Min (mm)	Max (mm)	Average (mm)
San 28	0.50	1.21	0.85
APMT	0.27 / 0.01	0.54 / 0.51	0.37 / 0.20
F-APMT	0.11 / 0.14	0.44 / 0.41	0.26 / 0.29
SF-APMT	0.10	0.32	0.20

Table 6-3. Max, min and average values of the material loss measurements of Sanicro 28, APMT and pre-oxidized APMT after field-exposure at 700°C for 400 h and 1000 h. The material marked SF-APMT was pre-oxidized at 1050°C for 8 h and F-APMT at 1100°C for 24 h.

Summary of the material loss measurements

Exposures in the Händelö boiler P14 at 600°C for 400 h and 1000 h showed a lower material loss for APMT with and without pre-oxidation than that of Sanicro28. In addition, the material loss for APMT without pre-oxidation was lower than for APMT with pre-oxidation. These results are in agreement of those obtained in the project KME 414.

Exposures in the Händelö boiler P14 at 700°C for 400 h and 1000 h showed a lower material loss for APMT with and without pre-oxidation than that of Sanicro28. In addition, the material loss was similar for APMT with and without pre-oxidation.

Crystalline structure of deposit detected by XRD

Deposit was collected from sample rings exposed for 24, 400 and 1000 hours in 600 and 700 °C. It was assumed that the same deposit is present on all rings exposed to one specific time and temperature. So deposit was collected from one sample ring from each time and temperature. The deposit was ground to a fine powder and analysed using a Siemens D5000 powder diffractometer to determine the present crystalline compounds. The instrument was equipped with a grazing-incidence-beam attachment together

with a Göbel mirror. The samples were exposed to a source of CuK_{α} radiation ($\lambda = 1.5418$ Å) with an incident angle of 1.5°. The moving detector collected data in the range of 15° < 20 < 65° with step size of 0.05°.

The same type of compounds was detected in the deposit on the probes exposed at 600 and 700 °C (*Table 6-4* and *Table 6-5*). The ground deposit also contained corrosion products from the sample rings, mainly Fe_2O_3 and Cr_2O_3 . The deposit mainly contained alkali salts e.g. NaCl and KCl together with $CaSO_4$. No sulfur containing compound was detected on the sample rings exposed for 1000 hours. There were indications of Al_2O_3 from several of the deposit powders but no clear identification was made. Interestingly KAlSiO₄ was identified in one deposit (see *Table 6-5*) which has also been identified in the laboratory studies on a pre-oxidized sample exposed together with KCl at 600 °C.

24h	400h	1000h	
Fe ₂ O ₃ , Cr ₂ O ₃ , NaCl, KCl,	Fe ₂ O ₃ , Cr ₂ O ₃ , NaCl, KCl,	Fe ₂ O ₃ , Cr ₂ O ₃ , NaCl, KCl	
CaSO ₄	CaSO₄		

Table 6-4. Compounds detected by XRD at samples exposed for 24, 400 and 1000 hours at 600 °C.

24h	400h	1000h	
Fe ₂ O ₃ , Cr ₂ O ₃ , NaCl, KCl,	Fe ₂ O ₃ , Cr ₂ O ₃ , NaCl, KCl,	Fe ₂ O ₃ , Cr ₂ O ₃ , NaCl, KAlSiO ₄ ,	
CaSO ₄	CaSO ₄		

Table 6-5. Compounds detected by XRD at samples exposed for 24, 400 and 1000 hours at 700 °C.

Microstrucural analyses

The probe exposure samples which was exposed for 24 and 1000 hours were chosen to investigate further using scanning electron microscope (SEM). The sample rings were mounted in epoxy and cut by a precision low speed saw to create a cross-section. Before the SEM/EDX analysis the cross-section was grounded dry with silicon carbide paper and coated with a thin gold layer in order to avoid charging effects. The majority of the corrosion products and the deposit were not in direct contact to the metal when analyzed in the microscope. It is difficult to determine if the oxide scale/deposit has spalled during exposure, during cooling of the probe or during mounting of the sample ring in epoxy.

Probes exposed at 600 °C for 24 hours

Both the non-treated APMT and the pre-oxidized (1100 $^{\circ}$ C, 24h) have a thick deposit layer on top of the oxide scale (*Figure 6-37* and *Figure 6-38*). The elemental maps in *Figure 6-37* and *Figure 6-38* shows that the deposit mainly

consists of K, Na, Cl, Ca, S. These elements correspond well to NaCl, KCl and CaSO₄ which were detected using XRD (see *Table 6-4* and *Table 6-5*). The APMT sample without pre-oxidation forms a mixed oxide of Fe, Cr and Al (*Figure 6-37*). The alloy does not form a continuous pure Al_2O_3 at the present environment. The continuous Al_2O_3 layer from the pre-oxidation of APMT (1100 °C, 24 h) does not show protective behavior and has failed already after 24 hours of exposure at 600 °C in the boiler (See *Figure 6-39*). A iron, chromium-rich oxide has formed over and under the former protective alumina layer. Chlorides and sulfur were detected in the oxide/alloy interface on both samples and is believed to be metal chlorides (e.g $CrCl_2$, $FeCl_2$) and sulfides of the alloying elements (See *Figure 6-37* and *Figure 6-39*). No depletion of the alloying elements was detected in the alloy beneath the scale on both samples.

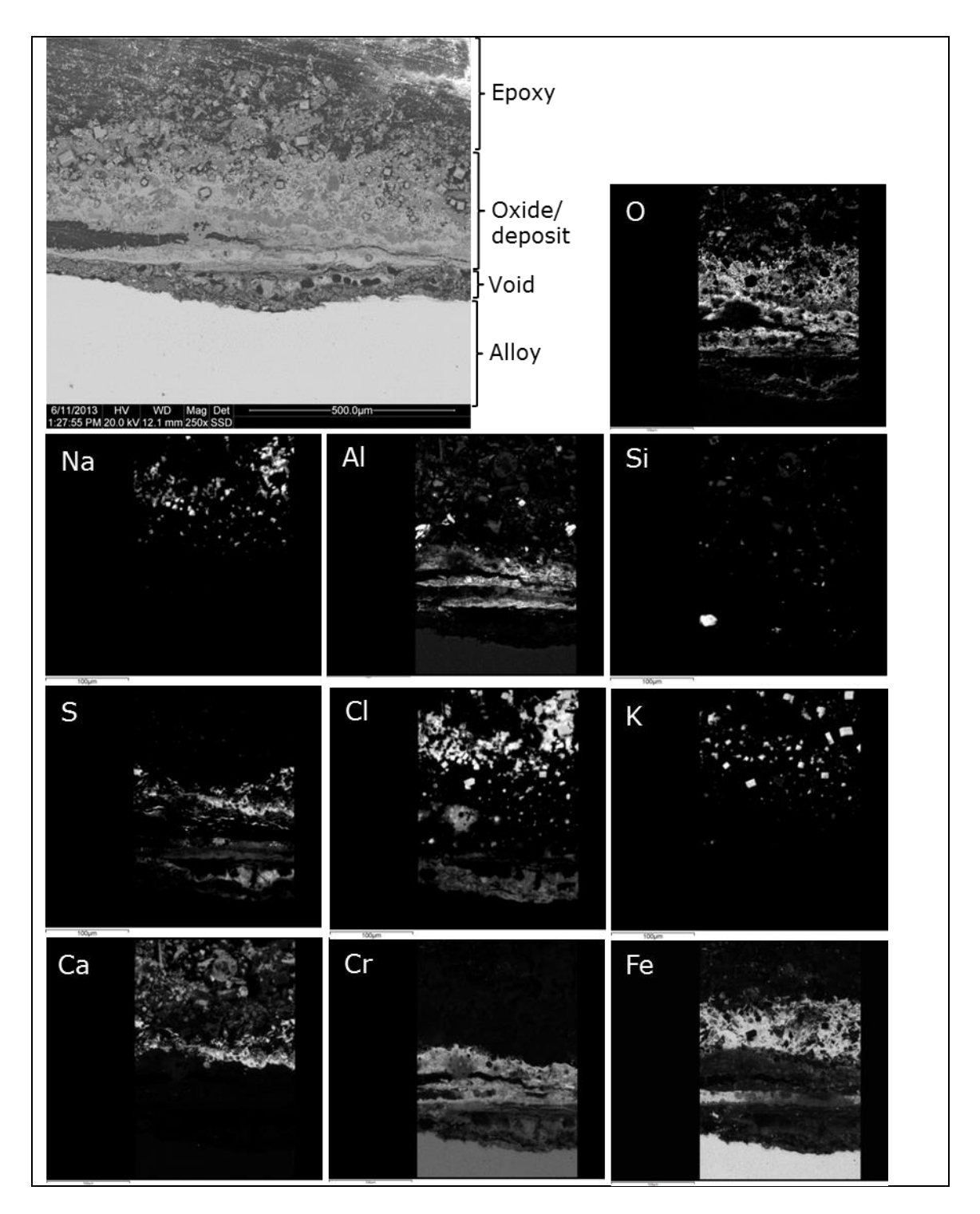


Figure 6-37. SEM-BSE image and elemental maps of the cross-section of APMT exposed for 24 hours at 600 °C.

Figur 6-37. SEM-BSE bild och element kartor av tvärsnittet på APMT exponerad i 600 °C under 24 timmar.

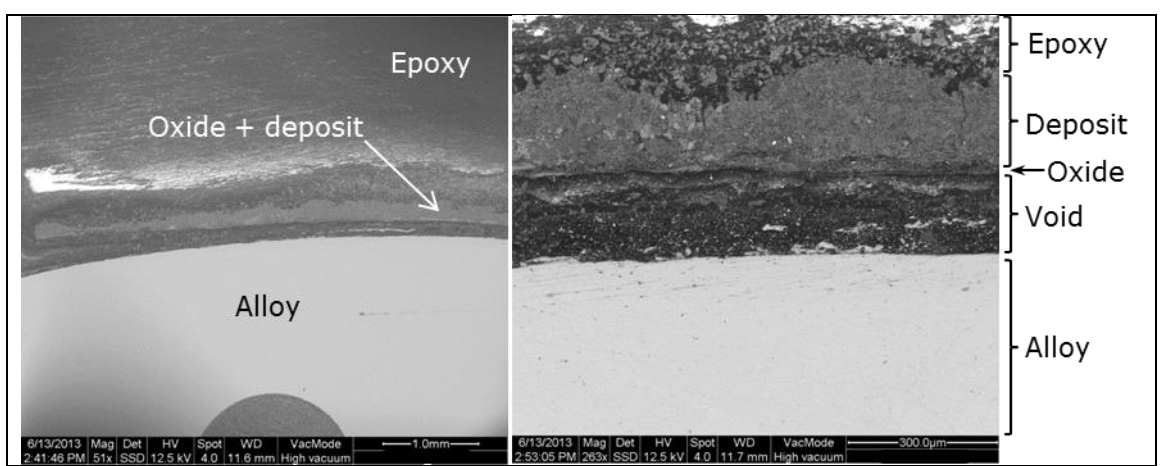


Figure 6-38. SEM-BSE images of the cross-section of pre-oxidized APMT (1100 °C for 24 h) APMT exposed for 24 hours at 600 °C.

Figur 6-38. SEM-BSE bilder på tvärsnittet av föroxiderad APMT (1100 °C for 24 h) exponerad i 600 °C under 24 timmar.

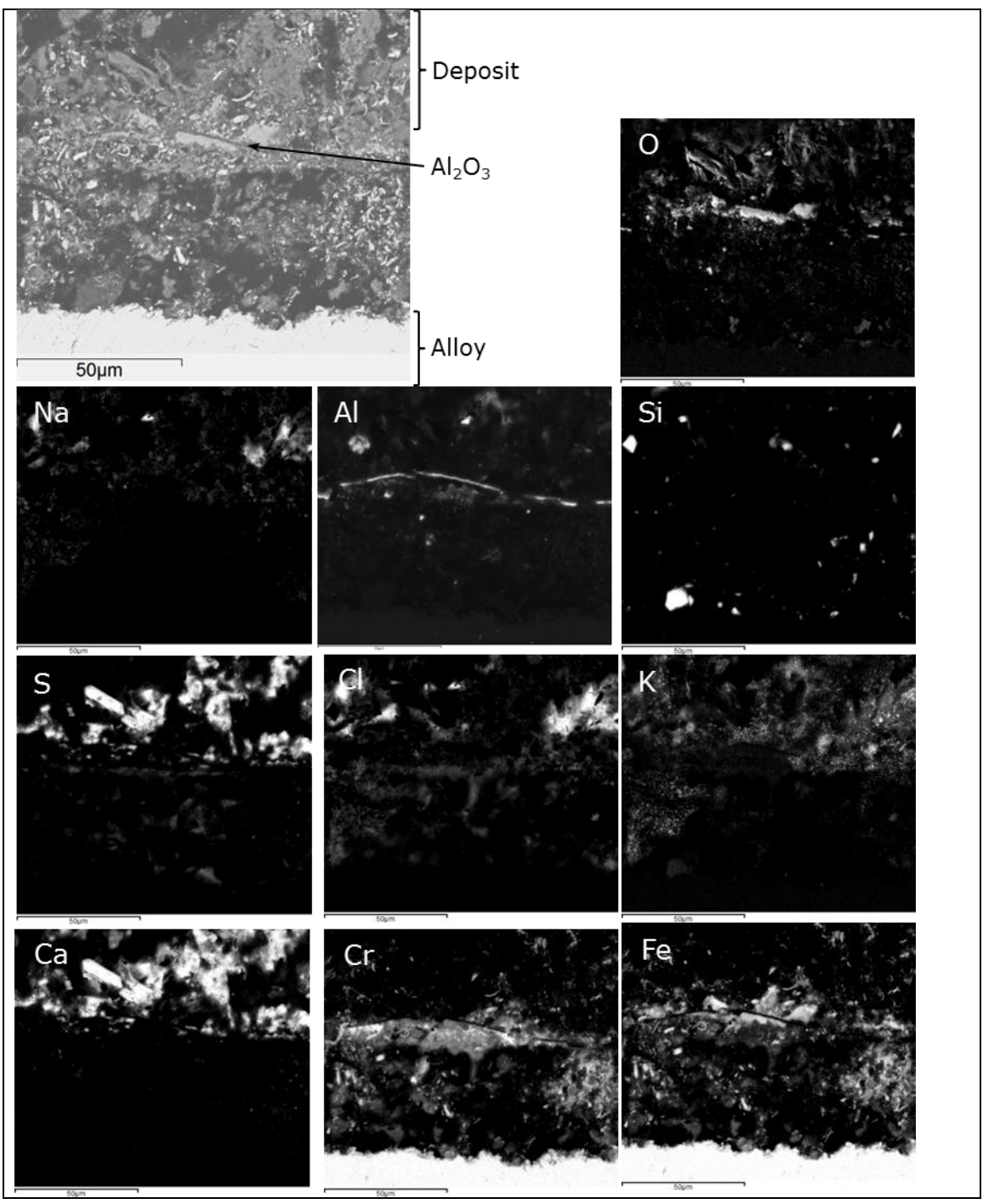


Figure 6-39. SEM-BSE image and elemental maps of the cross-section of pre-oxidized APMT (1100 °C for 24 h) exposed for 24 hours at 600 °C.

Figur 6-39. SEM-BSE bild och element kartor på tvärsnittet av föroxiderad APMT (1100 °C for 24 h) exponerad i 600 °C under 24 timmar.

Probes exposed at 600 °C for 1000 hours

The majority of the deposit layer is not present after 1000 hours of exposure at 600 °C, however some of the deposit was detected on the pre-oxidized sample and consisted of NaCl and KCl (*Figure 6-41*). No protective alumina layer was detected on the non-treated APMT or the pre-oxidized APMT (1100 °C, 24h). The present oxide scale is similar on both samples and consists of a mixture of Fe, Cr, Al oxides (*Figure 6-40* and *Figure 6-41*). Sulfur is found in the oxide while a \sim 60-100 μ m thick metal chloride layer is present between the oxide and alloy on both samples (*Figure 6-40* and *Figure 6-41*). No depletion of the alloying elements was detected in the alloy beneath the scale on both samples after 1000 hours exposure at 600 °C.

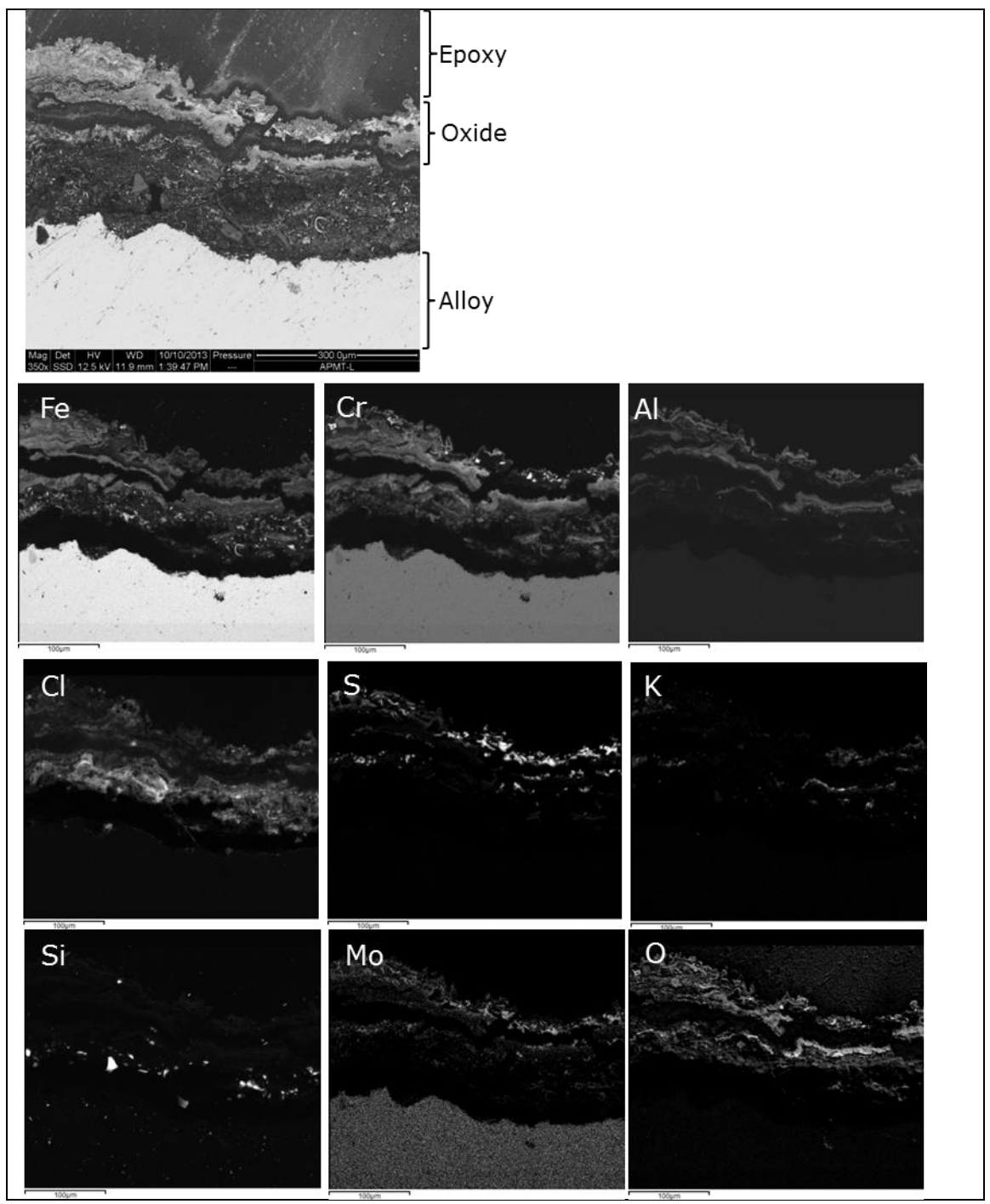


Figure 6-40. SEM-BSE image and elemental maps of the cross-section of APMT exposed for 1000 hours at 600 °C.

Figur 6-40. SEM-BSE bild och element kartor på tvärsnittet av APMT exponerad i 600 °C under 1000 timmar.

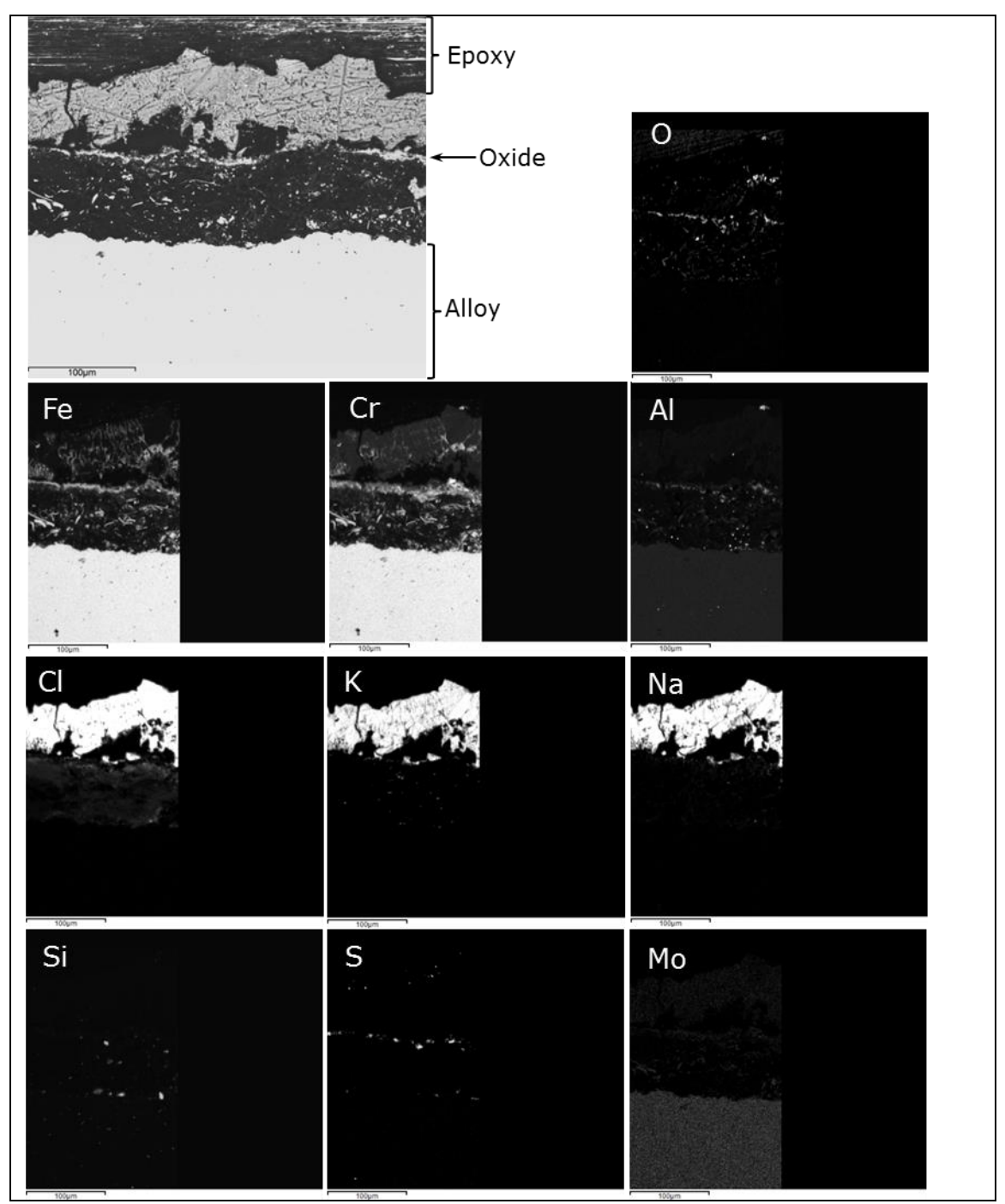


Figure 6-41. SEM-BSE image and elemental maps of the cross-section of pre-oxidized APMT (1100 $^{\circ}$ C for 24h) exposed for 1000 hours at 600 $^{\circ}$ C.

Figur 6-41. SEM-BSE bild och element kartor på tvärsnittet av föroxiderad APMT (1100 °C for 24h) exponerad i 600 °C under 1000 timmar.

Probes exposed at 700 °C for 24 hours.

The non-treated APMT coped better at 700 °C compared to 600 °C. The formed oxide at 700 °C seems denser and no iron-rich oxide is detected in the deposit layer as after 600 °C (compare *Figure 6-37*, *Figure 6-42* and *Figure 6-43*). The alloy tries to form a continuous alumina layer at least two times during the first 24 hours as can be seen in *Figure 6-43*. Instead of the desired alumina layer a mixed oxide of Fe,Al and Cr is formed similar as at 600 °C. Not as much metal chlorides were detected compared to 600 °C after 24 hours. Sulfur was detected at the oxide/alloy interface. Chromium rich metallic precipitates are detected in the alloy (*Figure 6-43*). Roughly 30 μ m of the alloy beneath the oxide scale is depleted in aluminium and chromium and is believed to be connected to the chromium-rich metallic precipitates.

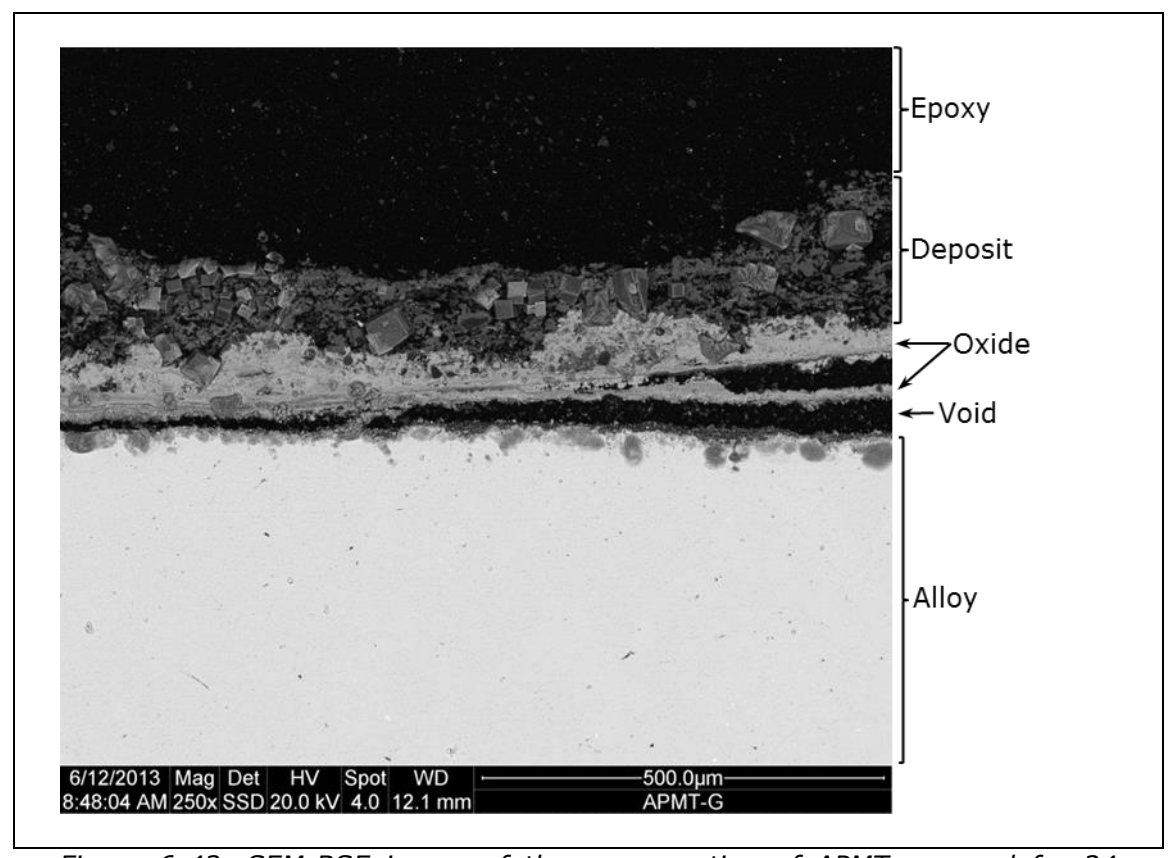


Figure 6-42. SEM-BSE image of the cross-section of APMT exposed for 24 hours at 700 °C.

Figur 6-42. SEM-BSE bild på tvärsnittet av APMT exponerad i 700 °C under 24 timmar.

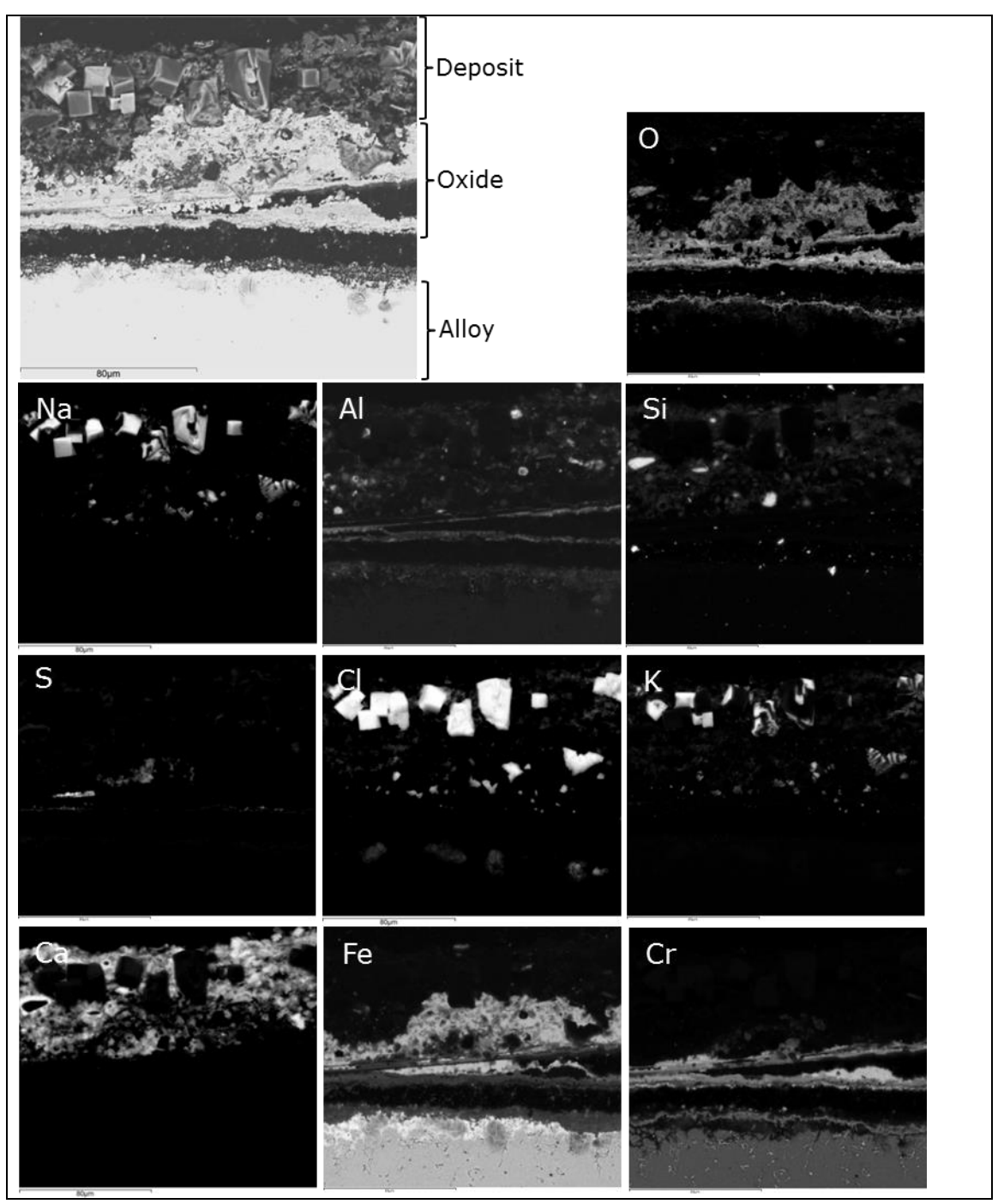


Figure 6-43. SEM-BSE image and elemental maps of the cross-section of APMT exposed for 24 hours at 700 °C.

Figur 6-43. SEM-BSE bild och element kartor av tvärsnittet på APMT exponerad i 700 °C under 24 timmar.

Pre-oxidized APMT (1100 °C for 24 h) exposed to 700 °C also coped better than the exposure at 600 °C. Nevertheless the alumina scale fails after only 24 hours of service in the boiler at 700 °C (*Figure 6-44*). The alumina scale from the pre-oxidation is considered protective at some parts of the sample surface where it still is in contact to the alloy with no iron-rich oxide underneath. The alumina scale however cracks with time (see *Figure 6-45*) and then the mixed oxide can start to form mainly inward underneath the alumina scale. The chromium rich metallic particles also form in the alloy on the pre-oxidized material. Sulfur is detected in the oxide scale and is believed to be sulfides of the alloying elements.

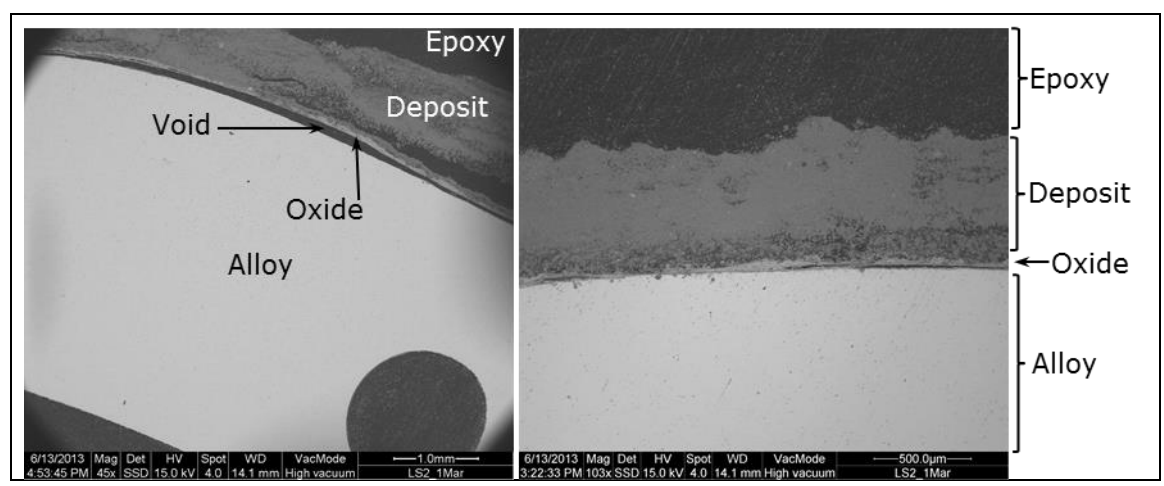


Figure 6-44. SEM-BSE images of the cross-section of pre-oxidized APMT (1100 °C for 24 h) APMT exposed for 24 hours at 700 °C.

Figur 6-44. SEM-BSE bilder på tvärsnittet av föroxiderad APMT (1100 °C for 24 h) exponerad i 700 °C under 24 timmar.

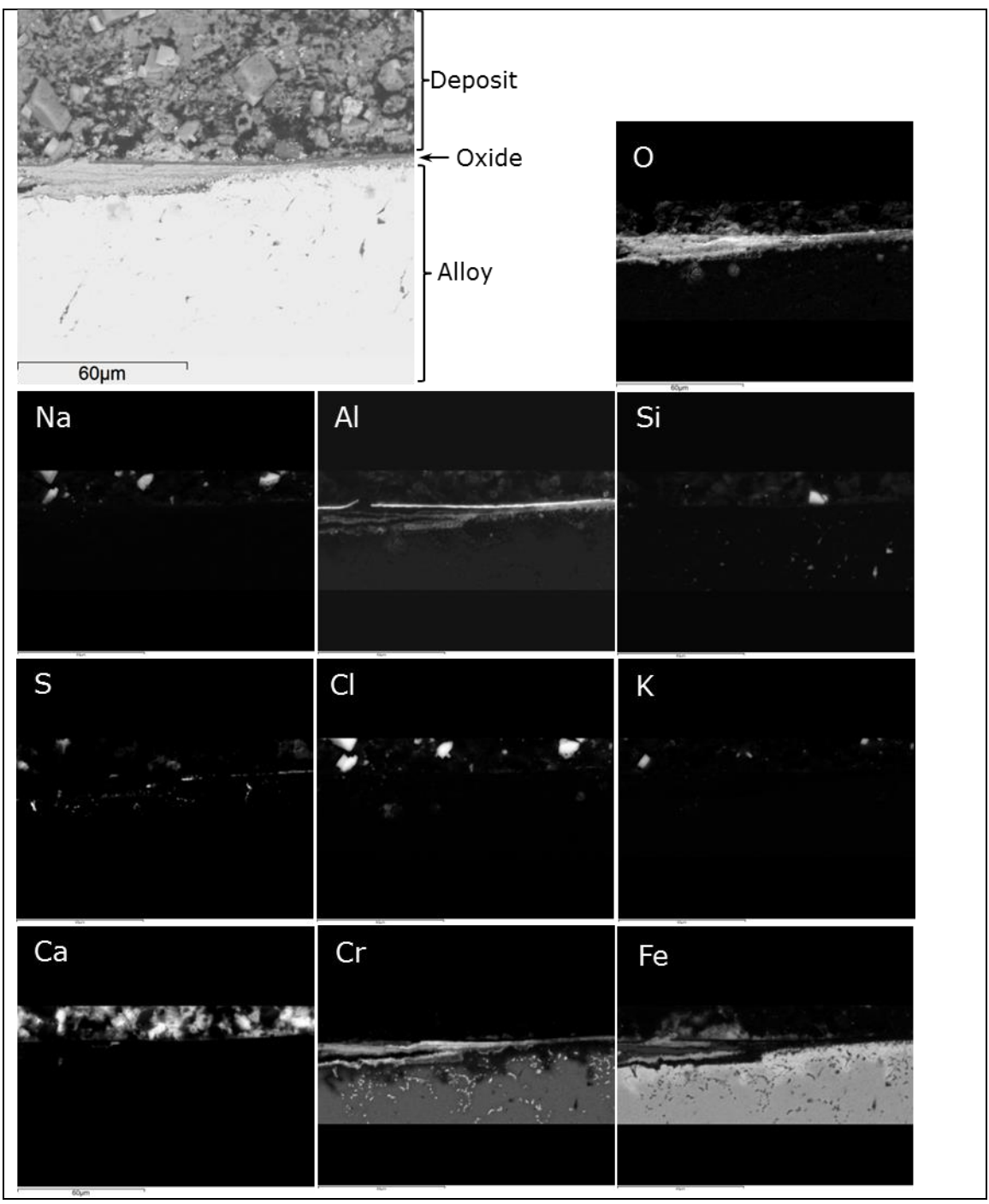


Figure 6-45. SEM-BSE image and elemental maps of the cross-section of pre-oxidized APMT (1100 °C for 24h) exposed for 24 hours at 700 °C.

Figur 6-45. SEM-BSE bild och element kartor på tvärsnittet av föroxiderad APMT (1100 °C for 24h) exponerad i 700 °C under 24 timmar.

Sandvik Heating Technologys standard pre-oxidation conditions (1050, 8h) was also tested throughout the exposures and was decided to be investigated further. The standard pre-oxidation (1050 °C, 8h) showed similar results as the sample pre-oxidized for 1100 °C for 24 hours (compare *Figure 6-44*, *Figure 6-45*, *Figure 6-46* and *Figure 6-47*).

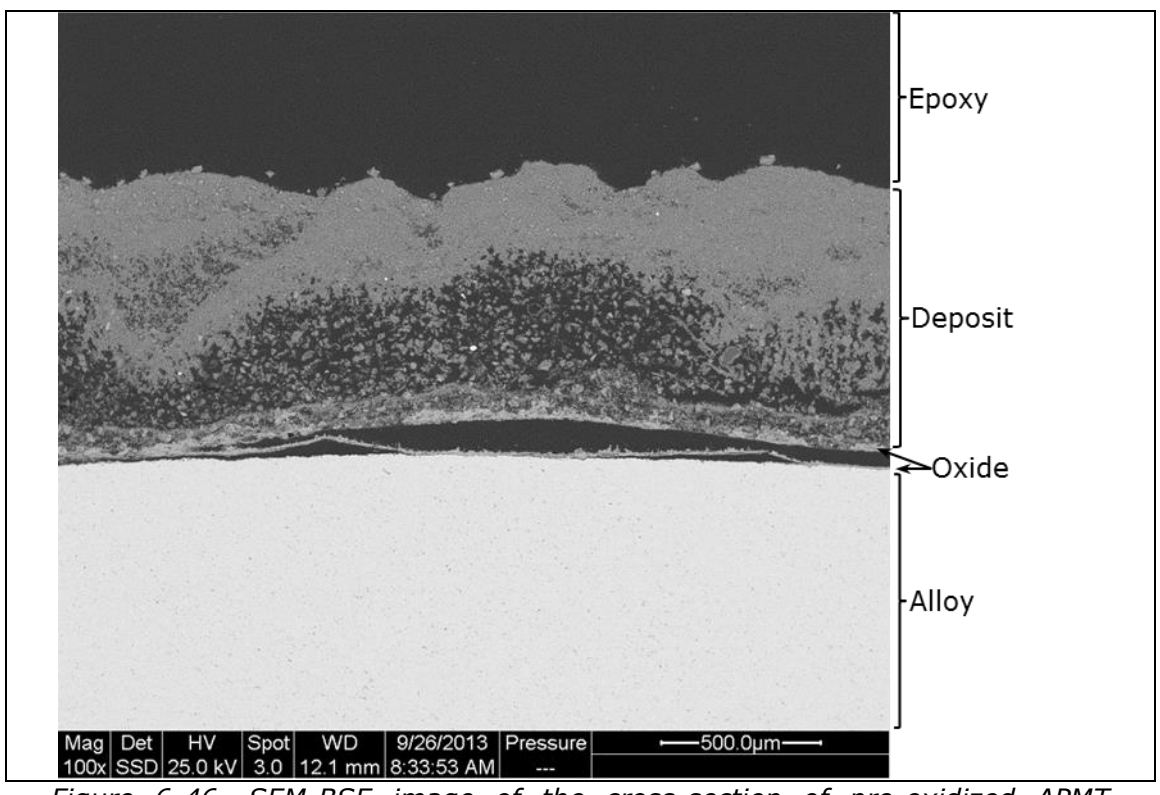


Figure 6-46. SEM-BSE image of the cross-section of pre-oxidized APMT (1050 °C for 8 h) APMT exposed for 24 hours at 700 °C.

Figur 6-46. SEM-BSE bilder på tvärsnittet av föroxiderad APMT (1050 °C for 8 h) exponerad i 700 °C under 24 timmar.

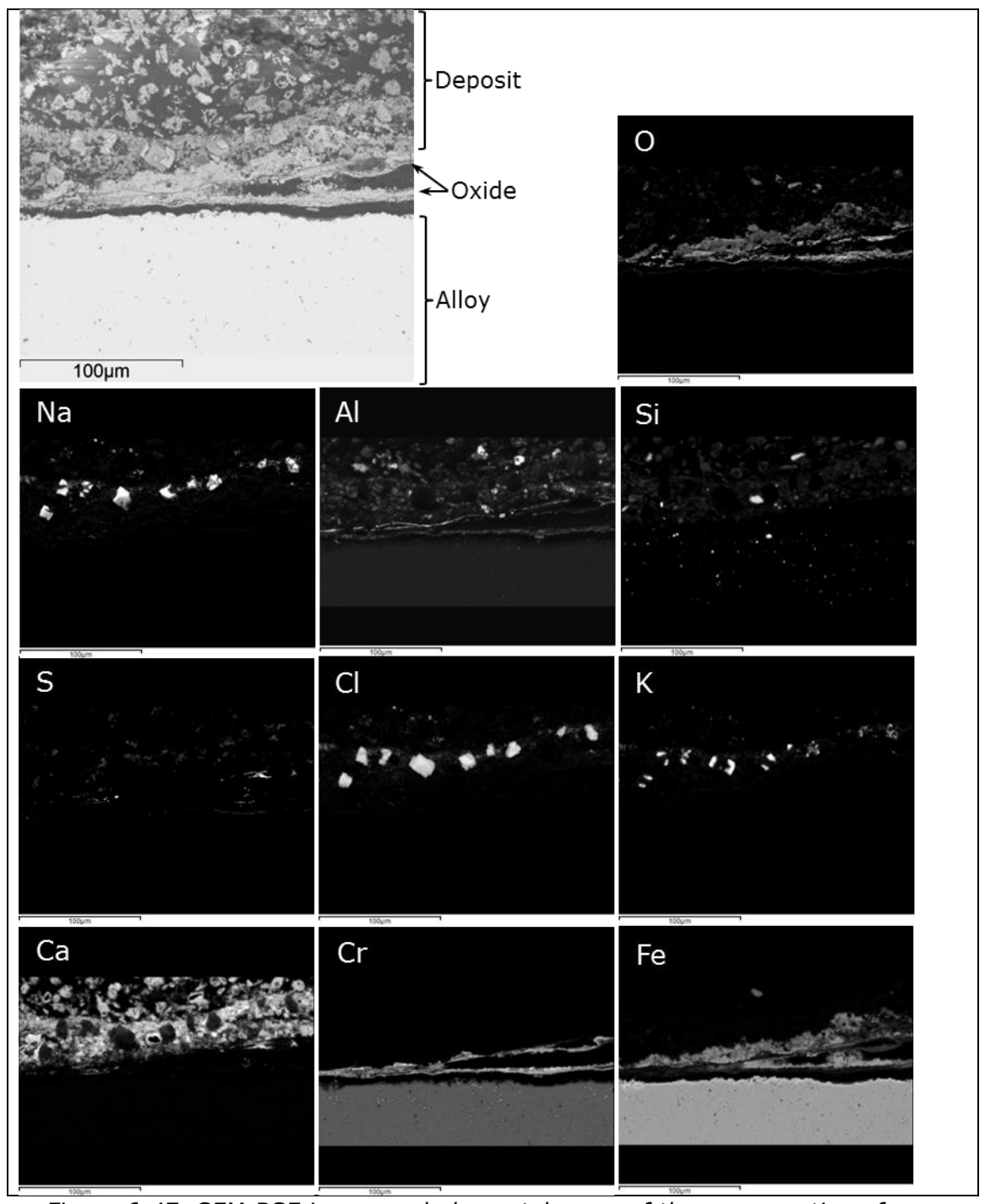


Figure 6-47. SEM-BSE image and elemental maps of the cross-section of pre-oxidized APMT (1050 $^{\circ}$ C for 8h) exposed for 24 hours at 700 $^{\circ}$ C.

Figur 6-47. SEM-BSE bild och element kartor på tvärsnittet av föroxiderad APMT (1050 °C for 8h) exponerad i 700 °C under 24 timmar.

San28 was chosen to add as a reference at 24 hours at 700 °C. Even on this material the oxide/deposit layer detaches from the surface on substantial amounts of the sample ring (*Figure 6-48*). An iron-rich oxide is present directly underneath the deposit layer which includes Na, K, Ca, Si and Cl. The deposit is most probably consisting mainly of NaCl, KCl, CaSO₄ which were detected by XRD (*Table 6-4* and *Table 6-5*). Underneath the iron-rich oxide an almost pure chromia layer is present. There is an oxidation affected zone in the alloy containing sulfur and oxygen with the alloying elements. Metal chlorides are also detected in the cross section (*Figure 6-49*).

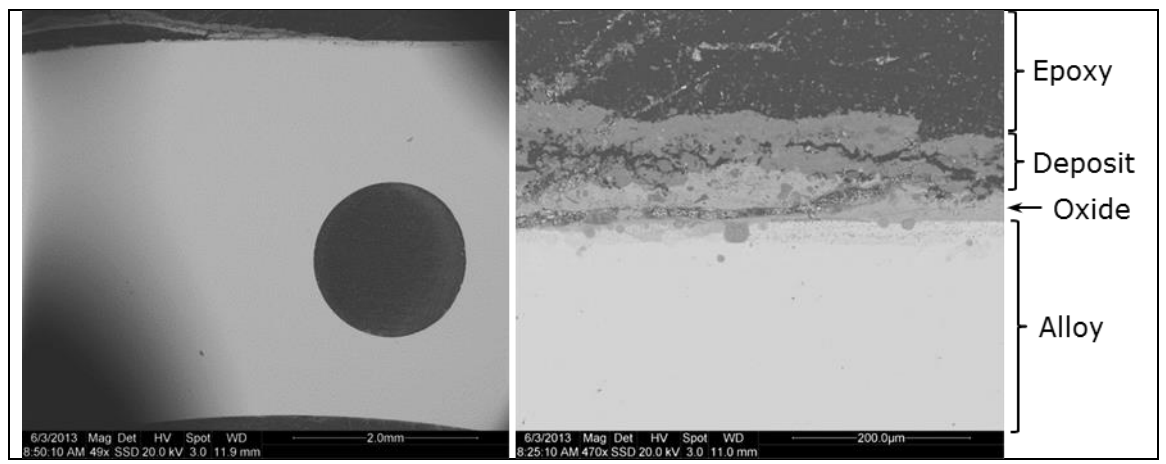


Figure 6-48. SEM-BSE images of the cross-section of San28 exposed for 24 hours at 700 °C.

Figur 6-48. SEM-BSE bilder på tvärsnittet av San28 exponerad i 700 °C under 24 timmar.

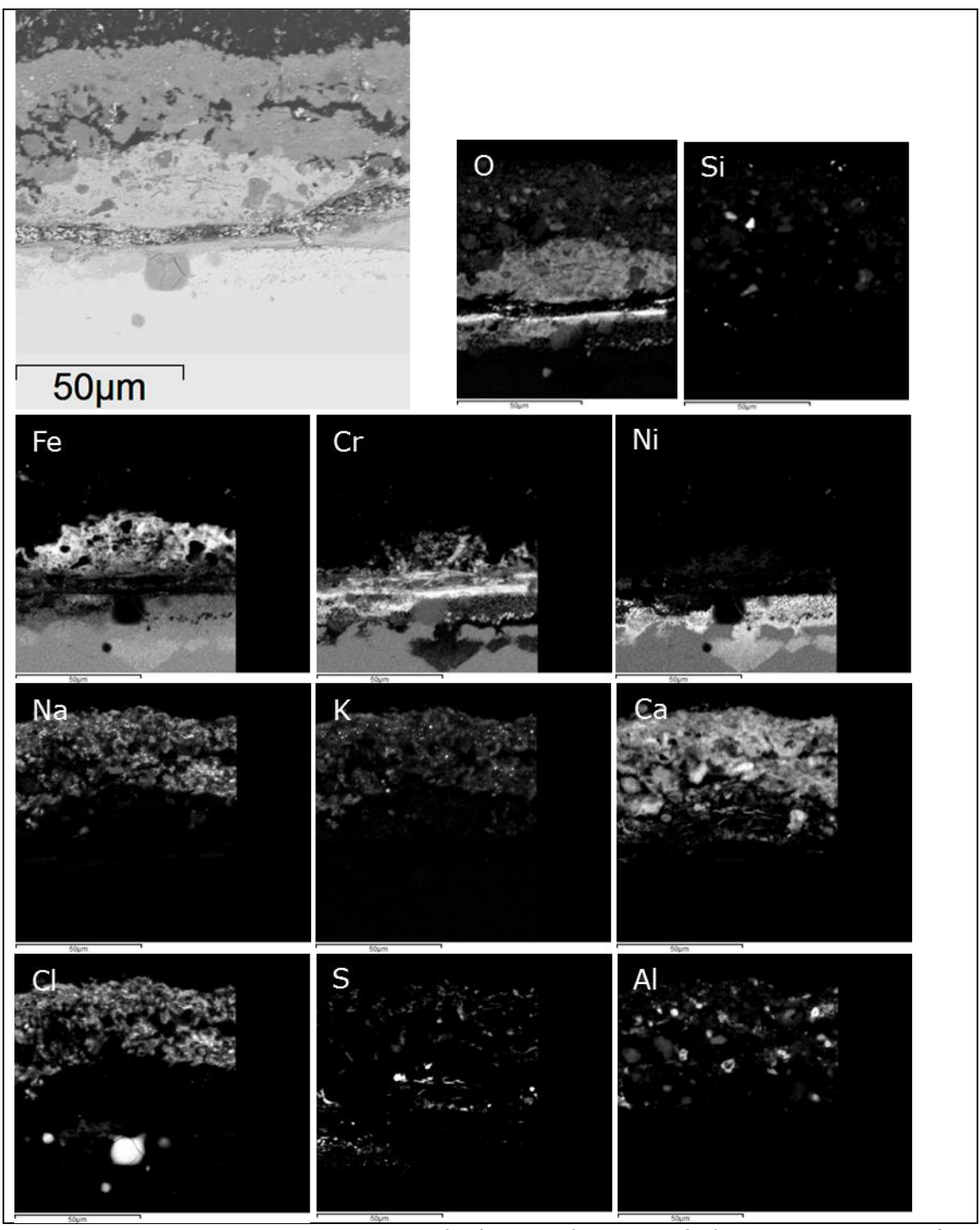


Figure 6-49. SEM-BSE image and elemental maps of the cross-section of San28 exposed for 24 hours at 700 °C.

Figur 6-49. SEM-BSE bild och element kartor på tvärsnittet av San28 exponerad i 700 °C under 24 timmar.

Probes exposed at 700 °C for 1000 hours.

No deposit was detected on the non-treated APMT after the boiler exposure at 700 °C for 1000 hours. A well adherent oxide scale is present on the alloy surface as can be seen in *Figure 6-50*. *Figure 6-51* reveals that the oxide scale is layered with an iron-rich oxide closest to the exposure environment and an aluminum/chromium-rich oxide closest to the alloy. Minor amounts of metal chlorides might be present and the chromium rich metallic particles are even more prominent after 1000 hours compared to 24 hours (compare *Figure 6-43* and *Figure 6-51*).

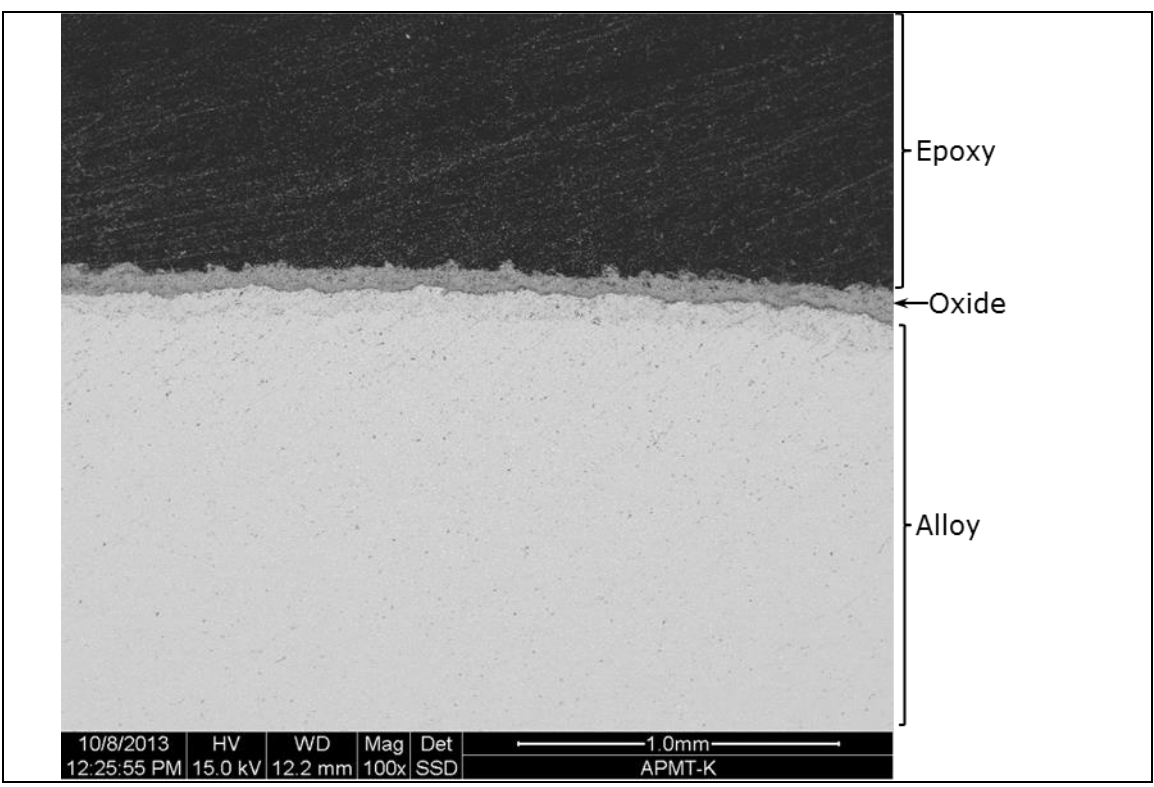


Figure 6-50. SEM-BSE image of the cross-section of APMT exposed for 1000 hours at 700 °C.

Figur 6-50. SEM-BSE bild på tvärsnittet av APMT exponerad i 700 °C under 1000 timmar.

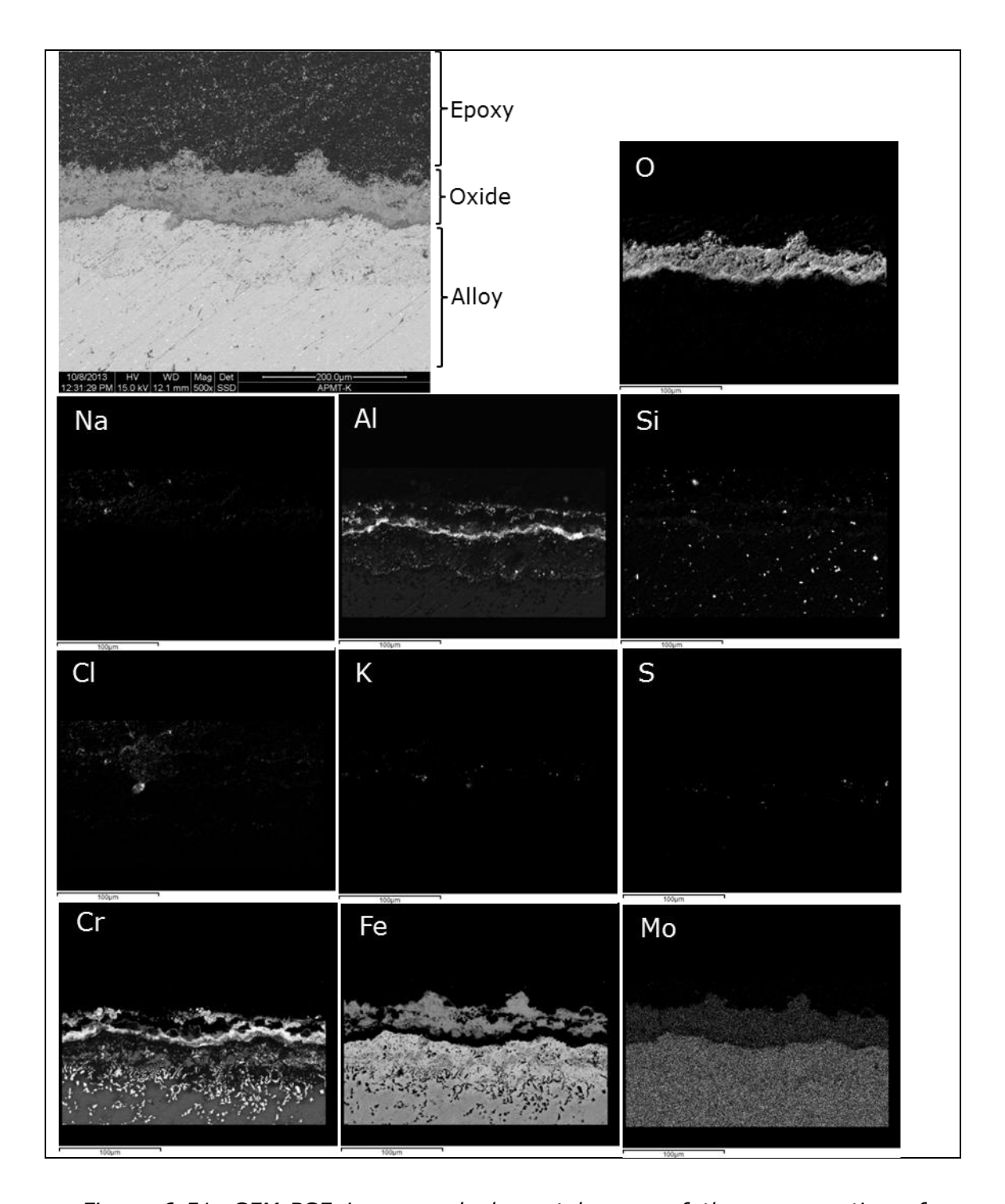


Figure 6-51. SEM-BSE image and elemental maps of the cross-section of APMT exposed for 1000 hours at 700 °C.

Figur 6-51. SEM-BSE bild och element kartor av tvärsnittet på APMT exponerad i 700 °C under 1000 timmar.

A roughly 600 μ m thick and porous oxide/deposit layer which has detached from the alloy is present on the pre-oxidized (1100 °C, 24h) sample after 1000 hours of exposure at 700 °C (*Figure 6-52*). The alumina scale from the pre-treatment was nowhere to be found. Instead a thick iron-chromium-rich oxide is present with an alumina enrichment at the oxide/alloy interface (*Figure 6-53*). Minor amounts of metal chlorides are present in the scale and sulfur is detected in the oxide/alloy interface. Sulfur signal also originates from the alloy bulk but is from the overlap between S and Mo, e.g. no sulfur is in the alloy matrix.

A roughly 50 μ m thick oxidation affected zone is present in the alloy substrate which contains aluminum nitride particles according to SEM/EDX point analyses (not shown). It is believed that the AIN formation depletes the surrounding alloy in aluminum and the chromium rich metallic phase forms which also contain iron and molybdenum according to SEM/EDX point analyses.

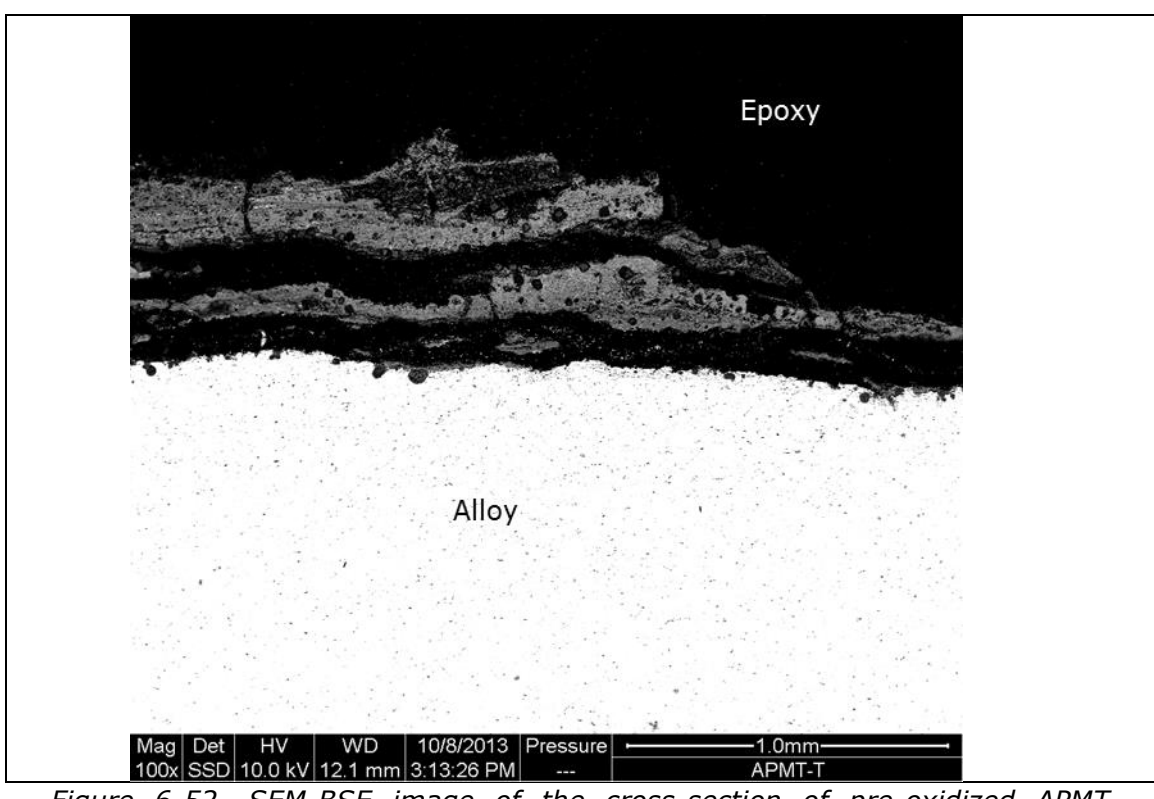


Figure 6-52. SEM-BSE image of the cross-section of pre-oxidized APMT (1100 °C for 24 h) APMT exposed for 1000 hours at 700 °C.

Figur 6-52. SEM-BSE bilder på tvärsnittet av föroxiderad APMT (1100 °C for 24 h) exponerad i 700 °C under 1000 timmar.

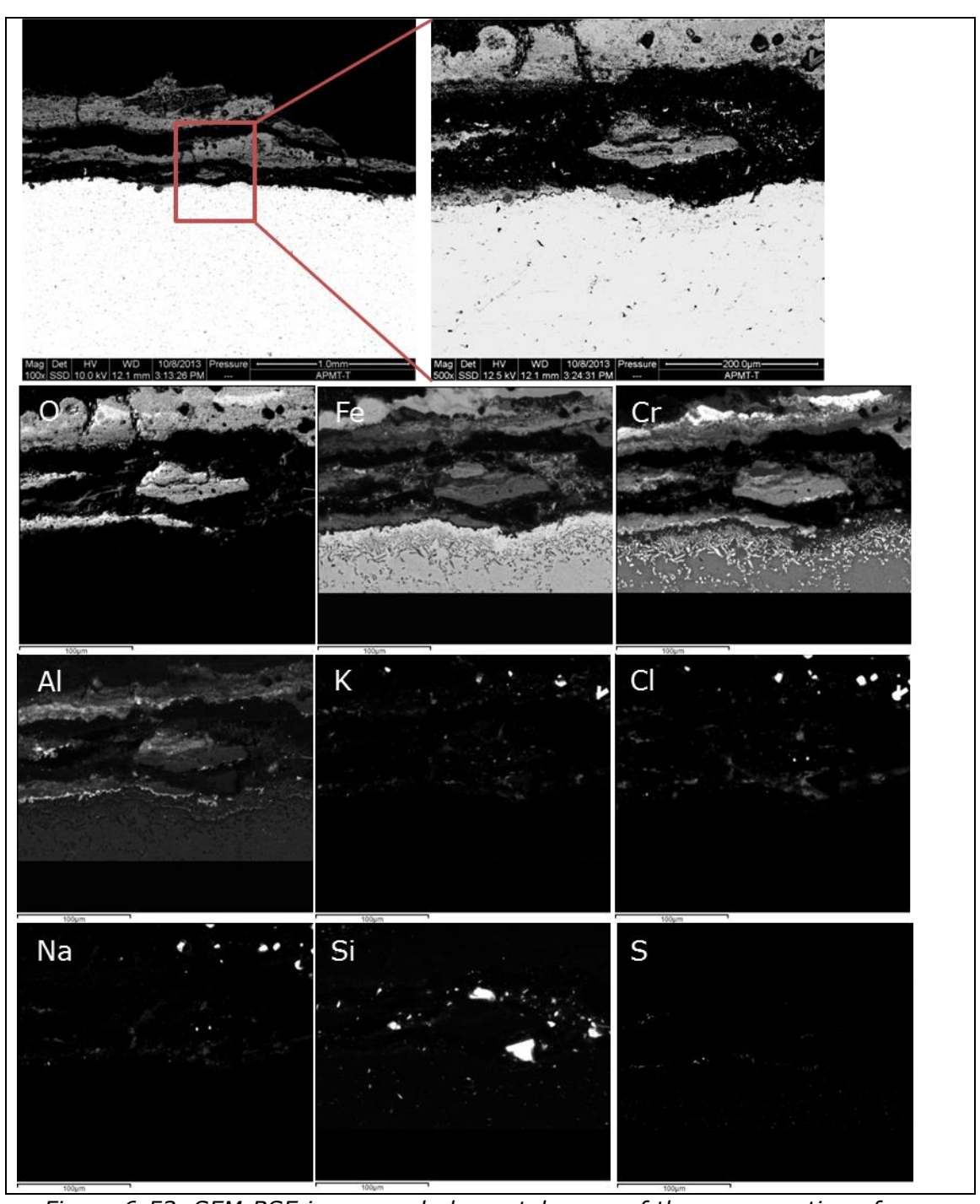


Figure 6-53. SEM-BSE image and elemental maps of the cross-section of preoxidized APMT (1100 °C for 24h) exposed for 1000 hours at 700 °C.

Figur 6-53. SEM-BSE bild och element kartor på tvärsnittet av föroxiderad APMT (1100 °C for 24h) exponerad i 700 °C under 1000 timmar.

6.2.2 Thermal shield tubes, Händelö and Idbäcken

Thermal shield tubes exposed at Händelö

The thermo element shield tubes exposed at Händelö were measured before exposure at 3 locations spread over the length of the tube. The tube thicknesses were similar over the entire length before exposure. After exposure the tube were measured again at the same locations and at an additional location were the tube were thinnest, e.g., were the largest metal loss had taken place. Images were taken of the tubes after being exposed from 2011-07-25 to 2011-11-11, when the tubes were taken out during a temporary shutdown of the boiler. In addition, images were also taken of the tubes after the exposure was finished. The tip of the thermal shield tubes were cut off and analyzed with XRD, see *Table 6-6*. These images and results are shown below.

Results for the thermal shield tubes exposed at the position KT024 and KT020 in the Händelö boiler P14, are shown in Figure 6-54. These thermal shield tubes are compared to each other because they are of different materials (IN 625 and pre-oxidized APMT) and are exposed at similar temperature (~810°C and ~840°C, respectively) at similar position in the boiler (see, Figure 5-12, Figure 5-13 and Figure 6-54). The images acquired 2011-12-05 shows that a thin yellowish deposit covered large parts of the surface of the material of both thermal shield tubes. The images acquired 2012-04-15 (Figure 6-55, Figure 6-56, and Figure 6-54) and the measurements of the diameter show that the material loss was larger on the pre-oxidized APMT material than on the IN 625, with a diminishment of the diameter of 5.1 and 1.6 mm, respectively. The most of the material of the thermal shield tubes were lost close to the wall of the boiler, as evident by the images acquired after the exposure. After exposure, the IN 625 material was more or less covered by a greenish oxide, and a thin layer of deposit covered some parts of the surface. The greenish oxide indicates the formation of NiO, which was confirmed by XRD, see Table 6-6. The thermal shield tube at the positions KT020 (APMT) was rust colored close to the boiler wall, the rest of the tube was covered with a thin yellowish deposit and rust-colored flaked areas. The XRD indicates the presence of iron-containing oxide ($(Fe,AI,Cr)_2O_3$), but also a weak peak corresponding to a-Al₂O₃ (Table 6-6). This aluminum oxide is probably not protective anymore judging from the rust-colored surface. Both IN 625 and APMT show medium strong peaks corresponding to the base material, indicating a similar scale thickness on both materials.

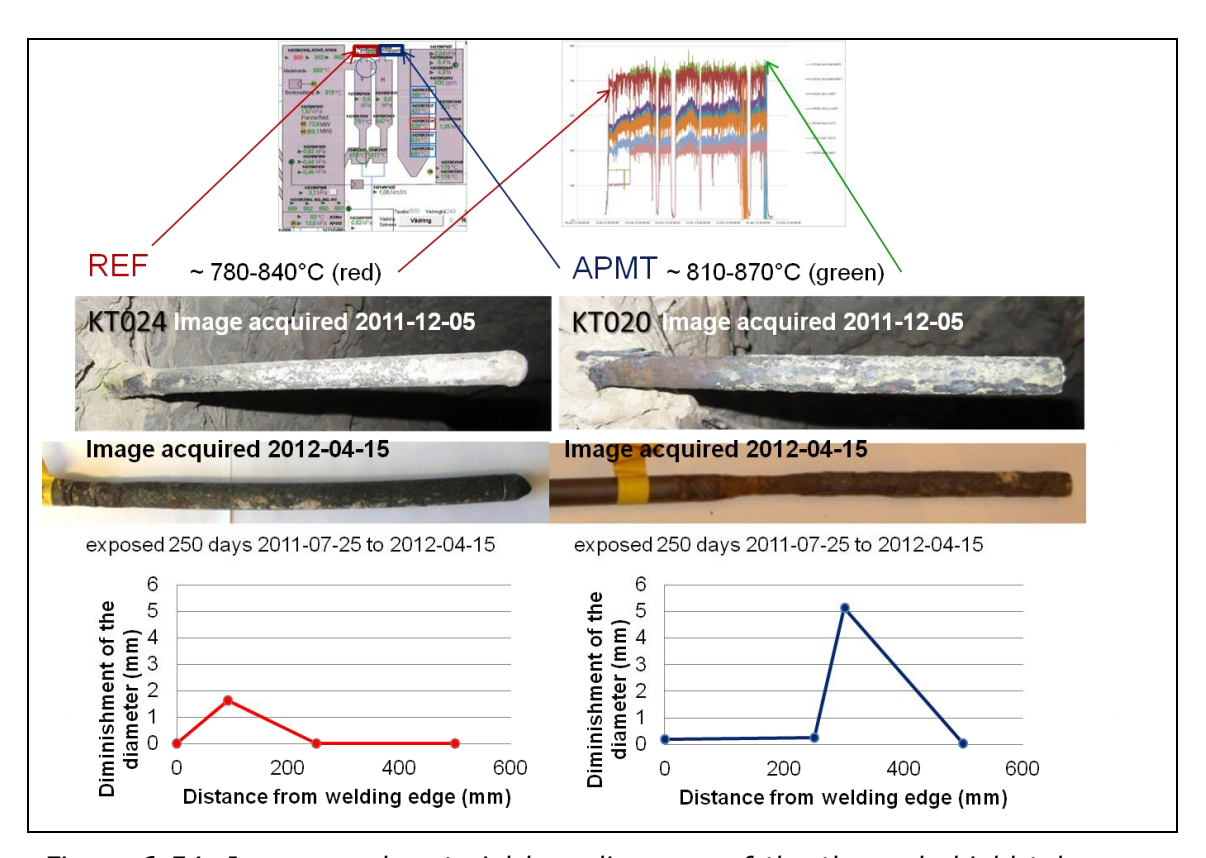
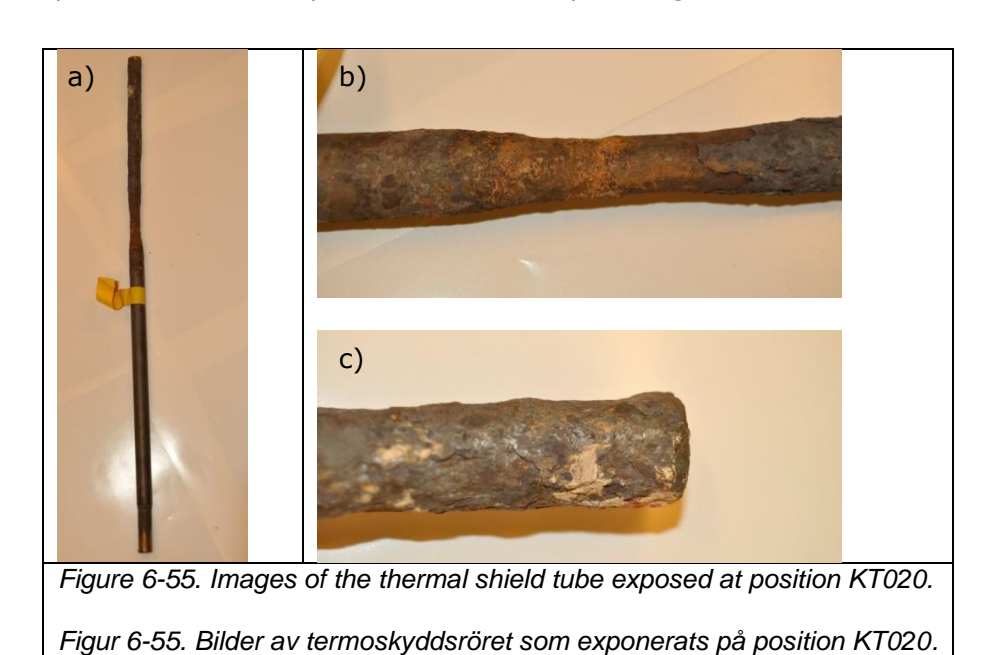


Figure 6-54. Images and material loss diagrams of the thermal shield tubes exposed at the positions KT020 and KT024, together with illustrations of the position and temperature during the exposure.

Figur 6-54. Bilder och materialförlustdiagram för termoskyddsrören som exponerats på position KT020 och KT024, tillsammans med illustration av positionen och temperaturen under exponeringen.



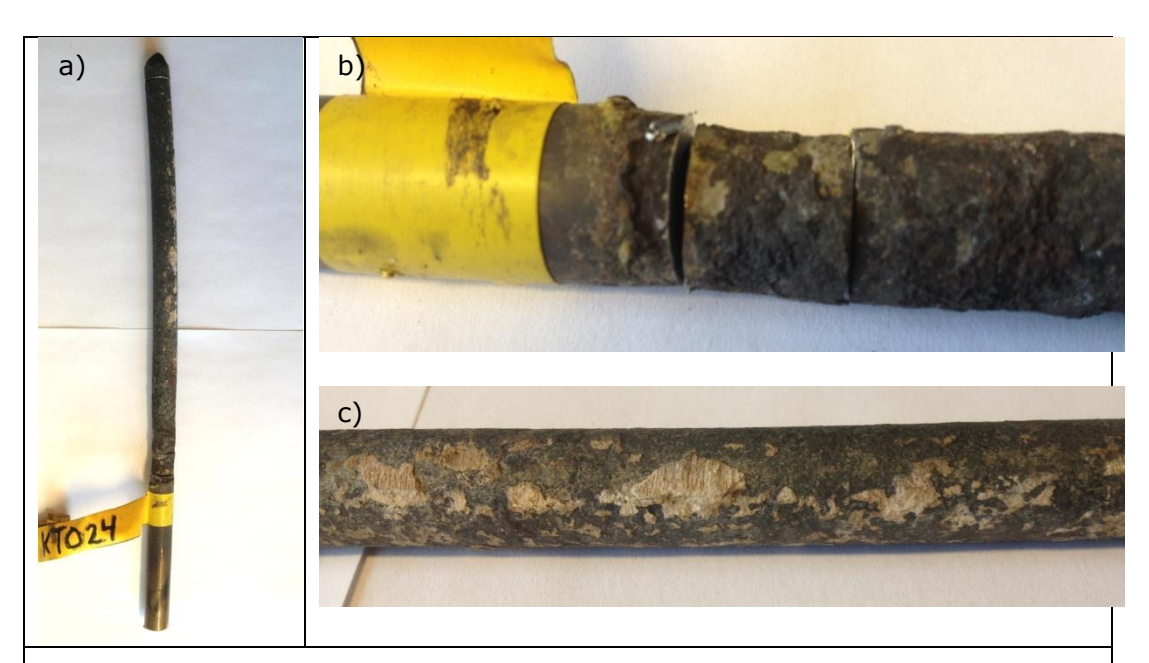


Figure 6-56. Images of the thermal shield tube exposed at position KT024. Figur 6-56. Bilder av termoskyddsröret som exponerats på position KT024.

				Deposit		
	a- Al ₂ O ₃	(Fe,Al,Cr) ₂ O ₃	substrate	KCl	NaCl	(Na,K)Cl
KT020	W	S	М			М
KT034	W	S	S	W	W	
KT037	1 peak	S	S	W	W	
KT041:1	М	W	S		W	
KT043		М	S			
					Deposit	
	NiO	NiCrFeO ₄	(Fe,Cr) ₂ O ₃	substrate	KCI	NaCl
KT024	S	М	W	M	М	S
KT039:1	S	W	М		S	S
KT039:2	S	S	М			W
KT041:Ö	S	S	М		S	W

Table 6-6. Results from XRD analyses of the tip of the thermal shield tubes exposed at Händelö. S, M and W denote strong, medium or weak intensity of the diffraction peaks.

The thermal shield tube, KT043, was made of pre-oxidized APMT and placed on the fifth floor of the boiler facility where the temperature was relatively 590° C. According to the measurements, KT043, narrowed increasingly from the welding edge to the tip of the probe, with a maximum material loss of 3.2 mm (*Figure 6-57*). Thus, the maximum material loss was significantly lower for KT043 exposed at ~590°C than for KT020 exposed at ~840°C. The surface color of KT043 was similar to that of KT020, a large proportion of the surface was rust-colored (*Figure 6-36* and *Figure 6-57*). The XRD analysis of KT043 showed peaks corresponding to iron-oxide ((Fe,Al,Cr)₂O₃) and a strong peak corresponding to the substrate (*Table 6-6*), indicating a thin layer of rust on the material surface.

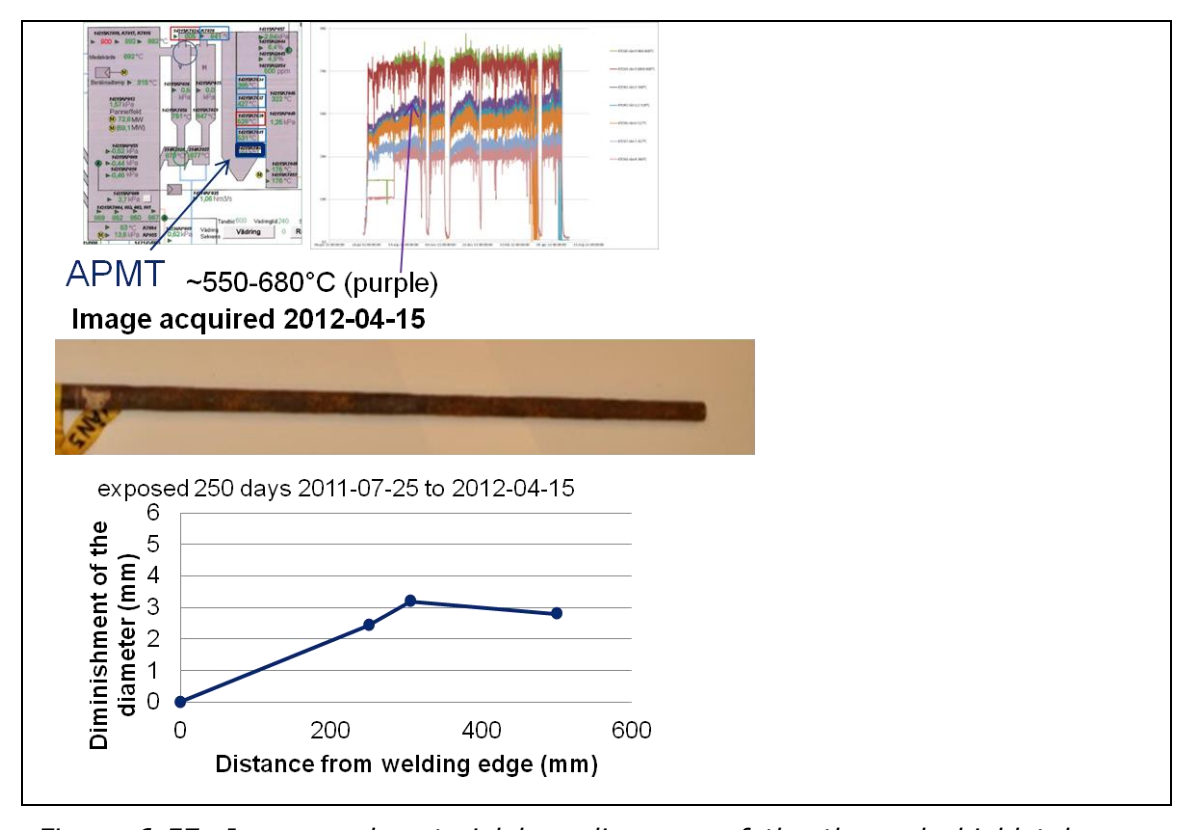


Figure 6-57. Image and material loss diagrams of the thermal shield tube exposed at the positions KT043, together with illustrations of the position and temperature during the exposure.

Figur 6-57. Bild och materialförlustdiagram för termoskyddsröret som exponerats på position KT043, tillsammans med illustration av positionen och temperaturen under exponeringen.



Figure 6-58. Images of the thermal shield tube exposed at position KT043. Figur 6-58. Bilder av termoskyddsröret som exponerats på position KT043.

Figure 6-59 shows the results for the thermal shield tubes at the positions KT034 and KT037. These thermal shield tubes were made of pre-oxidized APMT and the exposure temperature were approximately 410°C and 450°C, respectively. On the images acquired 2011-12-05, both thermal shield tubes appear intact. KT034 was covered by a thin layer of deposit, whereas KT037 had a thick layer of deposit built up on the side facing the wind. After the whole exposure time the thermal shield tubes still appeared intact and yellowish deposit covered parts of the surfaces (Figure 6-59, Figure 6-60, and Figure 6-61). The maximum material loss was measured to be 0.34 mm and 0.42 mm, respectively. These values are significantly lower than for the thermal shield tube at the position KT043 where the temperature is about 150°C higher. The XRD analyses showed similar results for both tubes (Table 6-6). The substrate peak was strong, indicating a thin oxide on the material. Peaks corresponding to the oxides (Fe,Al,Cr)₂O₃ and α -Al₂O₃ were found, indicating the presence of a protective oxide on the material surfaces.

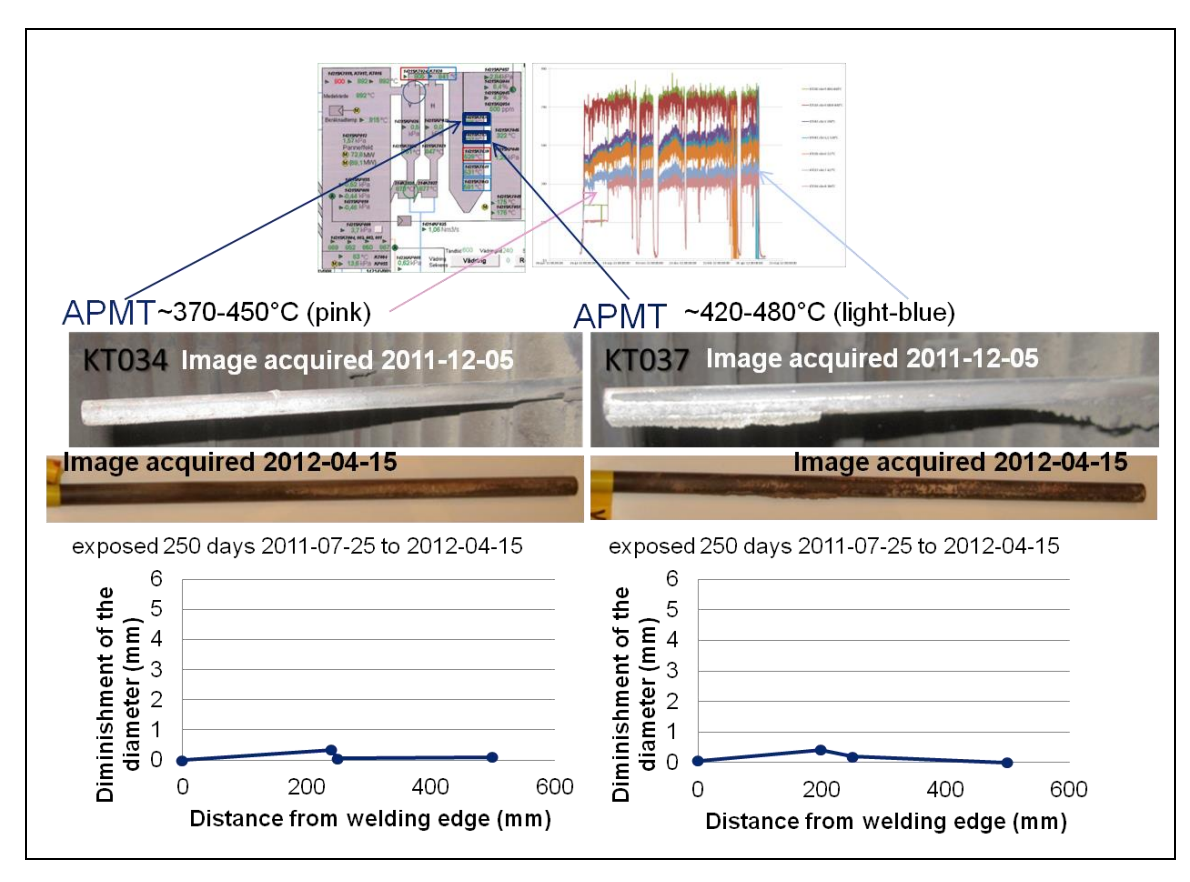


Figure 6-59. Image and material loss diagrams of the thermal shield tubes exposed at the positions KT034 and KT037, together with illustrations of the positions and temperatures during the exposure.

Figur 6-59. Bild och materialförlustdiagram för termoskyddsrören som exponerats på positionerna KT034 och KT037, tillsammans med illustration av positionerna och temperaturerna under exponeringen.



Figur 6-60. Bilder av termoskyddsröret som exponerats på position KT034.

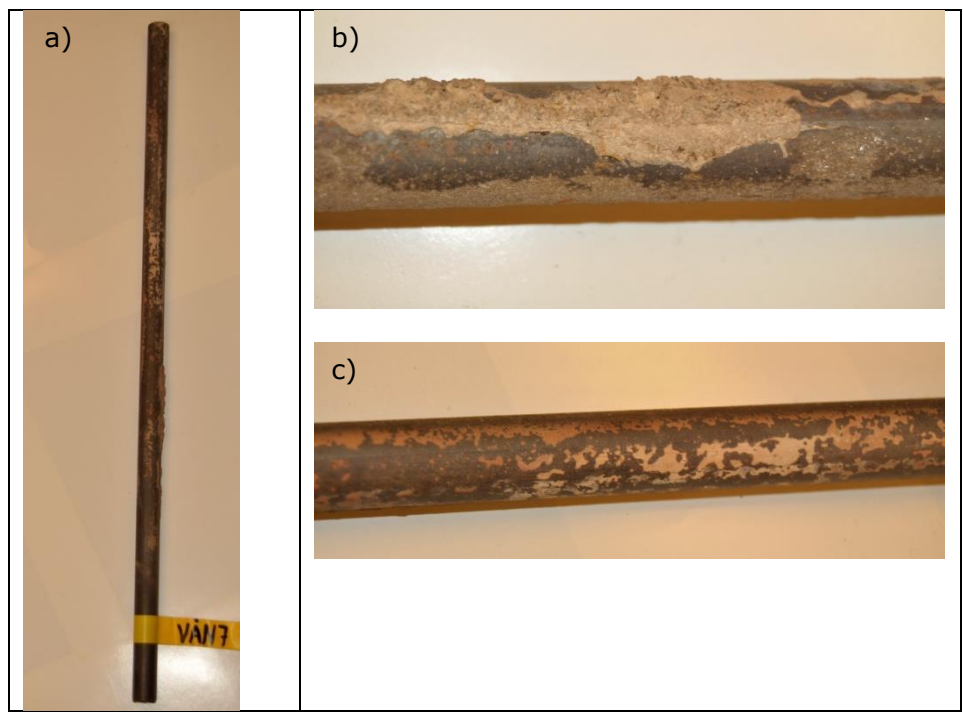


Figure 6-61. Images of the thermal shield tube exposed at position KT037. Figur 6-61. Bilder av termoskyddsröret som exponerats på position KT037.

Figure 6-62 shows the results for the thermal shield tubes at the positions KT039 and KT041. These thermal shield tubes were made of different materials, IN 625 and pre-oxidized APMT, respectively and the exposure temperature were approximately 560°C and 590°C, respectively. KT041 was placed between the fifth and sixth floors of the boiler. Because of its placement near KT039 (situated at the sixth floor), this rod was removed for comparison purposes when KT039 was removed because of failure. The original KT041 rod will be called KT041:1, and the original KT039 rod will be called KT039:1. Both rods was replaced after removal by rods made of Inc 625 and they will be called KT041:Ö and KT039:2, respectively. Measurements of KT041:1 prior to and after exposure can be found in Figure 6-62. A decrease in diameter of about half a millimeter was recorded, which is two and a half millimeter less than that of the reference rod KT039:1. Almost the entire surface of the rod KT041:1 was covered with a rust-colored coating (Figure 6-62 and Figure 6-63). XRD showed strong peaks corresponding to the base material, indicating a thin oxide scale. This was reinforced by the findings of peaks corresponding to a-Al₂O₃, peaks corresponding to $(Fe,Al,Cr)_2O_3$ were also found (*Table 6-6*). The thermal shield tube at the position KT039 had a thin light colored deposit on the surface and rust colored corrosion products. Close to the boiler wall a significant material loss can be observed (Figure 6-62 and Figure 6-64). In addition, visual analysis reveals a hole in the rod. XRD showed no peaks corresponding to the substrate, but peaks for the un-protective NiO (Table 6-6). Some peaks corresponding to NiCrFeO₄ and (Fe,Cr)₂O₃ were also found.

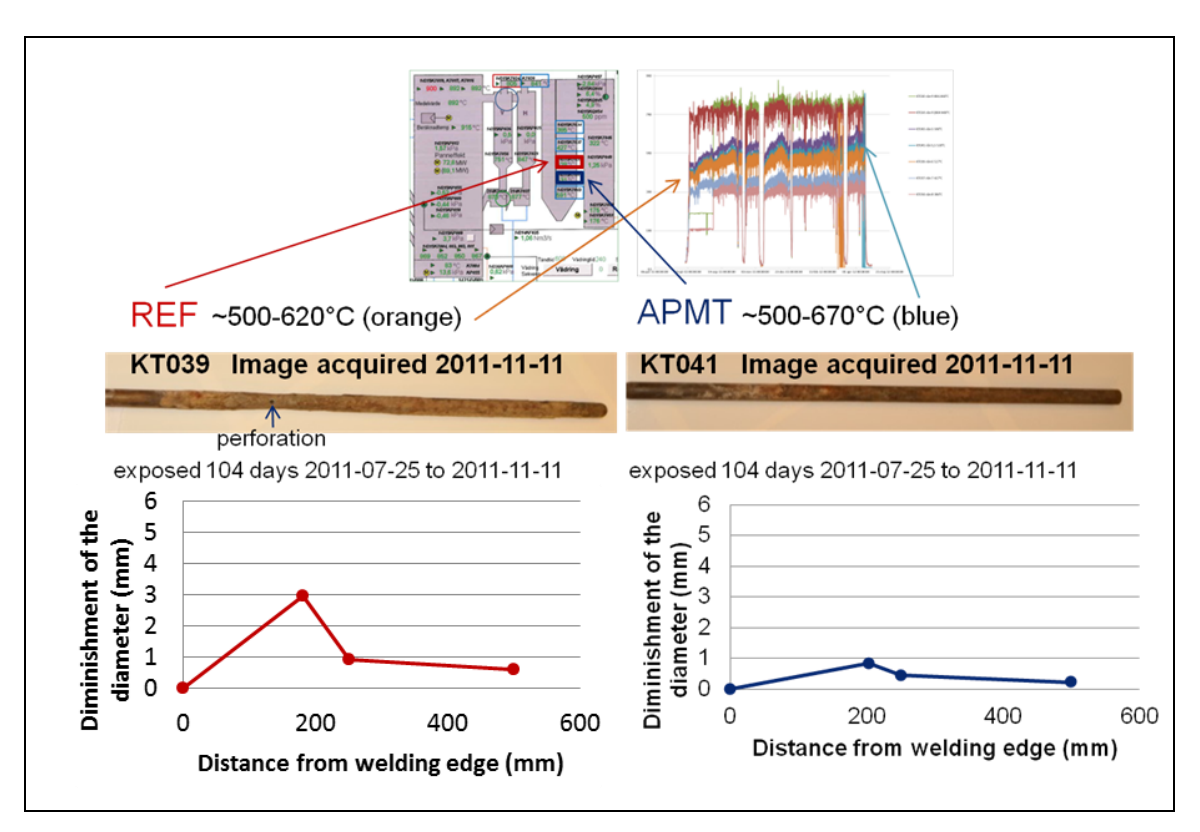


Figure 6-62. Image and material loss diagrams of the thermal shield tubes exposed at the positions KT039:1 and KT041:1, together with illustrations of the positions and temperatures during the exposure.

Figur 6-62. Bild och materialförlustdiagram för termoskyddsrören som exponerats på positionerna KT039:1 och KT041:1, tillsammans med illustration av positionerna och temperaturerna under exponeringen.

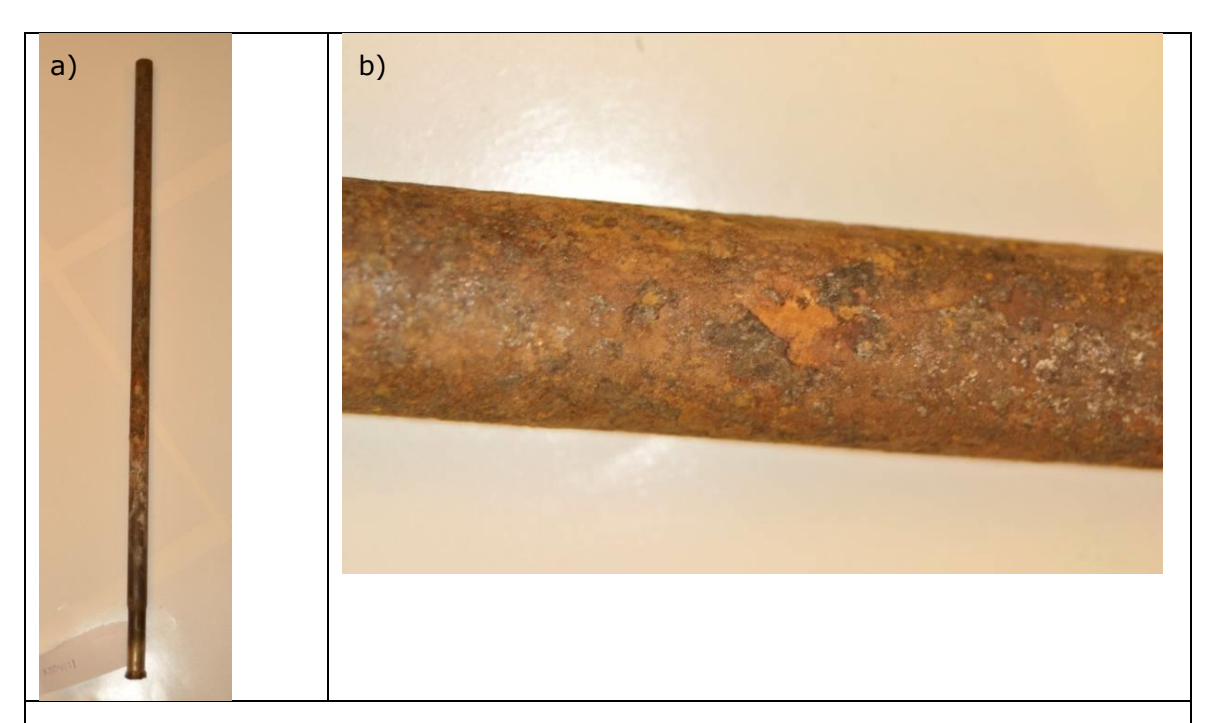


Figure 6-63. Images of the thermal shield tube exposed at position KT041:1. Figur 6-63. Bilder av termoskyddsröret som exponerats på position KT041:1.

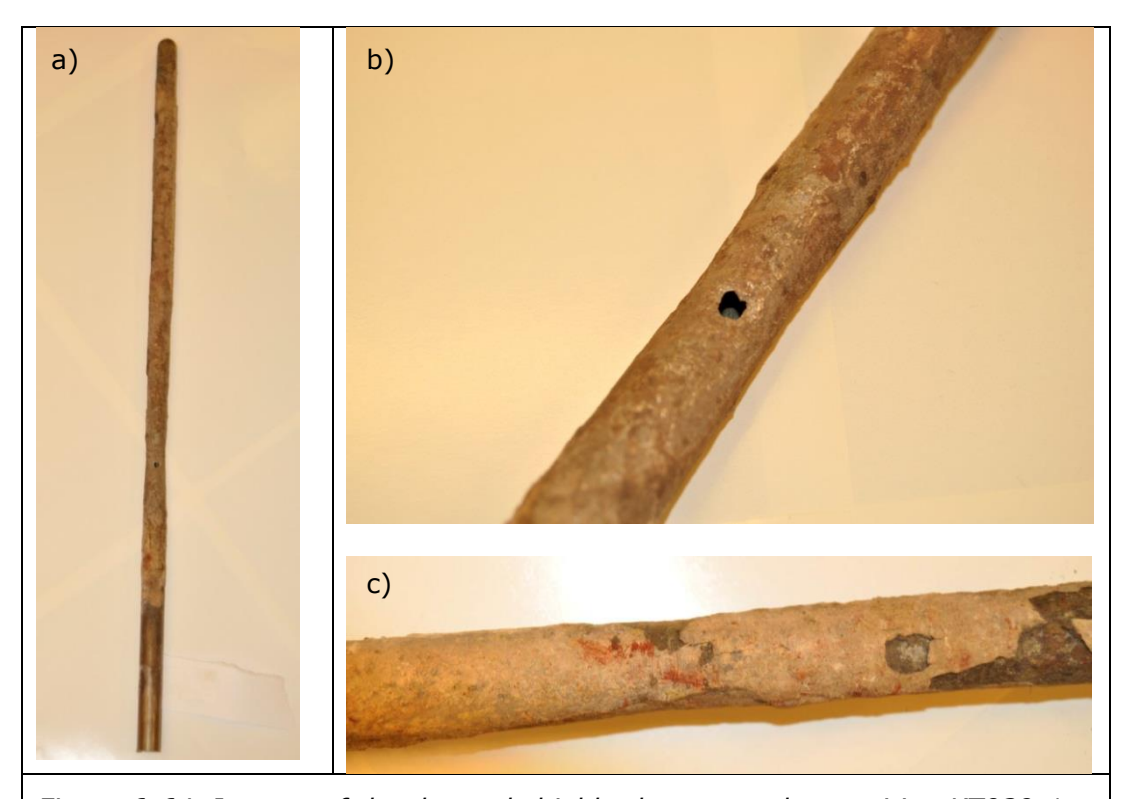


Figure 6-64. Images of the thermal shield tube exposed at position KT039:1. Figur 6-64. Bilder av termoskyddsröret som exponerats på position KT039:1.

KT041:Ö (inc 625) was in place from the time of removal of KT041:1 until removal of all rods for analysis, approximately 156 days. According to the diameter measurements, severe deterioration of KT041:Ö occurred. This is reinforced by the images in *Figure 6-65* and *Figure 6-66*. The surface of the rod corroded completely leaving an opening to center where the thermal element is placed. Also, a red colored corrosion product can be seen along with a yellowish deposit and gray areas in *Figure 6-66*.

The diameter of the rod KT039:2 had decreased with more than 8 mm after exposure which lasted for 118 days (*Figure 6-65*), as compared to 1 mm after 104 days of exposure mentioned above. The deterioration of KT039:2 is quite extense, as can be seen in *Figure 6-66*. The small section seen in *Figure 6-67* b reveals an area where large amounts of the rod have completely deteriorated. Yellowish and rust colored corrosion products can also be seen. The yellow color indicates the formation of chromates.

XRD analysis of the tip of both rods, KT039:2 and KT041:ö, showed no peaks corresponding to the substrate material but strong peaks for the un-protective oxide NiO (*Table 6-6*). In addition peaks corresponding to spinell oxide and corundum iron oxide were detected.

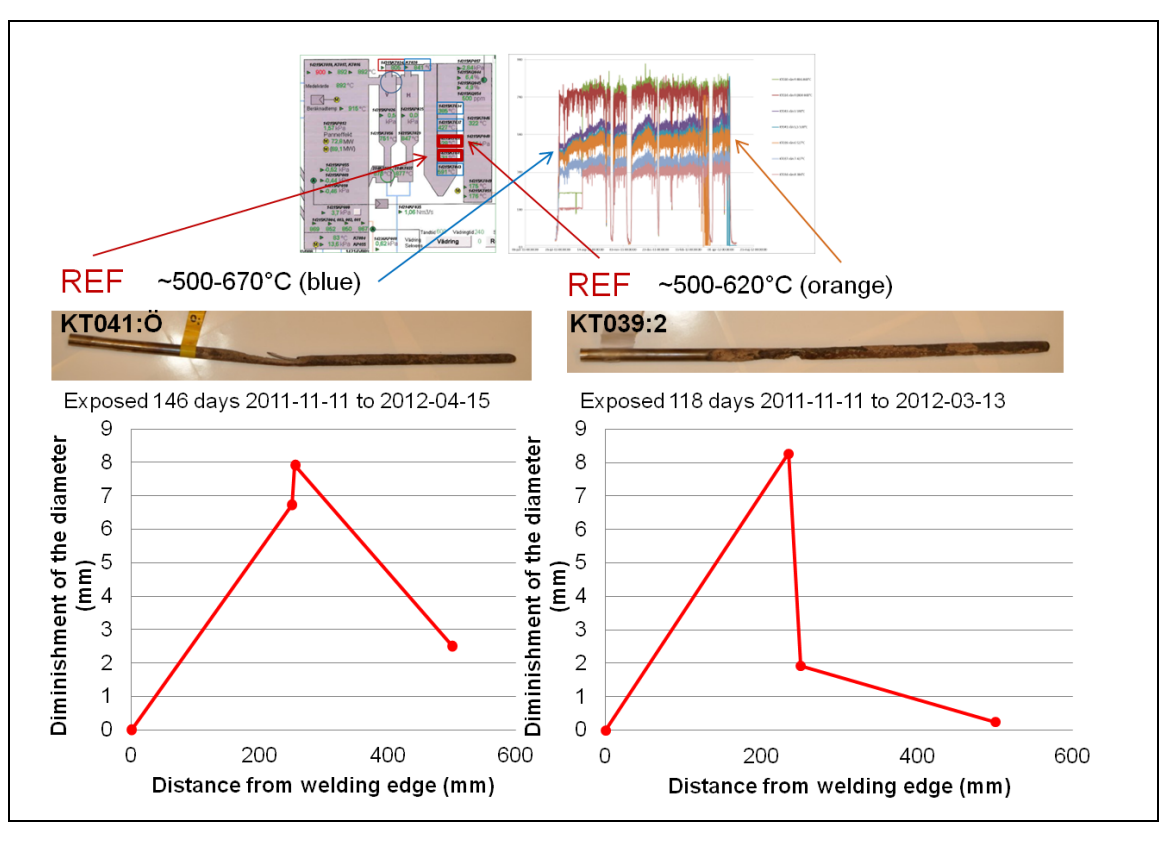


Figure 6-65. Image and material loss diagrams of the thermal shield tubes exposed at the positions KT039:2 and KT041:Ö, together with illustrations of the positions and temperatures during the exposure.

Figur 6-65. Bild och materialförlustdiagram för termoskyddsrören som exponerats på positionerna KT039:2 och KT041:Ö, tillsammans med illustration av positionerna och temperaturerna under exponeringen.

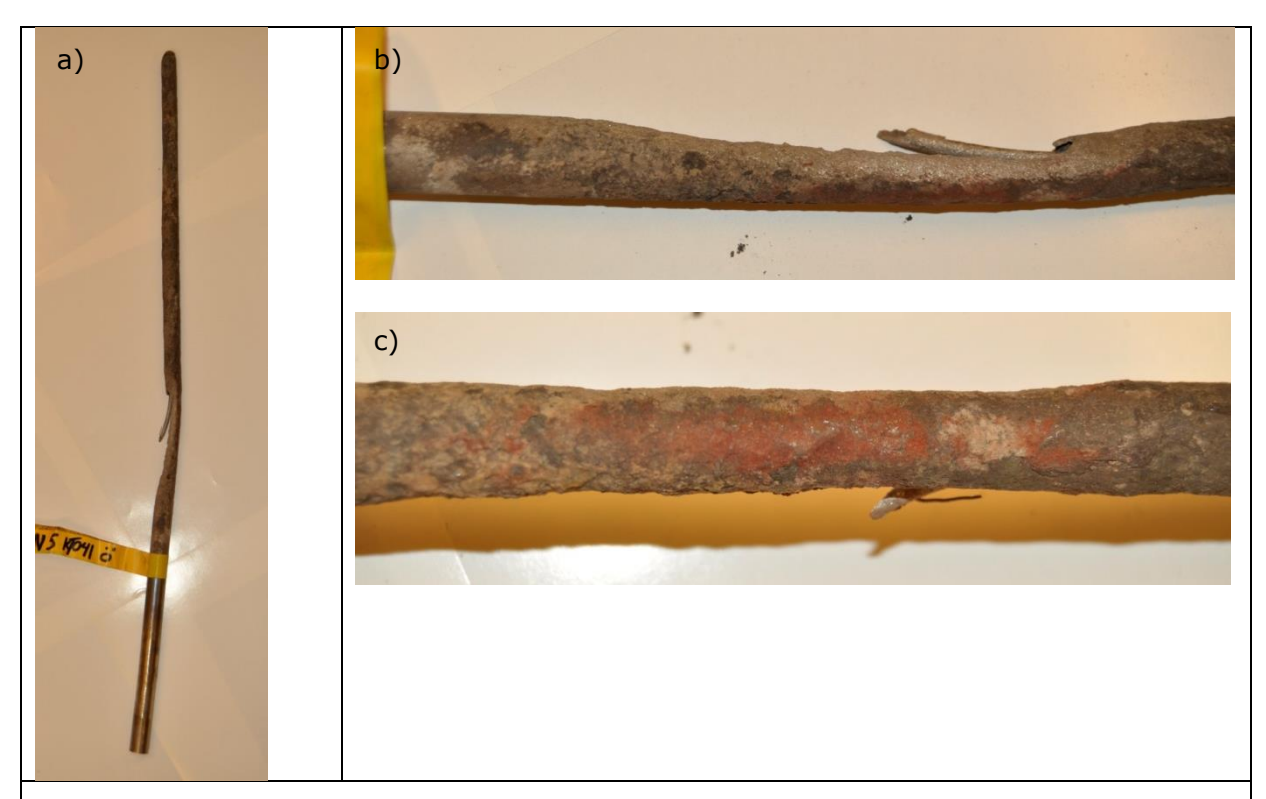


Figure 6-66. Images of the thermal shield tube exposed at position KT041:Ö. Figur 6-66. Bilder av termoskyddsröret som exponerats på position KT041:Ö.

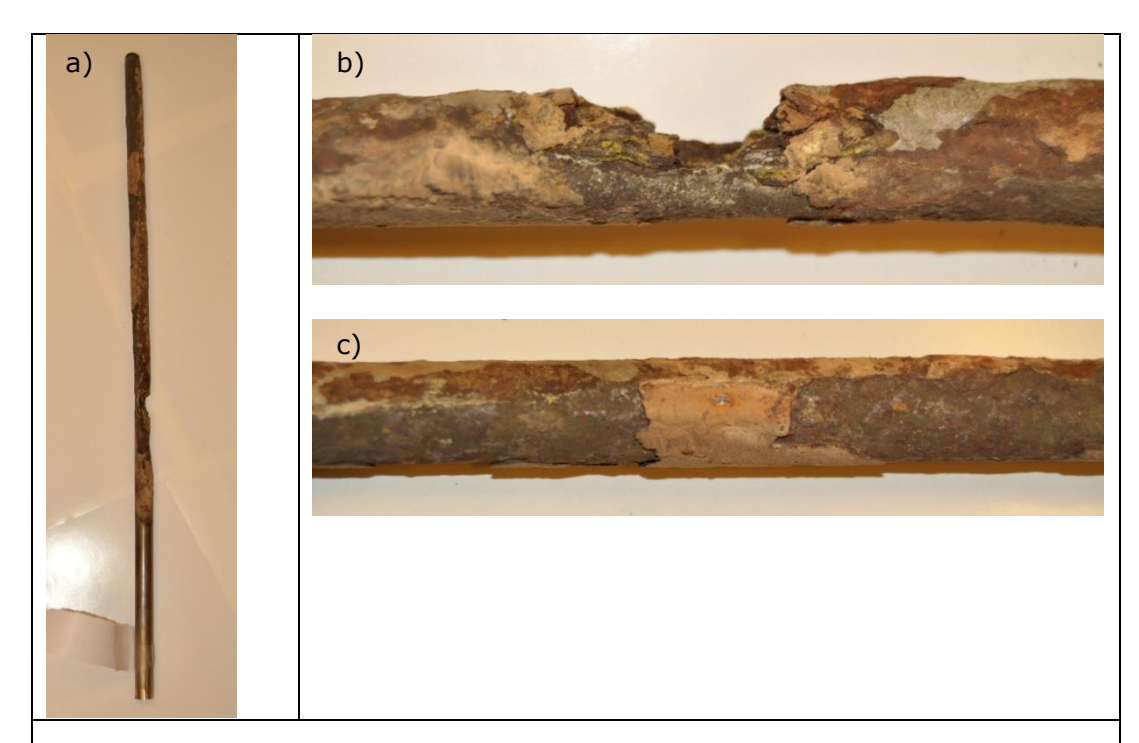


Figure 6-67. Images of the thermal shield tube exposed at position KT039:2. Figur 6-67. Bilder av termoskyddsröret som exponerats på position KT039:2.

Because the reference appears to brake quite quickly at position KT039, it was decided to test if the lifetime of the thermo shield tube could be increased by using alloy APMT instead. Hence, an APMT tube was put in 2012-04-29 at position KT039 and was taken 2013-10-21 which results in 540 days of exposure. The tube was still intact without any perforation into the thermo couple. Measuring of the tube shows that the maximum diminishment of the diameter is approximately 2.50 mm, which is far less than that of IN 625 (104 days – 3 mm, 118 days – 8 mm).

Thermal shield tubes exposed at Idbäcken

The thermal shield tubes exposed at Idbäcken were manufactured of Kanthal $A1^{\$}$. Two of the thermal shield tubes exposed at Idbäcken are shown in Figure 6-68 together with an un-exposed one. The third thermal shield tube that was exposed at Idbäcken was broken and lost due to an "explosion" in the boiler. Therefore, that tube will not be analyzed. The thermal shield tube B was exposed for 173 days at the position 3-TI-6017 under the sixth floor on the left side before the superheaters where the temperature was relatively 600°C, and tube C was exposed for 280 days at the position 3-TI-6406 at the third floor on the right hand close to the soot blowing hopper where the temperature was relatively 400°C.

Tub B appeared intact after the exposure with a thin grayish-brown deposit covering parts of the surface (*Figure 6-68*). The parts not covered by deposit revealed a grayish surface without any visible cracks or spallations. The part

of the rod that had been situated close to the boiler wall had some rust colored regions on the surface. The material loss measurements show only a small diminishment of the diameter (less than 50 μ m) of the second half of the tube length, which was situated closest to the wall of the boiler during exposure. The top of the tube were analyzed by XRD and showed peaks corresponding to the protective oxide a-Al₂O₃ (not shown).

The surface of Tube C is more affected of the exposure than tube B. The material appears to spall at some locations and form thick oxide products (Figure 6-68). A rust-colored deposit covers a large proportion of the surface of the tube. The material loss was higher than for tube C, with a diminishment of the diameter of up to 140 μ m. In accordance with the material loss on tube B, tube C also showed largest material loss on the part of the tube that had been situated close to the boiler wall during the exposure. The top of the tube were analyzed by XRD and showed peaks corresponding to the protective oxide α -Al₂O₃ (not shown). In addition peaks corresponding to iron oxides were present.

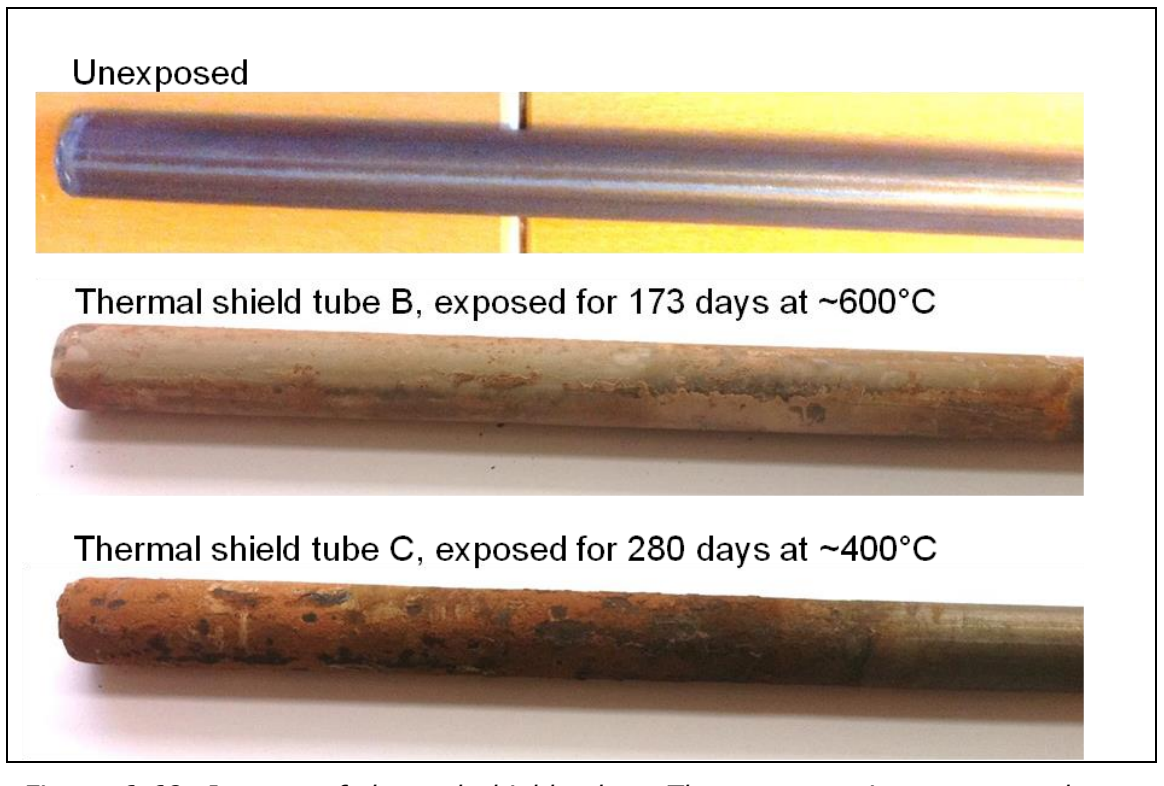


Figure 6-68. Images of thermal shield tubes. The upper on is not exposed. The ones below are exposed at Idbäcken, the middle one for 173 days at ~ 600 °C and the lower one for 280 days at ~ 400 °C.

Figur 6-68. Bilder på termoskyddsrör. Den övre är inte exponerad. De under är exponerad i Idbäckens anläggning, den i mitten under 173 dagar i \sim 600°C och den nedre under 280 dagar i \sim 400°C.

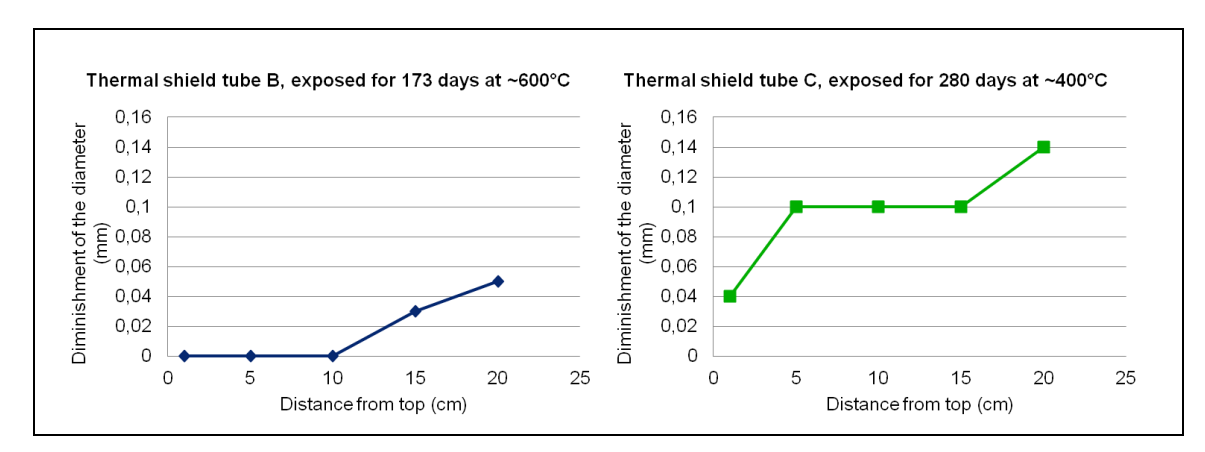


Figure 6-69. Diagrams showing the diminishment of the diameter of the thermal shield tubes after exposure at Idbäcken.

Figur 6-69. Diagram som visar minskningen av diametern hos termoskyddsrören efter exponering i Idbäckens anläggning.

Summary of the thermal shield tube results Händelö and Idbäcken

The lower the temperature, the lower the material loss of pre-oxidized APMT

- > APMT at around 800°C (5 mm material loss, 250 days)
- At lower temperatures ~550-680°C APMT withstand the environment much better than at ~800°C (3 mm material loss, 250 days)
- At lower temperatures ~370-480°C APMT withstand the environment much better than at ~550-800°C (> 1 mm material loss, 250 days)

Pre-oxidized APMT withstands the environment better than the reference, IN 625, at lower temperatures

- APMT withstand the environment better than the reference at position KT041 (\sim 600°C) (104 days, 1 mm 146 days, 4 mm).
- After 540 days APMT had a maximum diminishment of 2.50 mm at the position KT039 (~570°C), which is far less than for the IN 625 material (104 days 3 mm, 118 days 8 mm).

The reference withstand the environment better at higher temperatures than pre-oxidized APMT

- The reference appears to withstand the environment better than APMT at around 800°C (2 and 5 mm material loss, 250 days)
- However, this is one shot and different positions. Verifying of the results is needed

FeCrAl materials withstand the environment better in a biomass fired boiler compared to a waste fired

- ➤ After 173 days exposure at ~ 600 °C in a biomass fired boiler the metal loss of Kanthal® A1 is ~ 0 mm, compared to ~ 0,8 mm metal loss of APMT after 104 days exposure at ~ 590 °C in a waste fired boiler.
- ightharpoonup After 280 days exposure at \sim 400 °C in a biomass fired boiler the metal loss of Kanthal® A1 is \sim 0,1 mm, compared to \sim 0,37 mm metal loss of APMT after 250 days exposure at \sim 400 °C in a waste fired boiler

6.2.3 Shield sheets at the tertiary superheater, Händelö and Idbäcken

Händelö

Shield sheets for the tertiary superheaters were inserted in the Händelö boiler P14 and exposed from 2011-07-25 to 2012-04-15. The shield sheets were manufactured of 253Ma and pre-oxidized APMT. *Figure 6-70* shows images of the shield sheets acquired 2011-12-05. The 253Ma material has a black-green surface. The green color indicates the presence of NiO. The APMT material is covered with a brownish product, probably deposit from the flue gas. The appearance of the material is similar after the total exposure time.



Figure 6-70. Images showing the shield sheet at the tertiary superheaters exposed from 2011-07-25 to 2012-04-15 at the Händelö plant. The part of the shield sheet with a green-black surface is 253Ma and the part with a brownish color is pre-oxidized APMT.

Figur 6-70. Bilder som visar skyddsplåten för tertiäröverhettarna exponerad från 2011-07-25 till 2012-04-15 vid Händelöverken. Den svart-gröna biten av plåten är gjord av 253Ma medan den brunaktiga delen är består av föroxiderad APMT.

Examination of the pre-oxidized APMT and 253Ma materials was done through SEM/EDX and XRD analyses. A cross-section SEM image of the pre-oxidized APMT material is shown in *Figure 6-71*, together with EDX point analyses. The cross-section image reveals an alumina scale closest to the material surface as evident by the EDX points 7, 8, 9, and 3 with and composition of about 66at.% O and 33at.% Al. There appears to be internal oxidation close to the

alumina scale and an oxidation affected zoon where nitridation of the aluminum has occurred. On top of the alumina scale the rappers to be a Carich oxide deposited, also containing some Na and Ti. Point analysis 2 and 12 is indicated on dark spots in the substrate. However, the results show heavy elements, which give a bright contrast in BSE SEM images, This indicates that the beam has drifted during the measurement. Therefore, it is assumed that analyses are generated from the substrate (large bright region).

The SEM/EDX maps in *Figure 6-72* confirm the findings of the EDX point analysis. A continuous alumina scale is present on the material. Underneath the scale, there appear to be a zone with Cr enrichment. This is probably a result of Al depletion owing to the alumina scale growth and the oxidation affected zone reaching about 100 μ m into the substrate. In this zone aluminum and nitride overlaps, indicating the presence of AlN. On top of the alumina there is a Ca-rich deposit, also containing some Na, Ti and Si.

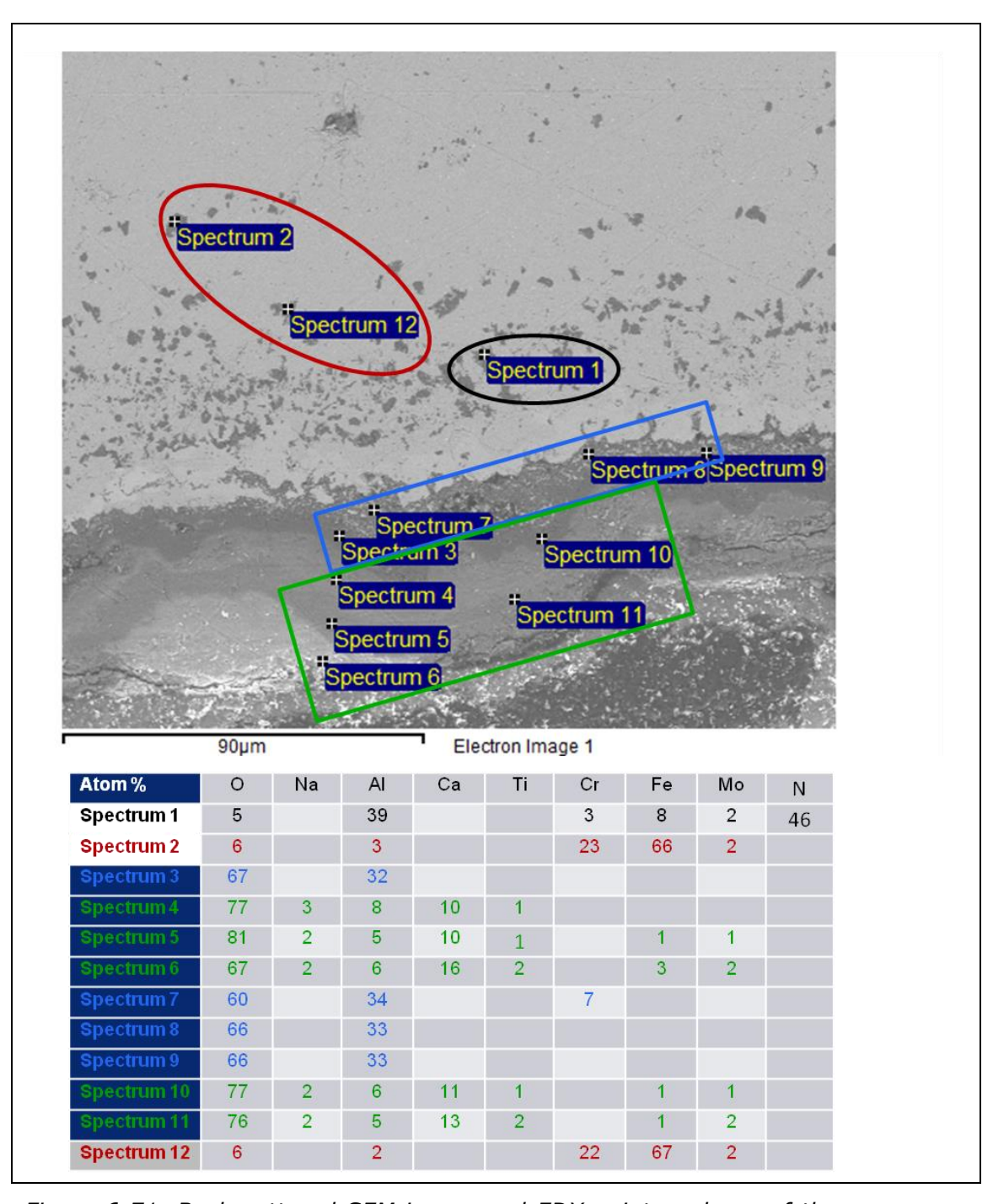


Figure 6-71. Backscattered SEM image and EDX point analyses of the crosssection of the pre-oxidized APMT sheet exposed at the tertiary superheaters at the Händelö plant, boiler P14.

Figur 6-71. Bakåtspridd SEM bild och EDX punkt analyser av tvärsnittet av den för-oxiderade APMT plåten som exponerats vid tertiäröverhettarna i kokare P14 vid Händelös anläggning.

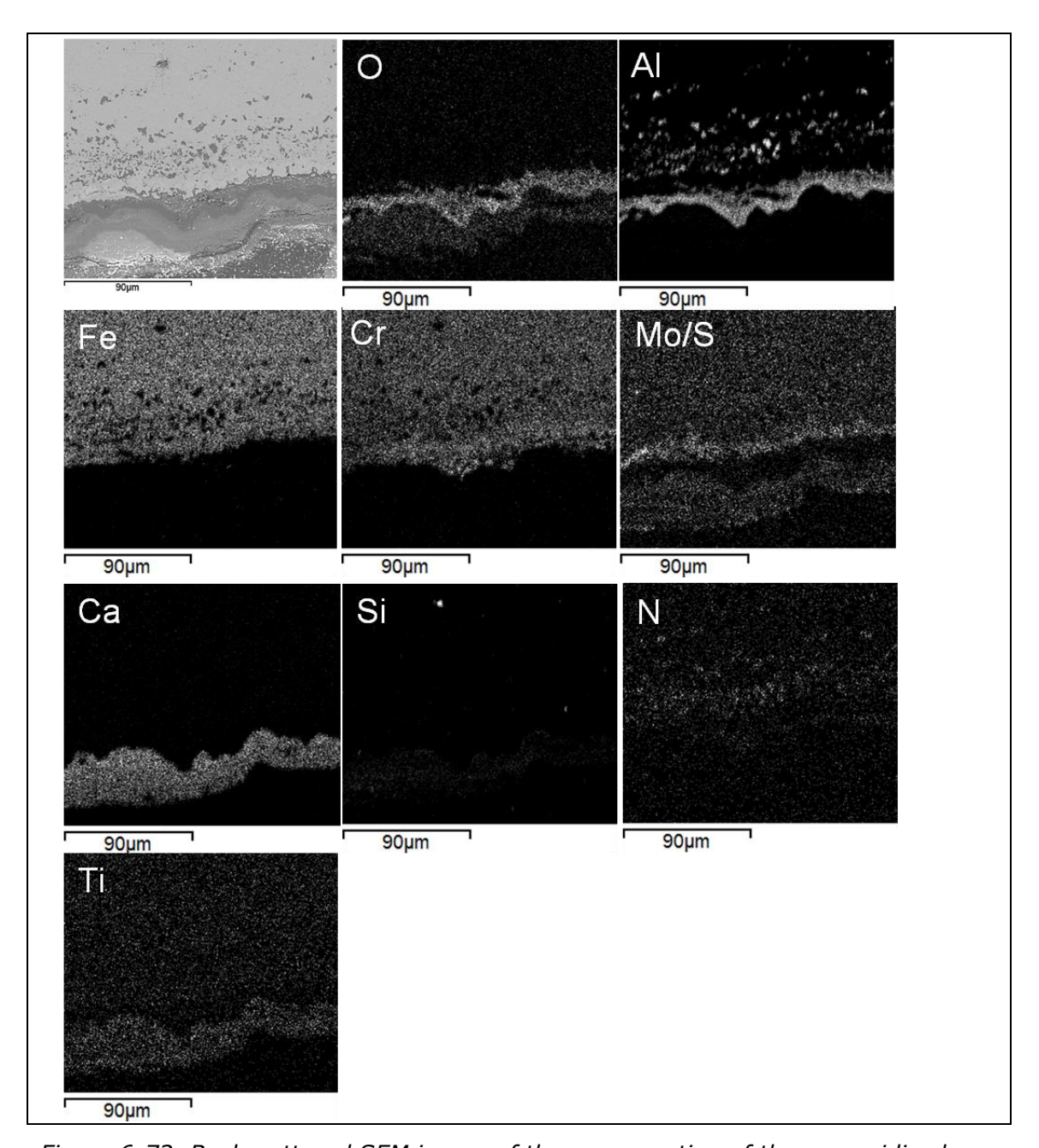


Figure 6-72. Backscattered SEM image of the cross-section of the pre-oxidized APMT sheet exposed at the tertiary superheaters at Händelö together with EDX maps for the elements O, Cr, Al, Fe, Si, Ca, N, Ti and Mo/S.

Figur 6-72. Bakåtspridd SEM bild av tvärsnittet av den för-oxiderade APMT plåten exponerad vid tertiäröverhettarna i Händelö tillsammans med EDX kartor för elementen O, Cr, Al, Fe, Si, Ca, N, Ti och Mo/S.

A cross-section SEM image of the 253Ma material is shown in *Figure 6-73*, together with EDX point analyses. The cross-section image reveals a mixed oxide consisting of Ni, Fe, Cr and Si on the surface of the material, as evident

by the EDX points 4, 5 and 6. The oxide is not continuous, it appears mixed with the substrate. Cr-oxide has formed as pegs into the substrate, see EDX point 3 consisting of 29 at.% Cr, 2 at.% Fe, 1 at.% Si and 69 at.% O. Point two shows the composition of the substrate.

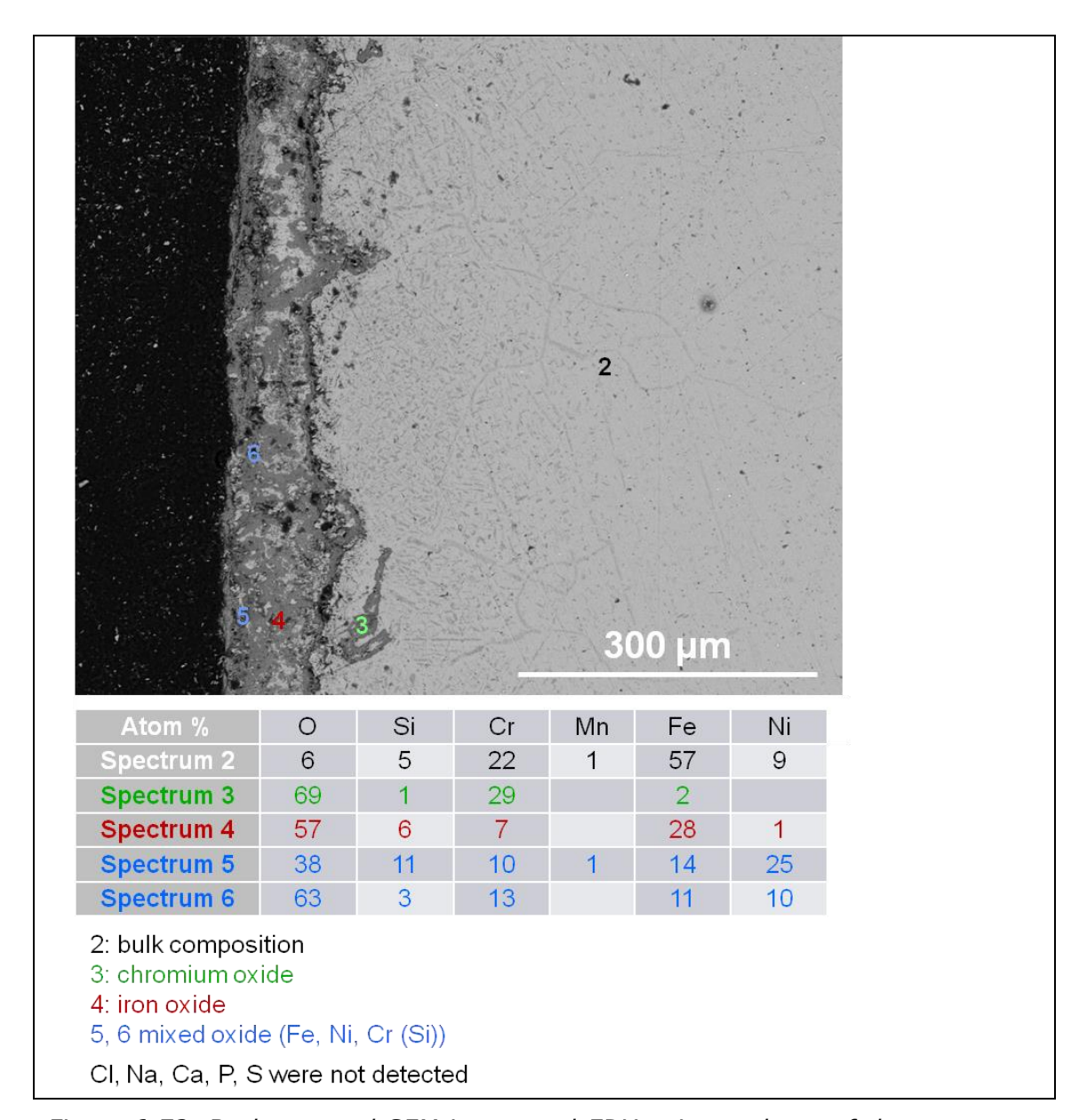


Figure 6-73. Backscattered SEM image and EDX point analyses of the cross-section of the 253Ma material exposed at the tertiary superheaters at the Händelö plant, boiler P14.

Figur 6-73. Bakåtspridd SEM bild och EDX punkt analyser av tvärsnittet av 253Ma materialet som exponerades vid tertiäröverhettarna i kokare P14 vid Händelös anläggning.

The SEM/EDX maps in *Figure 6-74* confirm the findings of the EDX point analysis. A discontinuous Fe-, Cr-, Ni- oxide can be seen on top of the surface. However there appears to be a continuous Cr-rich oxide scale closest to the substrate. Underneath this scale, there appear to be a zone with Ni enrichment/Cr depletion. This is probably a result of Cr depletion, owing to the Cr-scale growth and low diffusion rates of Cr.

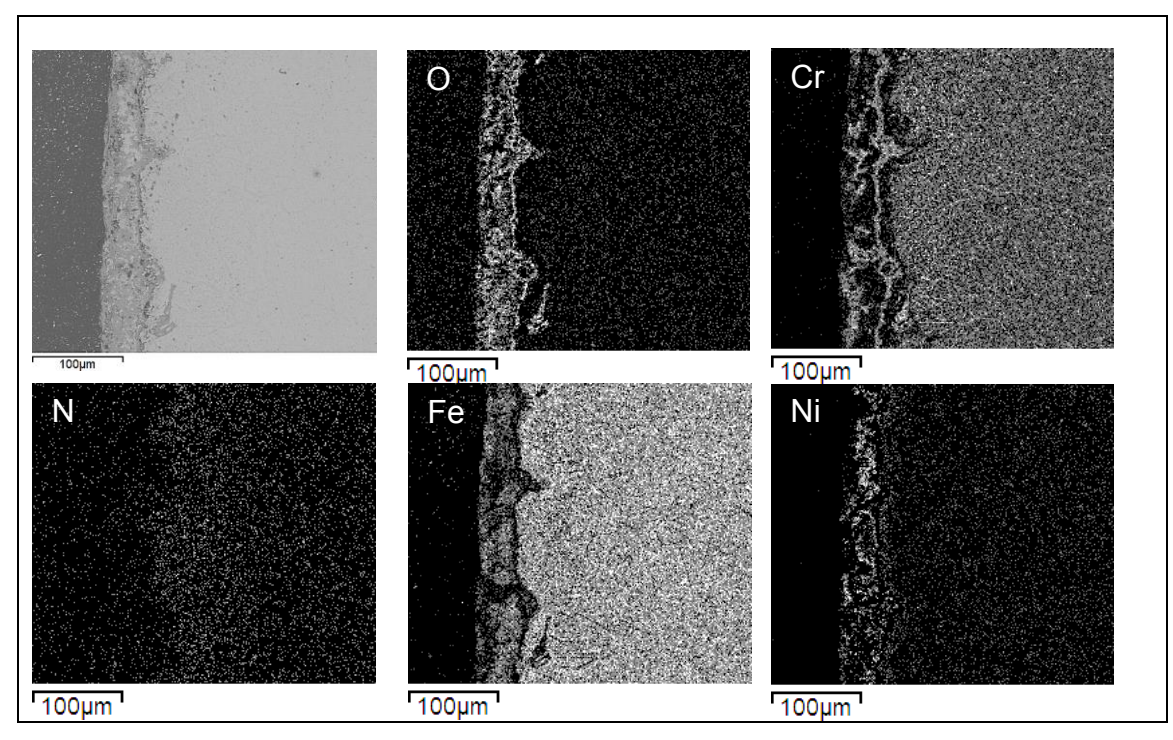


Figure 6-74. Backscattered SEM image of the cross-section of the 253Ma material exposed at the tertiary superheaters at Händelö together with EDX maps for the elements O, Cr, N, Fe, and Ni.

Figur 6-74. Bakåtspridd SEM bild av tvärsnittet av 253Ma materialet som exponerades vid tertiäröverhettarna i Händelö tillsammans med EDX kartor för elementen O, Cr, N, Fe, och Ni.

Idbäcken

The shield sheet for the tertiary superheater that was exposed at Idbäckens facility was manufactured of Kanthal APMT $^{\text{TM}}$. Figure 6-75 show images of the shield sheet after exposure. The major part of the surface is gray and appears unaffected by the exposure. There are also some regions that are rust-colored and some regions that are blackish.

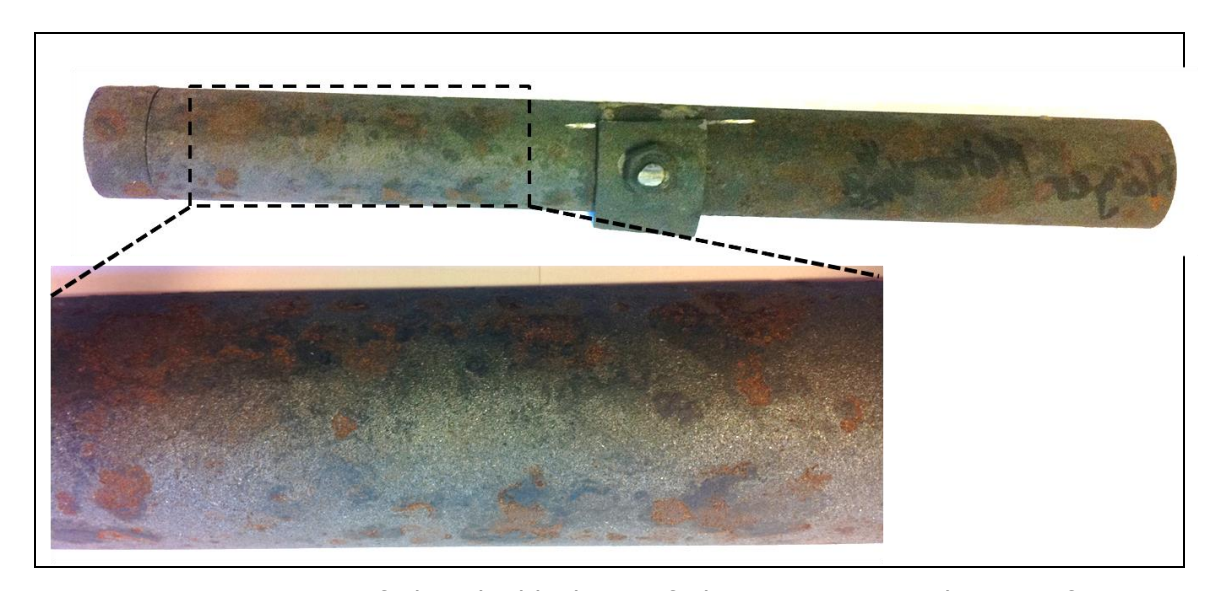


Figure 6-75. Images of the shield sheet of the tertiary superheater after exposure at Idbäckens facility.

Figur 6-75. Bilder på skyddsplåten för tertiäröverhettarna efter exponering i Idbäckens anläggning.

As described in section 5.4, the shield sheet was pre-oxidized prior to exposure to establish an $\alpha\text{-Al}_2\text{O}_3$ scale on the material surface. According to XRD analysis this scale is still present after exposure, as the diffraction pattern showed several peaks corresponding to $\alpha\text{-Al}_2\text{O}_3$. The XRD analysis was made from a gray region of the surface. There are also rust –colored regions, likely consisting of iron-oxide as detected with XRD.

Summary of the shield sheets at the tertiary superheaters, Händelö and Idbäcken

Händelö pre-oxidized APMT

- An alumina oxide was found closest to the metal, indicating the presence of an protective oxide.
- Aluminum nitrides appeared to have formed in the bulk close to the external alumina scale, depleting the bulk of Al likely resulting in difficulty to re-heal a damaged alumina scale
- > Ca-rich deposit

Händelö 253Ma

- > A continuous Cr-rich oxide is present on the substrate, indicating the presence of a protective scale
- Cr appears depleted in the bulk close to the Cr-rich oxide likely resulting in difficulty to re-heal a damaged chromia scale

- Pegs of Cr-rich oxide appear to grow into the bulk material
- A mixed Fe-Ni-Cr-oxide is present on top of the Cr-rich oxide
- Similar material thickness after exposure as pre-oxidized Kanthal APMT

Idbäcken pre-oxidized APMT

- > The major surface is intact after exposure with the Al₂O₃ scale, that was established on the material surface prior to exposure, still present.
- \triangleright The Al₂O₃ scale is damaged at some regions where rust is present.

6.2.4 Shield sheet at the vortex finder, Händelö

The shield sheet for the vortex finder at Händelö facility was manufactured of Kanthal APMTTM. Figure 6-76 shows images of the shield sheet before exposure (a), after exposure for 133 days (b) and after demounting after the total exposure time (265 days). From the images it can be seen that a yellowish deposit get caught on the shield sheet during exposure. The deposit appears to be rich in Ca and Na, see Figure 6-77 and Figure 6-78. The oxide scale appears layered and consists of an aluminium rich layer closest to the metal, an Cr-rich layer on top and an Fe-rich outer layer, see Figure 6-77 and Figure 6-78.



Figure 6-76. Images showing the shield sheet made of pre-oxidized Kanthal APMT material A) before exposure, B) after exposure from 2011-07-25 to 2011-12-05, and C) after exposure from 2011-07-25 to 2012-04-15 at Händelö plant.

Figur 6-76. Bilder på skyddsplåten tillverkad av AMPT material som föroxiderats A) innan exponering, B) efter exponering från 2011-07-25 till 2011-12-05, och efter exponering från 2011-07-25 till 2012-04-15 i Händelö anläggning.

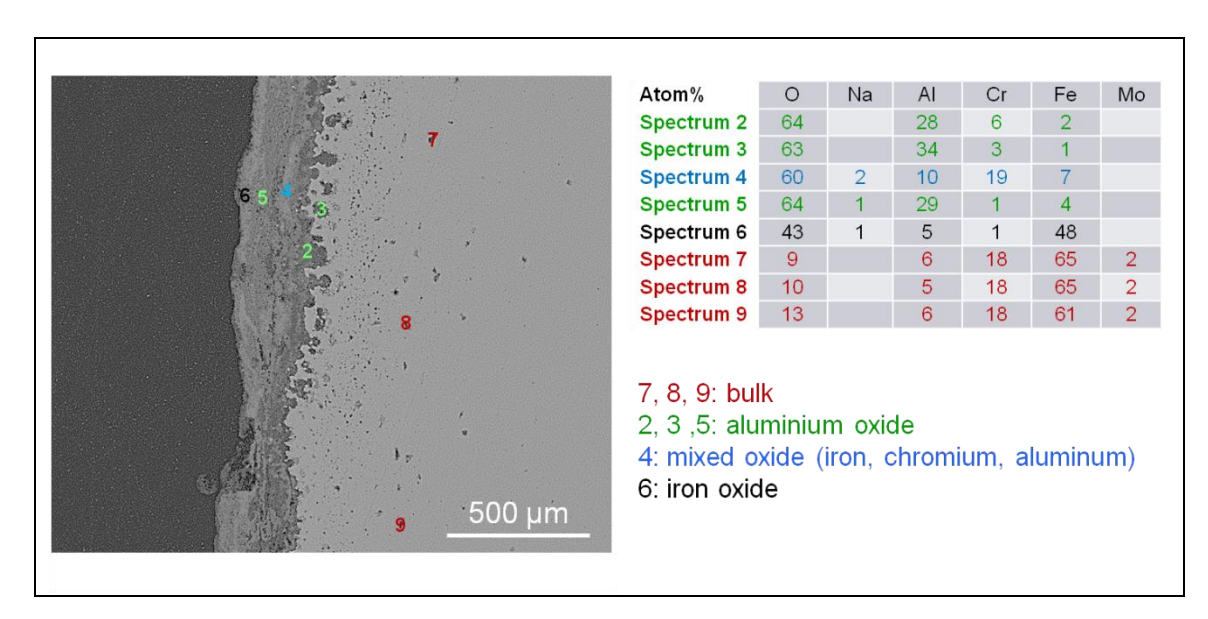


Figure 6-77. Backscattered SEM image and EDX point analyses of the cross-section of the pre-oxidized APMT sheet exposed at the vortex finder at the Händelö plant, boiler P14.

Figur 6-77. Bakåtspridd SEM bild och EDX punkt analyser av tvärsnittet av den för-oxiderade APMT plåten som exponerats vid centrumröret i kokare P14 vid Händelös anläggning.

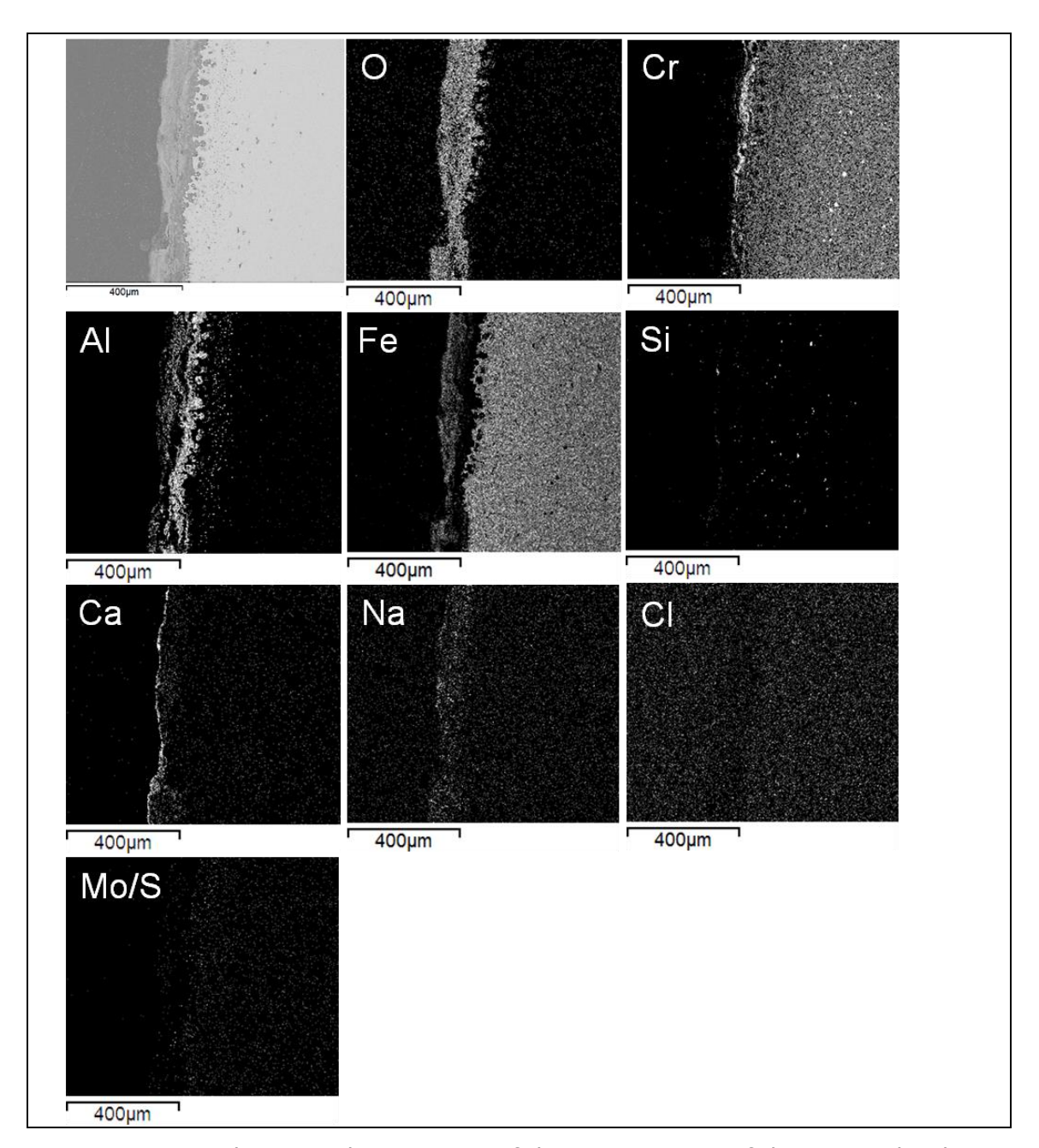


Figure 6-78. Backscattered SEM image of the cross-section of the pre-oxidized APMT sheet exposed at the vortex finder at Händelö together with EDX maps for the elements O, Cr, Al, Fe, Si, Ca, Na, Cl and Mo/S.

Figur 6-78. Bakåtspridd SEM bild av tvärsnittet av den för-oxiderade APMT plåten exponerad vid centrumröret i Händelö tillsammans med EDX kartor för elementen O, Cr, Al, Fe, Si, Ca, Na, Cl and Mo/S.

Summary of the results obtained for the shield sheet at the vortex finder

- ➤ The oxide was still rather protective with a high alumina content close to the metal, Cr in the middle and a Fe in the outer part (scale/gas interface)
- > Some Ca and Na was incorporated in the oxide scale

7 Analysis of the results

In this work both laboratory and field exposures were conducted. In addition, the field samples were exposed both cooled (corrosion probe) and uncooled (thermal shield tubes, shield sheet at the vortex finder, shield sheets at the tertiary superheater). It may be noted that the cooled samples will have a constant temperature that is lower than the flue gas in the boiler whereas the uncooled samples will follow the flue gas temperature. Consequently, condensation of flue gas components is very likely to occur on the cooled samples but not on the un-cooled. Also, the corrosion probe was inserted in a warm boiler, resulting in a large temperature difference between the flue gas and the corrosion probe initially, before the probe has been warmed up to the target temperature. Thus, condensation of flue gas components is more pronounced at start. The un-cooled components were inserted in a cooled boiler.

The results obtained from the laboratory and the field study accord with and complement each other. A more detailed understanding of the corrosion process can be deduced from the laboratory studies whereas the field studies show the effects of the corrosion. Both exposure environments contained KCI although the atmosphere in the boiler is more complex, evident by the detected compounds in the deposit on the corrosion probe samples (Cr₂O₃, Fe₂O₃, NaCl, KCl, CaSO₄). The same morphology and microstructure can be seen on both laboratory and field exposed samples. For example the surface of the tertiary superheater, exposed in Idbäcken, has the same surface features as the laboratory exposed samples, see Figure 6-20, Figure 6-21 and Figure 6-75, , most of the surface is covered with an intact Al₂O₃ scale and some isolated regions that are rust-coloured. In addition, the cross-section of laboratory exposed samples show similar oxide layers as short term exposed field samples, Figure 6-25, Figure 6-42, Figure 6-45 and Figure 6-47. Therefore, it can be concluded that similar oxidation behaviour is present both in the laboratory and the field exposures. For simplicity some of the discussion and analysis of the results of the laboratory study is placed in connection to the results (see, section 6.1).

The samples exposed for 1000 hours at 600 °C on the corrosion probe verified the results obtained in the KME 414 project. The material loss (total) obtained in this project and in KME 414 where surprisingly similar. The average material loss obtained for pre-oxidized APMT was 0.26 mm and 0.42 mm for KME 507 and KME 414 respectively, and 0.18 mm and 0.16 for APMT without pre-oxidation. The reference material was San28 in this project and 304L in KME 414 and both materials showed significantly larger material loss than APMT, the average values being 0.75 mm (San28) and 0.42 mm (304L). In this project the samples were also exposed for 400 hours. The material loss was then somewhat larger than after 1000 hours. (see *Figure 6-35*). This variance in corrosion rate is ascribed the different placement of the probes, which likely results in a somewhat different environment. The probe exposed for 400 hours has obviously experienced a more aggressive environment.

However, the results show the same trend as after 1000 hours, the material loss being largest for San28 and lowest for APMT without pre-oxidation. Thus, it can be concluded that APMT withstands the environment in a waste-fired boiler at 600 °C significantly better than both 304L and San28. In addition, it can be concluded that the pre-oxidation conditions chosen for APMT was disadvantageous at 600 °C. Also at 700 °C APMT has a lower material loss than the reference material (San28) (Figure 6-36). However no difference in material loss could be measured between the APMT samples with and without pre-oxidation at this temperature. The finding that pre-oxidation is disadvantageous at 600 °C is somewhat surprising. One could argue that the protective scale should at least initially, before being spalled off, inhibit corrosion and protect the material, resulting in less material loss. It is not obvious what causes the present results but one reason may be the different grain sizes of the pre-oxidized and non-pre-oxidised samples. The grain size in the as-delivered (non-pre-oxidized) material is approximately 1-2 µm whereas it is about 10-20 µm. At these low temperatures grain boundary diffusion is expected to dominate. Consequently, the diffusion rate is faster in the as received material leading to faster establishment of a somewhat protective layer. It should be emphasized that even if the present investigation shows that pre-oxidation does not improve the ability of FeCrAl alloys to withstand fireside corrosion in waste fired boilers at 600 and 700 °C, pre-oxidation should not be ruled out for components exposed at higher temperatures. Instead, the present results suggest that more research is needed to understand how and when pre-oxidation can be used to protect FeCrAl's. The results also show that the pre-oxidation conditions influence the protective behavior of the scale. Since the alumina scale is considered protective while no cracks and defects are present, it would be of great interest to find such a pre-oxidation process where a flawless alumina scale is obtained and withheld with time.

Both the laboratory and field exposed samples shows that APMT corrodes in a waste fired boiler environment although the material has been pre-oxidized to establish a protective α -Al₂O₃ scale before exposure. However, the lab tests showed that the corrosion attack was delayed by the presence of an external $a-Al_2O_3$ scale, see Figure 6-20, Figure 6-21 and Figure 6-22. The corrosion attack mainly starts at sharp edges but was also found to start at a few places on the flat surface. The sample pre-oxidized the longest time and at the highest temperature (24h, 1100 °C) prolonged the time before visible corrosion attack appeared on the surface. Hence, it is interesting to compare the alumina scales formed after the different pre-oxidations. Present and previous results have shown that oxidation of a FeCrAl alloy in an O₂-N₂ containing atmosphere results in a duplex alumina scale on the alloy surface ¹³⁻²¹. The alumina layers are separated by a Cr enrichment and the outer alumina layer is enriched in Fe. One factor influencing the protectiveness of an alumina layer is the alumina structure. There are different forms of alumina that can form, α , γ , δ and θ , α -alumina being the stable and most protective one and are known to form at approximately 1000 °C 8-10. After oxidation at 600 and 700 °C it was not possible to deduce the alumina structure. However, after pre-oxidation at 900 and 1100 °C it could be determined that the most protective form of alumina had formed (i.e. aalumina). Hence, the layer formed after oxidation at 700 °C might be one of the less protective forms of alumina and therefore resulting in a faster corrosion attack. Another difference between the alumina scales formed during pre-oxidation is the thickness of the layers. The outward growing layer had more or less a constant thickness on all samples, see *Figure 6-13*, whereas the thickness of the inner layer increased with exposure time and temperature. Hence, the protectiveness appears to rely on the thickness of the inner alumina layer. It may be noted that the thickness of the layers also varies over the surface. Consequently, the initiation of the corrosion attack might be at locations with thinner scale thickness. Another possibility is that corrosion is initiated at defects, such as pores or cracks, in the alumina scale. Cracks may have been introduced in the scale when the sample was subjected to stresses due to thermal cycling (cool-down after pre-oxidation, heating during field exposure) as the thermal expansion coefficient of the substrate and the scale differs.

The results from the pre-oxidation at 700 °C indicate that the start of the corrosion attack is connected to sites where chromate formation have taken place (reaction 2), see Figure 6-17. The K₂CrO₄ are believed to form from the Cr_2O_3 in the oxide scale, KCl(s), $O_2(g)$ and $H_2O(g)$, see Reaction 1. Some K₂CrO₄ particles are accompanied by iron oxide, likely a result of the removal of Cr in the oxide scale which is believed to create diffusion paths for corrosive species. However, corrosion does not start at all sites where chromates have formed, indicating that the protective scale is less protective at some locations. The corrosion production is accompanied with a volume increase which results in tension in the scale and cracks may then form in the oxide scale. It is suggested that the break-down of the scale starts at defects (crack or pores) or at sites with thinner scale thickness. This is supported by the results showing that the corrosion starts at a few sites and then spreads from these sites to eventually cover the entire surface, see Figure 6-22. When the protective oxide has been attacked by Reaction (2), it can then be penetrated by chloride ions leading to even more severe corrosion. It is proposed that chloride ions are produced through an electrochemical reaction in the presence of KCI. The chloride ions then diffuse inwards through the scale. Chloride ions are not expected to be soluble in the oxide. However, oxide grain boundaries are also oxide surfaces, and thus constitute paths for the chloride ions to the metal surface. Formation of transition metal chlorides occur when the chlorine ion encounter a metal ion. The location of the transition metal chloride depends on where the ions meet in the scale. The presence of metal chloride at the bottom of the scale shows that the alumina layer, formed during pre-oxidation, is readily penetrated by chloride species. It is suggested that thermally induced stresses after pre-oxidation cause's flaws (micro-cracks) in the alumina scale that act as paths for the transport of chloride species. The build-up of iron chloride beneath the oxide is suggested to accelerate corrosion by decreasing scale/alloy adhesion, finally resulting in spallation of the scale. Thus, the spallation of the alumina scale is likely a process that goes on during exposure. The spallation process may be accelerated after exposure during cool down, due to thermal expansion missmatch between the scale and the substrate.

The initial breakdown of the alumina layer in a waste fired boiler environment is still not fully understood. However, when the protectiveness of the alumina

scale is lost, an iron-rich oxide forms at the oxide/gas interface and a mixed oxide ((Cr,Al,Fe) $_2O_3$) layer form closest to the alloy substrate. In both cases, with and without an alumina scale before exposure, chloride and sulphur penetrate the scale, likely forming alloy sulphides and chlorides, which are known to decrease scale adherence. An oxidation affected zone containing aluminium nitrides are formed in the alloy close to the surface. The capturing of the aluminium in the nitrides likely obstructs the formation/re-healing of an alumina layer. Nevertheless, Al enriched layers are found also after longer exposure times. Nitridation of the alloy implies that the oxide scale is permeable to N_2 molecules. The absence of the formation of an alumina scale is likely also due to the slow Al diffusion in the bulk material at the exposure temperature, as described in the introduction.

However, raising the exposure temperature to 700°C is enough for the material to form an aluminium-rich layer, evident by the two alumina layers formed on the APMT exposed for 24 and 1000 h at 700°C in the boiler (Figure 6-43 and Figure 6-51). It has also been shown in the laboratory that an a- Al_2O_3 scale can form on the FeCrAl material Kanthal[®] AF at $700^{\circ}C^{^{\prime}22}$. However, the protectiveness of the alumina scale appears to be lost in a similar manner as described above, but a new scale can repeatedly be formed. The presence of this protective scale may be a reason for the lesser amount of chlorides found at the scale/alloy interface, compared to 600°C. Another is the higher volatility of CI-containing species at the higher temperature, which have two implications. The formed CI-containing species will evaporate more easily and the condensation of Cl-containing species in the flue gas will be decreased. In spite of the large material loss of San28, the material forms a chromia-rich layer close to the alloy at 700°C, although internal oxidation of Cr was detected in the substrate. It is suggested that the un-protective behavior of the chromia rich scale is due to the chromate and $CrO_2(OH)_2(g)$ formation that depletes oxide scale in chromium making it more permeable to corrosive

The materials appears to manage the boiler environment better at higher temperatures (above 800 °C), evident from the material exposed as shield sheet for the tertiary superheater and shield sheet at the vortex finder. The materials have intact protective scales on the material surfaces after the exposure. Thus, APMT has an alumina scale on the surface and 253Ma has a chromia scale. However, the protective scale constituent is depleted in the alloy of both materials, Cr due to internal oxide formation and Al due to aluminium nitride formation. The depletion of the bulk Al and Cr, respectively, likely results in difficulty to re-heal a damaged scale.

species. Sulfur and chlorides are found in the oxide scale and at the

oxide/alloy interface in accordance with alloy APMT.

The corrosion of the thermal shield tube exposed at Händelö was unevenly distributed over the length of the tubes. Most of the tubes had a small area with a significantly larger material loss than the rest of the tube. This area was located at a similar distance from the tube wall on all thermal shield tubes. A possible explanation is that the flue gas flow along the walls in the boiler is disturbed by the protruding thermal shield tube, resulting in a turbulent gas flow in the vicinity of the tube. This turbulence will cause an increase in erosion. The fact that the APMT tubes withstand the lower temperatures better than the higher ones were somewhat surprising because

the protective a-alumina layer was expected to be able to re-heal at the higher temperatures but not at the lower. The loss of the a-alumina layer and the inability to re-form is suggested to proceed in the same manner as described above.

Comparing the thermal shield tubes positioned at the lower temperatures shows that the APMT material was significantly better than the Inconel 625 tubes. However, at the higher temperatures (~800 °C) it appears as the reference material, Inconel 625, manages the environment better than Kanthal® APMT. It may be noted that the materials were not exposed at the exact same position and temperature. Thus it is not possible to conclude that the material Inconel 625 manages the higher temperature better than Kanthal® APMT. Besides the temperature difference, other factors may have influenced the material loss of these thermal shield tubes. The composition of the flue gas might be unevenly distributed in the boiler, depending on different fuels in different areas of the combustion zoon. Also, as mentioned above, erosion may be a contributing factor. Thus, additional exposures must be performed to inquire the best suitable choice of material at these positions. Comparing the thermal shield tubes exposed at similar temperatures in Händelö (waste fired boiler) and Idbäcken (biomass fired boiler) shows that the material loss is significantly lower in the biomass fired boiler. This fact is simply ascribed to the less corrosive environment.

8 Conclusions

- ➤ In contrast to the laboratory exposed samples, pre-oxidation had no beneficial effect on corrosion behavior at 600 and 700 °C in the fireside environment of the waste-fired boiler.
- The field exposed pre-oxidized samples formed scales similar to those observed on the samples without pre-oxidation, featuring a chloride layer closest to the alloy substrate. It is believed that the alumina scale breaks down in a similar manner as described for the laboratory exposed samples and that the corrosion proceeds similar to APMT without pre-oxidation.
- ➤ At higher temperatures (>700 °C) the alumina scale appears to stay intact in the boiler environment. However, the oxidation affected zone present in the alloy substrate clearly indicates a non-protective behavior of the alumina scale.
- ➤ The material loss was 3 times less for APMT (with pre-oxidation) compared to San 28 in the Händelö boiler at 600 °C for 400 and 1000 hours. In addition, the material loss for APMT without pre-oxidation was lower than for APMT with pre-oxidation. These results are in agreement of those obtained in the project KME 414. Also the 700 °C exposures showed a lower material loss for APMT compared to San28. At this temperature the material loss was similar for APMT with and without pre-oxidation.
- ➤ The material loss of un-cooled pre-oxidized APMT exposed in the Händelö boiler is dependent on the flue gas temperature. The lower the flue gas temperature, the lower the material loss. After 250 days at around 800 °C 5 mm material is lost, at ~550-680 °C 3 mm and ~370-480 °C less than 1mm.
- ➤ The material loss of un-cooled pre-oxidized APMT, exposed in the Händelö boiler, is less than the reference, inc625, at the lower flue gas temperatures. At ~600 °C for 104 days APMT lost 1 mm material whereas the reference lost 4 mm after 146 days. After 540 days APMT lost 2.50 mm at the position KT039 (~570°C), which is far less than for the IN 625 material (104 days 3 mm, 118 days 8 mm).
- The max material loss at higher flue gas temperatures was less for the un-cooled reference, IN 625, than for un-cooled pre-oxidized APMT. After 250 days exposure at around 800 °C in the Händelö boiler P14 the reference lost 2 mm whereas APMT lost 5 mm. However, this is one shot and different positions. Verifying of the results is needed.

- ➤ FeCrAl materials withstand the environment better in a biomass fired boiler compared to a waste fired. After 173 days exposure at a flue gas temperature of ~600 °C in a biomass fired boiler the metal loss of Kanthal® A1 is ~0 mm, compared to ~0,8 mm after 104 days exposure at ~590 °C in a waste fired boiler. After 280 days exposure at ~400 °C in a biomass fired boiler the metal loss of Kanthal® A1 is ~0,1 mm, compared to ~0,37 mm after 250 days exposure at ~400 °C in a waste fired boiler.
- ➤ The laboratory exposures show that Kanthal® APMT performs excellent in oxygen and in oxygen/water vapour mixtures at 600 °C. The scale contains corundum type (Fe,Cr,Al)₂O₃.
- \blacktriangleright KCl strongly accelerates the corrosion of Kanthal® APMT in $O_2 + H_2O$ at 600 °C. Chromia in the scale reacts rapidly with $O_2 + H_2O$ forming K_2CrO_4 and gaseous HCl. Chromate formation depletes the protective scale in Cr, triggering the formation of a fast-growing iron-rich scale. There was little evidence for alloy chlorination and it is believed to be of secondary importance in the present case. K_2CrO_4 is reduced on the scale surface according to an electrochemical process where the electrons are supplied by means of alloy oxidation.
- ➤ In the field exposure, APMT without pre-oxidation formed a layered scale. The bottom part of the scale was enriched of chlorides of the alloying elements while the upper part consisted of a mixture of oxides dominated by (Fe,Cr,Al)₂O₃ and iron-oxide. The deposit consisted mainly of NaCl, KCl and CaSO₄.
- > The sub-scale metal chloride formation is suggested to form through an electrochemical reaction in the presence of KCl. The chloride ions then diffuse inwards through the scale. Formation of transition metal chlorides occur when the chlorine ion encounter a metal ion. It is suggested that the build-up of iron chloride beneath the oxide accelerates corrosion by decreasing scale/alloy adhesion.
- ▶ Pre-oxidation of alloy APMT at 700 °C results in the formation of a thin oxide layer which is dominated by alumina (likely meta-stable) and contains significant amounts of iron and chromium. Pre-oxidation at 900 and 1100 °C results in a continuous duplex α -Al₂O₃ scale, the alumina layers being separated by a Cr enrichment.
- In the laboratory study, all pre-oxidations of Kanthal® APMT show a protective behavior at 600 °C in the presence of KCl, as long as no flaws are present in the alumina scale indicated by the corrosion event; localized corrosion attacks that spreads over the surface with time.
- ➢ Flaws (defects) in the alumina scale are suggested to be introduced during the formation of the alumina scale. Flaws (cracks) might also evolve during thermal stresses. The K₂CrO₄ formation is believed to start at the present flaws in the alumina scale accompanied by iron

oxide formation. The iron oxide formation causes a volume increase leading to more cracks resulting in accelerated corrosion.

9 Goal fulfilment

The project exposed FeCrAl materials in a range of different temperatures in a waste fired boiler. In addition some exposures were performed in a biomass fired boiler. Both corrosion probe and un-cooled exposures were successfully performed. Different components (shield sheet for the vortex finder, thermal shield tubes, and shield sheets for the tertiary superheaters) were manufactured in a reference material and in a FeCrAl material (with and without pre-oxidation) and exposed. The analysis of the results gives directions to where these materials can be used, as was the goal. Also, the results were compared to KME 414. Laboratory studies were also conducted and gave results on the oxide nature in different atmospheres. In addition, the effect of pre-oxidation was examined in the laboratory, giving hint on why the scale fails. That is, the project fulfilled the goal to examine the usability of FeCrAl alloys in waste- and biomass- fired boilers.

10 Suggestions for future research work

- Further investigations of the usability of FeCrAl materials in biomass and waste fired boiler environments (field and lab.), especially at higher temperatures (above 700 °C) to verify the results obtained in this project.
- The results in this project show that the corrosion resistance of FeCrAl alloys is significantly better than for the steels used nowadays in a waist fired boiler at temperatures ≤ 700 °C. However, the FeCrAl alloys do not withstand the pressure in the superheater tubes. Thus, to make use of the corrosion resistance of the FeCrAl material for superheaters, the FeCrAl material must have a bearing material. Hence, to investigate the performance of different alumina forming coatings/compound tubes in biomass and waste fired boiler environments would be of great interest for the development of more corrosion resistant superheater tubes.
- Investigate the effect of applying an external alumina coating before exposure, not by pre-oxidizing which affects the composition of the substrate material, with for example a sol-gel method or similar.

11 Literature references

- (1) Asteman H., S. J.-E., Johansson L.G. Evidence for chromium evaporation influencing the oxidation of 304L: the effect of temperature and flow rate. *Oxidation of Metals* **2002**, *57*, 193-216.
- (2) Asteman, H.; Svensson, J. E.; Johansson, L. G. Oxidation of 310 steel in H2O/O2 mixtures at 600 °C: the effect of water-vapour-enhanced chromium evaporation. *Corrosion Science* **2002**, *44*, 2635-2649.
- (3) Pettersson C., J. E. S., L.G. Johansson. The Influence of Small Amounts of KCl(s) on Initial Stages of the Corrosion of Alloy Sanicro 28 at 600°C. Oxidation of Metals **2008**, 70, 241-256.
- (4) Pettersson C. , J. P., H. Asteman, J.E. Svensson, L.G. Johansson. KCl-induced high temperature corrosion of the austenitic Fe-Cr-Ni alloys 304L and Sanicro 28 at 600°C. *Corrosion Science* **2006**, *48*, 1368-1378.
- (5) Segerdahl K., J. P., J.E. Svensson, L.G. Johansson. Is KCl(g) corrosive at temperature above its dew point? Influence of KCl(g) on initial stages of the high temperature corrosion of 11% Cr steel at 600°C. *Materials Science Forum* **2004**, 461-464, 109-116.
- (6) Petteresson J., H. A., J.E. Svensson, L.G. Johansson. KCl Induced Corrosion of a 304-type Austenitic Stainless Steel at 600°C; the Role of Potassium. *Oxidation of Metals* **2005**, *64*, 23-41.
- (7) Jonsson, B.; Berglund, R.; Magnusson, J.; Henning, P.; Hattestrand, M. High temperature properties of a new powder metallurgical FeCrAl alloy. *High Temperature Corrosion and Protection of Materials 6, Prt 1 and 2, Proceedings* **2004**, *461-464*, 455-462.
- (8) El Kadiri, H.; Molins, R.; Bienvenu, Y.; Horstemeyer, M. F. Abnormal High Growth Rates of Metastable Aluminas on FeCrAl Alloys *Oxidation of metals* **2005**, *64*, 63-97.
- (9) Badini, C.; Laurella, F. Oxidation of FeCrAl alloy: influence of temperature and atmosphere on scale growth rate and mechanism. *Surface & Coatings Technology* **2001**, *135*, 291-298.
- (10) Berthome, G.; N'Dah, E.; Wouters, Y.; Galerie, A. Temperature dependence of metastable alumina formation during thermal oxidation of FeCrAl foils. *Materials and Corrosion-Werkstoffe Und Korrosion* **2005**, *56*, 389-392.
- (11) 6.2, F. Databases: Fact53, ELEM, BINS.
- (12) Engkvist, J.; Israelsson, N.; Bexell, U. The initial effect of KCl deposit on alumina scales characterized by ToF-SIMS and AES. *SURFACE AND INTERFACE ANALYSIS* **2013**, *45*, 445-448.
- (13) Liu, F.; Götlind, H.; Svensson, J.-E.; Johansson, L.-G.; Halvarsson, M. Early stages of the oxidation of a FeCrAIRE alloy (Kanthal AF) at 900 °C: A detailed microstructural investigation. *Corrosion Science* **2008**, *50*, 2272-2281.
- (14) Engkvist J., S. C., K. Hellström, A. Järdnäs, J.-E. Svensson, L.-G. Johansson, M. Olsson and M. Halvarsson. Alumina Scale Formation on

- a Powder Metallurgical FeCrAl Alloy (Kanthal APMT) at 900–1,100 °C in Dry O2 and in O2 + H2O. Oxidation of Metals **2009**, online.
- (15) Liu, F.; Josefsson, H.; Svensson, J. E.; Johansson, L. G.; Halvarsson, M. TEM investigation of the oxide scales formed on a FeCrAIRE alloy (Kanthal AF) at 900 degrees C in dry O-2 and O-2 with 40% H2O. *Mater High Temp* 2005, 22, 521-526.
- (16) Blachère, J. R.; Schumann, E.; Meier, G. H.; Pettit, F. S. Textures of alumina scales on FeCrAl alloys. *Scripta Materialia* **2003**, *49*, 909-912.
- (17) Marechal, L.; Lesage, B.; Huntz, A. M.; Molins, R. Oxidation behavior of ODS Fe-Cr-Al alloys: Aluminum depletion and lifetime. *Oxidation of Metals* **2003**, *60*, 1-28.
- (18) Pint B. A., A. J. G.-R. a. L. W. H. Analytical Electron-Microscopy Study of the Breakdown of a-Al2O3 Scales Formed on Oxide Dispersion-Strengthened Alloys. *Oxidation of Metals* **2001**, *56*, 119-145.
- (19) Montealegre, M. A.; Strehl, G.; González-Carrasco, J. L.; Borchardt, G. Oxidation behaviour of novel ODS FeAlCr intermetallic alloys. *Intermetallics* **2005**, *13*, 896-906.
- (20) Unocic, K. A.; Essuman, E.; Dryepondt, S.; Pint, B. A. Effect of environment on the scale formed on oxide dispersion strengthened FeCrAl at 1050 degrees C and 1100 degrees C. *Mater High Temp* **2012**, *29*, 171-180.
- (21) Mennicke, C.; Schumann, E.; Ruhle, M.; Hussey, R. J.; Sproule, G. I.; Graham, M. J. The effect of yttrium on the growth process and microstructure of .alpha.-Al2O3 on FeCrAl. *Oxidation of Metals* **1998**, 49, 455-466.
- (22) Josefsson H. , F. L., J.-E. Svensson, M. Halvarsson, L.-G. Johansson. Oxidation of FeCrAl alloys at 500-900°C in dry O_2 . *Materials and Corrosion* **2005**, *56*, 801-806.

12 Publications

One publication is planned but not yet written

Appendices

Λ ++	2+0	hm	an+	1.
Att	all.		em	_1:

	Water content	Ash %	Ash % TS	Sulphur %	Sulphur % TS	Chlorine %	Chlorine % TS	Attatci
	%	2		8	2			
2010 week 45-47	35,6	13,0	20,2	0,29	0,46	9,0	6,0	
2010 week 50-52	41,8	11,2	19,2	0,22	0,37	0,2	0,4	
2011 week 6-8	40,1	12,2	20,3	0,43	0,72	0,4	0,7	10,2
2011 week 12-14	39,2	10,3	17	0,31	0,51	9,0	6,0	11,7
2011 week 18-20	33,8	15,6	23,5	0,48	0,72	0,7	1,1	11,3
2011 week 25-27	32,1	16,0	23,5	0,58	0,85	0,5	0,7	11,9
Average	37,1	13,1	20,6	0,4	9,0	0,5	8,0	11,1
	Carbon %	Carbon % TS	Hydrogen %	Hydrogen % TS	Nitrogen %	Nitrogen % TS	Oxygen %	Oxygen % TS
2010 week 45-47	30,3	47,1	8,0	6,2	8,0	1,2		23,9
2010 week 50-52	26,2	45,1	8,2	0,9	0,7	1,2		27,7
2011 week 6-8	27,3	45,5	8,0	0,9	0,7	1,1		25,6
2011 week 12-14	30,2	49,7	8,3	6,4	0,5	8,0		24,6
2011 week 18-20	29,8	45,0	9,7	2,7	0,7	1,0		22,9
2011 week 25-27	30,9	45,5	2,6	5,9	6,0	1,4		22,1
Average	29,1	46,3	8,0	0,9	2,0	1,1		24,5



SVENSKA ELFÖRETAGENS FORSKNINGS- OCH UTVECKLINGS - ELFORSK - AB

Elforsk AB, 101 53 Stockholm. Besöksadress: Olof Palmes Gata 31 Telefon: 08-677 25 30, Telefax: 08-677 25 35 www.elforsk.se